Volume 27
Number 45
7 December 2025
Pages 14391-14734

Green Chemistry

Cutting-edge research for a greener sustainable future

rsc.li/greenchem

ISSN 1463-9262

ROYAL SOCIETY OF CHEMISTRY

CRITICAL REVIEW

Vjekoslav Štrukil *et al.*

Mechanochemical ball milling as an emerging tool in chemical recycling and upcycling of waste polymers

25 YEARS ANNIVERSARY

Green Chemistry

CRITICAL REVIEW

View Article Online
View Journal | View Issue

Cite this: *Green Chem.*, 2025, **27**, 14401

Mechanochemical ball milling as an emerging tool in chemical recycling and upcycling of waste polymers

Anamarija Briš, Davor Margetić and Vjekoslav Štrukil *

Exponential growth of global plastic production in the past 70 years has unfortunately not been followed by at least comparable recycling rates, ultimately leading to a plastic pollution crisis we are currently facing. The very same physical and chemical properties of polymeric materials, which have been tailored for specific purposes, now pose a challenge to researchers who strive to come up with solutions to reverse them and enable full depolymerization to the monomer level. This approach lies at the core of chemical recycling, a promising technology that has the potential to convert currently present plastic wastes into valuable feedstock for the production of virgin-grade polymers and/or upcycling to novel functional materials. While traditional methods rely on thermochemical or thermocatalytic processes under high temperatures and pressures, new opportunities in chemical recycling of plastics have emerged with mechanochemical ball milling. In a short period, this methodology has been proven as highly efficient and selective for the depolymerization of commodity plastics, with significant advancements in the recycling of even challenging addition polymers. This review article aims to provide readers with a systematic overview of recent contributions in this field, focusing on the application of ball milling as an environmentally friendly, robust and easy-to-implement technique.

Received 9th July 2025,
Accepted 22nd September 2025

DOI: 10.1039/d5gc03507d

rsc.li/greenchem

Green foundation

1. Mechanochemistry has been recognized as a powerful tool to address the waste plastic-related problems. A specific solid-state reactivity that enables chemical reactions under ambient conditions with minimum or no solvent use, high efficiency, selectivity and product purity makes the breakdown of polymers more straightforward and environmentally friendly.
2. Waste plastic pollution is one of the key challenges that requires an urgent response from scientists around the globe. Mechanochemistry, with its potential to change the chemical processes in the upcoming decades, has made possible unprecedented waste polymer conversion rates and monomer yields through implementation of ball milling technique.
3. Mechanochemistry is an exciting area with new discoveries being extensively reported in the literature. This comprehensive review of the latest developments in mechanochemical treatment of waste polymers by ball milling aims to provide scientists with a state-of-the-art overview of the field and a source of inspiration for future research.

1. Introduction

The growing accumulation of plastic waste has emerged as one of the most pressing environmental challenges of the 21st century. Since the beginning of the mass production of synthetic polymers on an industrial scale in the 1950s, a moment in the modern history that has been recognized as the beginning of the "plastic age",[1] a staggering amount of more than 8 billion metric tons of plastics has been manufactured. Excellent physical and chemical characteristics of plastics, as well as their cheap production and availability, have made it irreplaceable across different industries like packaging, construction, automotive and electronics. The rate of global plastic production increases every year with 413.8 million metric tons produced in 2023. Fossil-based plastics accounted for 90.4%, and less than 9% came from circular schemes including mechanical recycling with 8.7% and chemical recycling with only 0.1% contribution.[2] Another mounting problem is related to single-use plastics that are thrown away in a life span counting only minutes but at the same time occupy 50% of the plastics market share.[3] The above numbers also testify to the low rate of recycling, where majority of post-consumer plastics end up in landfills or are incinerated. Degradation of waste plastics in the environment due to weath-

Laboratory for Physical Organic Chemistry, Ruđer Bošković Institute, Bijenička cesta 54, 10000 Zagreb, Croatia. E-mail: vstrukil@irb.hr

ering leads to the generation of micro- and nanoplastic particles that find their way into living organisms with potential to engage in interactions with biomolecules resulting in mostly unrecognized health effects.[4] With this in mind, it is fair to say that decades of irresponsible plastic waste management and neglecting the negative environmental impact that it produces have brought our society to the brink of plastic catastrophe. While there are ways to combat these issues, *e.g.* to phase down single-use plastics or use alternative bio-based and bio-degradable products, the global plastic production rate figures, growing demand and the huge amount of mixed plastic wastes that are already present make this task challenging. Furthermore, mechanical recycling, as a dominant circular technology,[5] still requires collection and sorting facilities for mixed waste streams followed by pre-treatment to ensure high-quality feedstock that can be processed into, *e.g.*, recycled food contact materials compliant with strict food safety regulations.[6] In the last decade, chemical recycling (also known as "advanced" or "molecular" recycling) has emerged as an innovative and promising solution for the recycling of waste polymers unsuitable for mechanical treatment.[7] This method relies on the chemical degradation of polymer chains down to the monomer level, and their recovery as feedstock for the production of new virgin-like polymers or upcycling to value-added products.[8]

Over the last twenty years, we have witnessed a tremendous development of mechanochemistry for the synthesis of organic,[9] inorganic[10] and functional materials.[11] Solid-state environment has made chemical transformations in the absence of bulk solvents possible, while new modes of reactivity through liquid- (LAG),[12] ion- and liquid- (ILAG),[13] polymer- (POLAG)[14] and ionic liquid-assisted grinding approach (IL-AG)[15] facilitated the discovery of pharmaceutically-relevant polymorphs, boosted reaction efficiencies and made synthesis procedures more clean and straightforward. The integration of ball milling with different energy sources such as heat,[16] light,[17] sound[18] or even electricity,[19] has enabled mechanochemistry to join forces with other chemical disciplines and create opportunities for new advancements. In parallel, the development of techniques for real-time *in situ* monitoring of mechanochemical reactions[20] has allowed in-depth study of kinetics and reaction mechanisms in the solid state at a molecular level. Hence, it is not unusual that mechanochemistry with all its benefits has been sourced as an attractive alternative for chemical polymer recycling[21] that goes beyond conventional high-temperature and high-pressure technologies and allows the development of depolymerization strategies under ambient conditions. Although polymer mechanochemistry has evolved over the decades into a discipline in its own right with significant advancements in the design of polymeric molecules based on the mechanophore concept,[22] reviews on the use of mechanochemistry to degrade waste commodity polymers are still lacking in the literature. It was only recently that Rizzo and Peterson published an excellent comprehensive review covering many aspects of modern polymer science at the interface with mechanochemistry, including polymer recycling and modifications with ball mill grinding.[23] In our contribution, we will specifically focus on the chemical recycling by means of degradation and depolymerization reactions, and the upcycling of commodity plastics, conveniently carried out in laboratory-size ball mills, as well as provide several examples of a successful scale-up of mechanochemical reactions involving waste polymers. In addition, the latest results on the recycling and upcycling of polymer types such as polyurethanes and polyfluoroalkyl compounds will be highlighted (Table 1). Given the high interest in the application of ball milling to recycle waste plastics and a fast-growing number of research articles published recently, we thought it was of great importance to systematically present these contributions based on different polymer types with an emphasis on practical and mechanistic investigations as critically important aspects of full implementation of mechanochemistry for reducing the waste plastics pollution and moving towards a plastic circular economy.[24]

2. Mechanochemical ball milling in waste polymer processing

2.1. Condensation polymers

Polyesters and polycarbonates. Poly(ethylene terephthalate) (PET) is by far the most important representative of synthetic thermoplastic polymers from the polyester family. PET resins find applications in the packaging industry (beverage bottles, food trays, and cups), production of textile fibres and films, *etc.*[25] PET is produced on an industrial scale from ethylene glycol (EG) *via* two main routes: (a) condensation with purified terephthalic acid (TPA) and (b) transesterification of dimethyl terephthalate (DMT). Both processes initially produce bis(2-hydroxyethyl) terephthalate (BHET) as an intermediate in the antimony(III) oxide-catalysed polymerization reaction. The final stages of polycondensation are typically operated at elevated temperatures under high vacuum in order to achieve the desired physical properties such as intrinsic viscosity (IV), the main quality control parameter that determines further processing of PET.[26] Other physical characteristics, specifically tailored for different applications, are modified by a range of additives (chain extenders, impact modifiers, crystallization promoters, UV stabilizers, *etc.*).[27] Thus, the depolymerization strategies related to PET revolve around the breakage of ester bonds to convert the waste polyester back to either TPA, DMT, BHET or EG.[28]

Our group reported in 2021 the first example of quantitative depolymerization of waste PET into TPA and EG monomers by mechanochemical ball milling at ambient temperature and pressure, *via* the alkaline ester hydrolysis approach (Scheme 1).[29]

The method is based on using stoichiometric quantities or slight excess (1.1 eq.) of sodium hydroxide in combination with non-treated or pre-milled PET bottles or polyester textile to isolate TPA after aqueous workup and acidification with a mineral acid (Fig. 1a). In stark contrast to existing protocols for PET depolymerization which rely on solvent-based chemistry at high temperatures and pressures, as well as excess base

Table 1 Summary of the selected reaction parameters for the mechanochemical recycling and upcycling of waste plastics by ball milling covered in this review article

Entry	Polymer[a]	Type of ball mill	Milling media[a]	Type of recycling or upcycling reaction	Reaction scale	Size/number or mass of balls	Reaction conditions[a]	Ref.
1	PET	Mixer	SS	Alkaline hydrolysis	0.5 g 4.0 g	15 mm/1 20 mm/2	NaOH (1.1 eq.), NaCl, 30 Hz, 2–3 h	29
2	PET	Mixer	SS, WC, Al_2O_3	Alkaline hydrolysis	1 g	20 mm/1	NaOH (1 eq.), 30 Hz, up to 40 min	30
3	PEF, PBF	Mixer	SS	Alkaline hydrolysis	0.25 g 2.50 g	10 mm/1 15 mm/2	NaOH (1 eq.), NaCl, 30 Hz, 30 min–1 h	38
				Methanolysis	0.166 g 1.66 g	10 mm/1 15 mm/1	CH_3OH (10–20 eq.), CH_3ONa (0.5 eq.), 30 Hz, 1–2.5 h	
4	BPA-PC	Planetary	SS	Methanolysis	5.0 g	5 mm/500	1. DMC (2 eq.) 30 min; 2. CH_3OH (30 eq.), 600 rpm, 6 h	39
	PLA				2.2 g	5 mm/250	CH_3OH (20 eq.), 600 rpm, 6 h	
	PET				2.8 g	5 mm/300	CH_3OH (35 eq.), 650 rpm, 6 h	
5	PET, PBT	Mixer Planetary	SS	MOF synthesis	0.2 g 12.0 g	18 mm/2 8, 12, 15 mm/12	1. NaOH (1 eq.), 30 Hz, 2 h; 2. Metal salt (1 eq.), 2 h, 30 Hz or 400 rpm	40
6	PU	Mixer	SS	Alkaline hydrolysis	220 mg	10 mm/3	MeOH or H_2O, Cu/$MgAlO_x$ 25 Hz, 90 min, 60 °C-90 °C	50
7	PE	Mixer	SS	Fenton reaction	1 g	10 mm/8	30% H_2O_2/H_2O Fe_2O_3 (5 wt%) 15–25 Hz, 1–2 h	64
8	PE	Planetary	SS	H_2 gasification to light hydrocarbons	50 mg	10 mm/10	γ-Al_2O_3/Fe cat. H_2 (170 bar), 21 h, 450 rpm	65
9	PE	Planetary	ZrO_2	Degradation *via* H_2O activation	50 mg	10 mm/10	γ-Al_2O_3 cat., H_2O (5–12.5 μL), 12 h, 500 rpm	66
10	PE, PP	Planetary	HS	Gasification to H_2	1.55 g	5 mm/500 g	Mn granules 36 h at 400 rpm	68
11	PVA PE PS	Mixer	SS	Macroradical formation for dehalogenation Macroradical formation for sp^3 C–F fluorination	200 mg 300 mg 300 mg	10 mm/1	Haloalkane (0.2 mmol), $SiH(SiMe_3)_3$ (1.2–2.4 eq.), 35–6 °C, 30 Hz, 1 h Alkane (0.2 mmol), Selectfluor (2.2 eq.), LAG, 60 °C, 30 Hz, 1 h	69
12	PP	Mixer	SZ, WZ	Depolymerization to light hydrocarbons	2 g	10 mm/5	SZ or WZ balls, 30–35 Hz, 1 h	70
13	PS	Mixer	HS, WC, Si_3N_4	Depolymerization to styrene	1.5 g	BPR between 10 : 1 and 13 : 1	Spex 8000 ball mill, 12 h	74
14	PMS	Mixer	SS	Depolymerization to α-methylstyrene	3 mg	7 mm/2	30 Hz, 8 min	75
15	PS	Mixer	SS	Post-polymerization modification (grafting with CF_3)	0.81 mmol	8 mm/2	10 mol% $TMSCF_3$, 40 mol% AgOTf, 40 mol% KF, DCE, 30 Hz, 4 h, N_2	78
16	PS	Mixer	SS	Post-polymerization modification (Birch reduction)	20 mg	10 mm/1	Li (10 eq.), EDA (12 eq.), THF (15 eq.), 30 Hz, 1 min	81
17	PS	Planetary	ZrO_2-yttria	Wet milling grafting with graphene	*ca.* 8 g	1, 2, 3, 5 mm/ 202 g	Graphite, wet grinding, 300 rpm, 36 h	82
18	PE, PS, PMMA, PPS, PSF	Mixer	SS	Grafting with luminophore	50 mg	10 mm/2	Luminophore (0.014 mmol) 30 Hz, 30 min	84
19	PMMA, PEMA, PnBMA, PBnMA, PPhMA, PiPMA	Mixer	SS	Depolymerization to alkyl or phenyl methacrylate	3 mg 100 mg	5 mm/15 10 mm/2	*t*-BuOH slurry, 43 °C, 30 Hz, 8 min 15 cycles of 2 min milling @ 43 °C + 5 min@95 °C open	87
20	PVC	Planetary	SS	Degradation to alkene residue	3 g	15 mm/7	CaO (1–4 eq.), 700 rpm, up to 5 h	92
21	PVC	Planetary	SS	Degradation to alkene residue	3 g	15 mm/7	Ball milling with different additives: CaO, SiO_2, Al_2O_3, CaO-quartz, Fe_2O_3, La_2O_3, $CaSO_4$, $CaSO_4{\cdot}2H_2O$	93–98

Table 1 *(Contd.)*

Entry	Polymer[a]	Type of ball mill	Milling media[a]	Type of recycling or upcycling reaction	Reaction scale	Size/number or mass of balls	Reaction conditions[a]	Ref.
22	PVC	Planetary	SS	Degradation to hydrocarbons using oyster shells	3 g	15 mm/7	Oyster shells (4 eq.), 400 rpm, 4 h	99
23	PVC	Planetary	HS	Gasification by $KMnO_4$-promoted oxidation	0.5 g	3, 5, 10 mm/ BPR 55 : 1	$KMnO_4$ (1.2 eq.), 800 rpm, 12–48 h	100
24	PVC	Mixer	SS	Degradation by dechlorination, epoxidation, ring-opening and hydrolysis	0.5 g	12 mm/3	(1) DBU (1 eq.), 30 Hz, 3 h; (2) *m*-CPBA (1 eq.), 30 Hz, 3 h; (3) NaOH (1 M), 30 min, stirring RT	101
25	PVC	Planetary	ZrO_2	Dechlorination. Cross-linking and carbonization to porous carbon	N/A	N/A	KOH in PEG-800 (2 M solution), 900 rpm, 10 h	102
26	PVC	Planetary	SS	Grafting of azole-containing drugs	0.5 g	10 mm/4	Azoloazine sodium salt (2 eq.), LAG, 500 rpm, 4 h	103
27	PTFE, FEP, PVF, PVDF, PFA, ETFE, ECTFE, PVDF-HFP, PCTFE	Mixer	SS vessel, HS balls	PFAS destruction by defluorination	0.5 g (total loading)	7 g/2	K_3PO_4 (1.25 eq. per F) or $K_4P_2O_7$ (0.625 eq. per F), 35 Hz, 3 h	113
28	PET	Mixer	PTFE vessels, ZrO_2 ball	Enzymatic hydrolysis	300 mg	10 mm/1	RAging (5 min milling at 30 Hz + 55 °C HiC), Na-PB buffer	37
29	PET/cotton textiles	Mixer	PTFE vessels, ZrO_2 ball	Enzymatic hydrolysis	200 mg	10 mm/1	RAging (5 min milling at 30 Hz + aging 55 °C HiC, CTec2), NaPi buffer	119
30	PET	Mixer	SS	Enzymatic hydrolysis	200 mg	5 mm/2	RAging (5, 10, 20 or 30 min milling at 30 Hz + 55, 50, 40, 30 min aging), KPi buffer	120
31	PLA	Mixer	PTFE vessels, ZrO_2 ball	Enzymatic hydrolysis	300 mg	10 mm/1	MAging (15 min milling at 30 Hz + aging 55 °C HiC), Tris-HCl buffer	123
32	PEN	Mixer	SS	Enzymatic hydrolysis	200 mg	3.5–4 g/1	MAging (30 min milling at 30 Hz + aging 55 °C HiC), NaPi buffer, 30 days	124
33	PET	Kneader	N/A	Alkaline hydrolysis	30 g	N/A	NaOH (13 g), EG (15 g), 160 °C, 40 rpm, 5 min	127
34	PET	Twin-screw extruder	N/A	Neutral hydrolysis	feed rate 1.11 kg h^{-1}	N/A	H_2O/PET 0.68 : 1, 300 °C, screw speed 10 min^{-1}, H_2O (0.75 kg h^{-1}), 4757 kPa, 9 min	128
35	PET	Twin-screw extruder	N/A	Alkaline hydrolysis	Feed rate 20 kg h^{-1}	N/A	NaOH, 160 °C, screw speed 200–400 min^{-1}	129
36	PVC	Horizontal TS-type reactor	SS	Degradation to alkene residue	1 kg PVC-CaO (1 : 4)	10 mm/172 kg and a 50% fill rate	CaO, inner cylinder 300 rpm, outer cylinder 70 rpm, 10 h	92
37	PVC	Horizontal ball mill	SS	Degradation to alkene residue	100–200 g	6.4, 9.5, 12.7, 15.9 mm/ 200–3200	0.5–1.0 M NaOH in EG, 190 °C, 15–60 rpm	130
38	PVC	Eccentric vibratory ball mill	SS vessel, WC balls	Degradation to alkene residue	100 g	35 mm/30 kg	$CaCO_3$ from eggshells, rotational speed 960 min^{-1}, 12 h	132

[a] See the list of abbreviations.

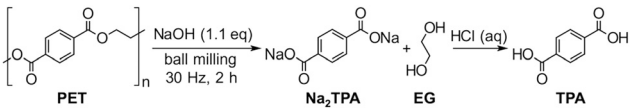

Scheme 1 Mechanochemical depolymerization of waste PET with NaOH to monomers TPA and EG in the solid state.[29]

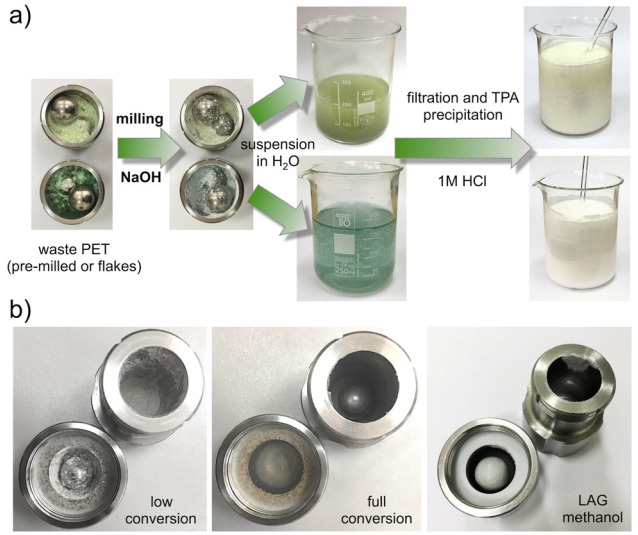

Fig. 1 (a) Schematic diagram of TPA isolation from waste PET. (b) Rheology changes during ball milling PET and NaOH under solvent-free or LAG conditions.[29]

or acid to promote the ester hydrolysis reaction,[28] our method represents a significant step forward in environmentally friendly chemical recycling of waste PET. The optimization of reaction conditions including milling time, media (size and material of balls and jars), bases and different liquids for liquid-assisted grinding (LAG) revealed that NaOH was the preferred base during two hours of solvent-free ball milling with a single 15 mm stainless steel ball at 30 Hz frequency. Since the crude reaction mixtures were consistently compacted on the jar walls or displayed rheological behaviour known as the "snow-balling effect" in the literature (Fig. 1b), we decided to use dry sodium chloride as an inert grinding auxiliary to keep the mixtures in the form of a free-flowing powder to facilitate collection of the product and ensure high reproducibility. As it would turn out, further mechanistic studies carried out by Sievers *et al.* (*vide infra*) showed that this type of rheology transformation actually indicated a change in reaction regime associated with enhanced kinetics and sudden increase in monomer yields.[30] Still, the addition of NaCl led to dilution effect and slower kinetics yielding sodium terephthalate (Na_2TPA) with minor contamination in the form of sodium mono(2-hydroxyethyl) terephthalate (NaMHET) due to incomplete hydrolysis. The addition of slight excess of NaOH (1.1 eq.) resulted in complete depolymerization of PET with ≥99% isolated yields and ≥98% purity of TPA after acidification. This ball milling approach was demonstrated to work with the same efficiency on a gram scale (2.00 g or 4.00 g of PET) with transparent and coloured waste PET bottles, as well as coloured polyester fabric. In the case of mixtures of plastics composed of different amounts of low-density polyethylene (LDPE), polypropylene (PP), polystyrene (PS) and PET, normally encountered in the post-consumer waste stream, only the polyester component was selectively depolymerized.

In an interesting extension of this methodology, we next showed that pre-milled PET could also be depolymerized by a low-energy method of aging a stoichiometric PET–NaOH mixture in a humid atmosphere or solvent vapours. The process was facilitated under high relative humidity (RH = 75% or 100%) with PET conversion of *ca.* 65% after 3 days and 80% after one week at room temperature. The aging time could be reduced to 3 days by mild heating of the PET–NaOH mixture to 45 °C or 60 °C, whilst keeping the conversion at RH = 100% at high levels of 86 and 89%, respectively. Similarly, a short 5 minute milling of the PET–NaOH reaction mixture to ensure homogenization, improve contact surfaces between reactants, and partially initiate the process before it was exposed to humidity had a profound effect on the PET reactivity profile at room temperature during 3 days of aging (Fig. 2).

Under such conditions, 66% isolated TPA yield at low humidity was achieved, while the PET conversion went up to excellent 84% at high RH. We also found that aging in methanol vapours was even more efficient with quantitative 99% PET conversion, albeit the purity of TPA was compromised due to the presence of 11% of mono-methyl terephthalate (MMT) contamination detected by ^{1}H NMR and Fourier transform infrared spectroscopy-attenuated total reflectance (FTIR-ATR). Presumably, methoxide anions could be generated by NaOH-promoted deprotonation of methanol and act as nucleophiles in the transesterification of PET molecules.

Highly efficient PET depolymerization by ball milling at ambient temperature and pressure sparked an interest among other research groups to investigate the great potential of mechanochemistry to break down other types of plastics and possibly scale up these processes to levels interesting for commercial production. With a focus placed on polyesters, Sievers performed an important systematic study on the kinetics of alkaline PET hydrolysis under ball milling conditions by chan-

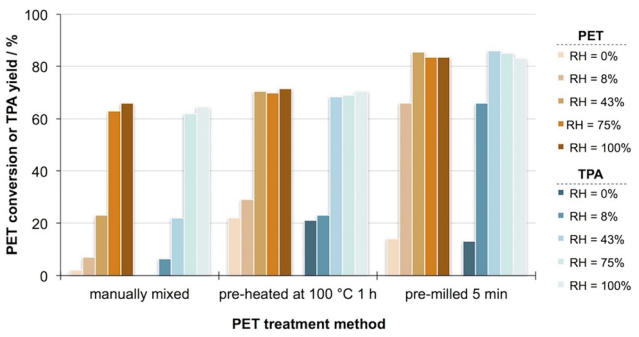

Fig. 2 PET conversion and TPA yield during aging at different humidity levels for 3 days at 25 °C as a function of the PET treatment method.[29]

ging the milling frequency, ball mass and temperature.[30] In this way, the authors proposed a kinetic model describing the PET depolymerization in single-ball milled experiments and analyzed the contribution of thermal and mechanical effects to observed solid-state reactivity. Using a 20 mm stainless steel ball in a 25 mL jar at 30 Hz frequency as standard conditions, a linear relationship between the Na_2TPA monomer yield and milling time was found up to 12.5 minutes with *ca.* 40% PET conversion. Then, an inflection point was observed where the reaction rate was significantly accelerated resulting in the fast and almost quantitative conversion of the rest of PET over the next 5 minutes of milling, while the appearance of the reaction mixture changed from powdery to a wax-like consistency compacted on the jar walls and grinding ball (Fig. 3a). The selectivity of Na_2TPA decreased slightly from 98 to 91% on account of NaMHET yield at this stage, also suggesting that Na_2TPA reactivity may play a role besides the PET depolymerization as the primary process. Gel permeation chromatography (GPC) measurements of the weight-average molecular weight (M_w) of unreacted PET indicated a small decline from 52 800 to 50 100 during the first 7.5 minutes of the reaction, down to 43 700 after 15 minutes of milling. As the milling time approached 12.5 minutes, when the rheology change occurred, the M_w distribution curves displayed narrow profiles, suggesting the loss of the longest and shortest polymer chains with the bulk of unreacted polymer intact.

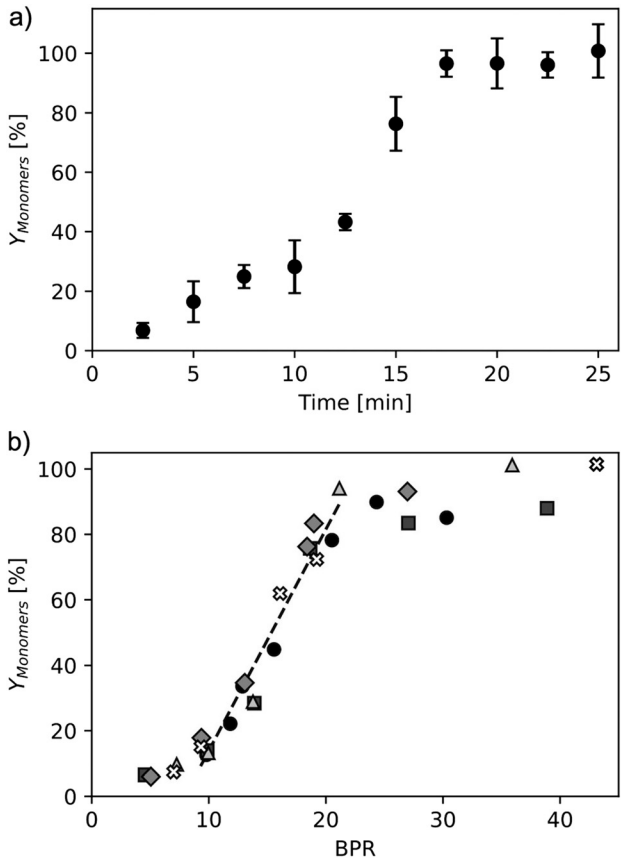

Fig. 3 (a) Na_2TPA yield change during ball milling PET/NaOH mixture with a 20 mm stainless steel ball at 30 Hz with a sigmoidal kinetics curve. (b) Na_2TPA yield as a function of BPR for PET depolymerization showing linear correlation for BPR between 10 and 20. Reprinted with permission from A. W. Tricker, A. A. Osibo, Y. Chang, J. X. Kang, A. Ganesan, E. Anglou, F. Boukouvala, S. Nair, C. W. Jones and C. Sievers, Stages and Kinetics of Mechanochemical Depolymerization of Poly (ethylene terephthalate) with Sodium Hydroxide, *ACS Sustainable Chem. Eng.*, 2022, **10**, 11338–11347. Copyright 2022 American Chemical Society.[30]

A more detailed look into the contribution of mechanical energy revealed that lower milling frequencies of 27.5 and 25 Hz led to slower kinetics with complete depolymerization achieved after 25 and 40 minutes, respectively. In parallel, the change from powder to waxy phase occurred at a later stage during milling. Additionally, the effect of ball mass (20 mm diameter) was probed by changing the material from stainless steel (ρ = 7.5 g cm^{-3}) to tungsten carbide (ρ = 15.6 g cm^{-3}) and aluminium oxide (ρ = 3.95 g cm^{-3}). As expected, the WC ball performed best with complete reaction after 7.5 minutes, while the lighter Al_2O_3 ball gave only 45% conversion after 30 minutes without the characteristic rheology change. Although the use of WC ball increased the temperature by 20 °C, further experiments with a stainless steel ball at *ca.* 90 °C showed that the rate of PET depolymerization seemed to be unaffected in comparison to room temperature ball milling. The low-temperature experiments at −35 °C, achieved by cooling the milling assembly with liquid nitrogen, indicated a slow kinetics with 42% yield and complete absence of the waxy phase. The investigation of the effect of ball-to-powder ratio (BPR), one of the characteristic parameters in ball milling, on the Na_2TPA yield during a 20 minutes of milling at 30 Hz revealed a curve with three stages corresponding to BPR values <10, 10–20 and ≥20. While for BPR < 10, the reaction was limited by the available surface area and BPR ≥ 20 led to complete depolymerization, the BPR values between 10 and 20 were in a linear correlation with the monomer yield (Fig. 3b).

Based on these experimental measurements, the authors hypothesize that the mechanochemical PET depolymerization could be explained by the shrinking core model (Fig. 4). Polymer chains on the surface of PET particles remain in contact with the NaOH phase, where the alkaline ester hydrolysis reaction occurs. In this reactive zone, monomer products Na_2TPA and EG are formed, while the PET chains in the inside of particles remain largely unreacted as evidenced by the slow decline in average M_w values of the PET residues. As the depolymerization reaction approaches completion, the remainder of unreacted PET particles shrink until quantitative conversion is achieved. In contrast to shrinking core models describing solution reactions where the concentration gradients play a major role, in the case of mechanochemical reactions, the energy of ball milling would be the parameter that governs the kinetics. During milling, the PET particles as well as the outer coating made of NaOH, Na_2TPA and EG undergo compaction, stress, and deformation from energy transfer, leading to cracks and surface defects, resulting in an increased surface area and non-uniform reaction rates. Collisions against the vessel wall expose fresh PET reactive surfaces until all of the starting

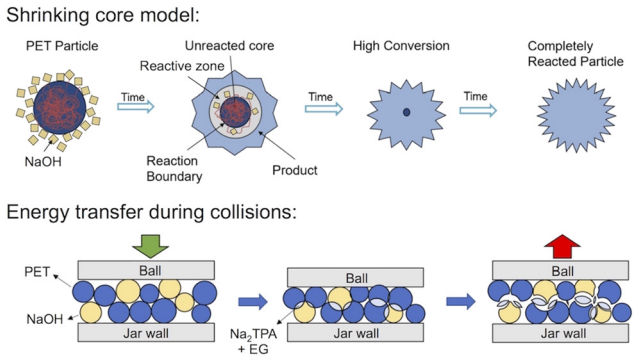

Fig. 4 Shrinking core model proposed for the alkaline PET depolymerization under ball milling conditions. Reprinted with permission from A. W. Tricker, A. A. Osibo, Y. Chang, J. X. Kang, A. Ganesan, E. Anglou, F. Boukouvala, S. Nair, C. W. Jones and C. Sievers, Stages and Kinetics of Mechanochemical Depolymerization of Poly(ethylene terephthalate) with Sodium Hydroxide, *ACS Sustainable Chem. Eng.*, 2022, **10**, 11338–11347. Copyright 2022, American Chemical Society.[30]

material is consumed. Such a picture is consistent with the observed linearity between the monomer yield and milling time in the first stage of the PET depolymerization, where the reaction mixture was in the form of a powder. However, the sigmoidal kinetics associated with the transformation from the powder phase to wax,[31] where the rate of PET depolymerization is rapidly increased, implies other mechanistic modes of action. For example, the reduction of PET crystallinity upon ball milling[32,33] would produce amorphous PET with polymer chains disentangled and thus more susceptible to NaOH hydrolysis. Furthermore, the highly viscous nature of the waxy phase might provide an environment where frequent inelastic collisions occur with more effective energy transfer per collision from the ball to the reaction mixture. These considerations led the authors to an expression for the PET conversion as a function of milling time, derived from the milling intensity as the energetic descriptor. The apparent rate constant k' for the studied single-ball milled reaction was calculated to be $8.6 \pm 0.5 \times 10^{-10}$ s^2, where the rate is proportional to BPR and the third power of milling frequency.

Boukouvala *et al.* reported the application of mathematical modelling using discrete element method (DEM) simulations to describe the PET alkaline depolymerization in a ball mill, in order to devise an accurate representation of this mechanochemical reaction, necessary for process design and optimization as the next step in the implementation towards larger scales.[34] Following the calibration of material and contact parameters in the DEM model, the extraction of collision frequencies and kinetic energy from DEM simulations allowed correlation with the experimental data on monomer yields. Interestingly, a linear relationship emerged again between the monomer yield and the cumulative kinetic energy supplied to the milling system up to *ca.* 4600 J. This corresponds to the experimentally observed first stage of the reaction up to ~40% conversion where the mixture remained in the powder form ("powder phase"). For the cumulative energy dose between 4600 and 7100 J, the linearity is lost and a transition to a mixed powder-wax phase could be expected ("wax phase"), whereas higher energy input would result in a homogenous waxy phase and quantitative yields ("complete depolymerization").

Obviously, the effects of ball milling on polymer structure seemed to play an important role in promoting effective depolymerization by reducing the particle size through compression and shearing, increasing the surface area, changing the degree of crystallinity, but also introducing structural defects and creating reactive spots that could initiate and facilitate further depolymerization reactions. In this sense, we discuss here several publications related to physical changes that the PET polymer undergoes during milling as the basis for better understanding of possible mechanisms that accompany mechanochemical transformations. Namely, it was shown by Vasiliu Oprea *et al.* that ball milling of pre-dried PET powder in an inert atmosphere of nitrogen or argon in stainless steel media induced homolytic polymer chain scission reactions that led to production of macroradical species.[35] In contrast to full depolymerization which results in the breakdown of polymer structure to its monomer constituents, polymer chain scission often occurs at the centre of the chain and produces half-molecular-weight or even smaller chains, which is reflected in the reduced molecular mass.[36] Viscometry measurements in phenol : *o*-cresol mixture (1 : 1) and end-group analysis by titration were employed for the determination of changes in weight-average molecular weight, and revealed that low temperatures down to −32 °C, where PET polymer chains are more rigid, favoured reduction of M_w value from 35 200 to 28 170 after 3 hours of ball milling. The presence of moisture accelerated the rate of mechanochemical destruction of PET polymer chains with a *ca.* 40% drop in M_w values against *ca.* 30% when moisture was excluded (Fig. 5). This was accompanied by an increase in acid values, suggesting the hydrolysis of ester linkages in PET and formation of chains with free carboxylic end-groups. Despite

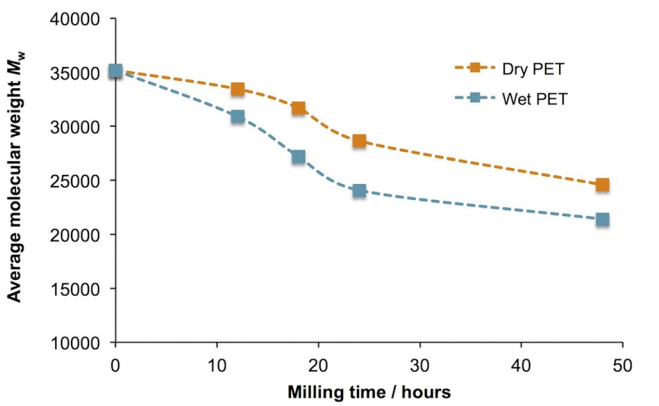

Fig. 5 The effect of moisture on PET polymer chain scission during ball milling of dry and wet samples. M_w values were measured in a phenol : *o*-cresol (1 : 1) mixture by solution viscometry.[35]

these observations, the authors did not attempt further depolymerization of PET to the monomer level and isolation of TPA.

Experiments in gaseous (air or nitrogen oxides) or liquid media (hydrocarbons and amines) showed that PET macroradicals formed by milling can react with other radical species if present (*e.g.* the nitrogen content in PET residue increased linearly with milling time and reached ~4% after 48 hours) and that the rate of polymer chain destruction was lower in inert hydrocarbon liquids than in gases. The observation that polymer chains were homolytically cleaved by milling to afford macroradicals was used to prepare PET grafted with vinyl chloride, vinyl acetate and acrylonitrile as co-polymers. After ball milling for 12–48 hours, gaseous vinyl chloride was more reactive and yielded *ca*. 23% of grafted PET against 8% with vinyl acetate and 11% with acrylonitrile as liquid co-monomers.

Balik *et al.* investigated changes in the properties of powdered PET samples (4.0 g scale) upon high-energy ball milling with 40 g of SS balls in a SPEX shaker mill, at different temperatures – around 5 and 50 °C, as well as under cryomilling conditions at −180 °C.[32] PET flakes of flattened morphology, initially present in the as-ground polymer obtained by grinding commercial PET pellets at −180 °C, were cold-welded during the first 30 minutes of ball milling at 50 °C or cryomilling conditions, leading to an increase in average particle size. Further milling resulted in a narrow particle size distribution with dimensions of 10 to 40 μm. Polarization microscopy revealed that ball milled samples were birefringent due to biaxial stretching and molecular orientation of polymer chains in PET particles, caused by collisions between balls and the milled material irrespective of the temperature. The degree of crystallinity (X_c) of PET milled at different temperatures was shown to change drastically during the first hour of milling and converged to 26%–36%, independent of the initial X_c which was 4% for low-crystallinity and 47% for high-crystallinity samples. Powder X-ray diffraction (PXRD) analysis suggested that mechanochemical treatment disrupts PET crystals by shearing parallel to the (010) planes and prolonged ball milling creates locally oriented, but rotationally disordered amorphous morphology.

In relation to this study, Zaker and Auclair recently assessed the effects of ball milling frequency on PET microstructure.[33] Four samples of PET materials with different initial degrees of crystallinity X_c (amorphous film = 5.5%, beverage bottle = 38%, textile = 39% and high-crystallinity powder = 42.5%) and size were milled in a 15 mL stainless steel jar with a single 12 mm stainless steel ball at frequencies of 5, 15 and 30 Hz. Under gentle ball milling at 5 Hz for 90 minutes, no significant changes in X_c or average particle size were observed. When the milling frequency was set to 15 Hz, an increase in the crystallinity of the amorphous PET to 9% and a decrease for other samples towards 27% were detected. At the same time, the temperature of the milling jar increased to *ca*. 35 °C. While the average particle size of amorphous PET remained stable, semi-crystalline samples were brought in the range of *ca*. 100 μm particle size after 60 minutes milling. Finally, ball milling at 30 Hz revealed substantial changes to both X_c values and average particle size in the first 15–30 minutes, with the increase in temperature to 55 °C. Interestingly, the amorphous PET film underwent crystallization while semi-crystalline samples were amorphized until stabilization of X_c at around 26%–32%, which is in an excellent agreement with the earlier report by Balik (Fig. 6a).[32] Particle size reduction to the level of *ca*. 50 μm regardless of the initial PET properties was also observed. High reproducibility of measurements, inferred from the low standard deviation, was in line with the narrower particle size distribution when compared to milling at lower frequencies. The differential scanning calorimetry (DSC) measurements were further supported by PXRD (Fig. 6b), and scanning electron microscopy (SEM) analyses showed a higher surface area of milled PET and generation of lamellar particles with a thickness <10 μm and a diameter of 40–60 μm.

The authors next demonstrated different reactivities of ball-milled PET samples towards enzymatic hydrolysis with HiC (Novozym 51032) in aqueous solutions at 60 °C for 7 days. The PET samples of crystallinity X_c = 26% with smaller average particle size (41.5 μm) gave 11% of TPA, whereas the ones with

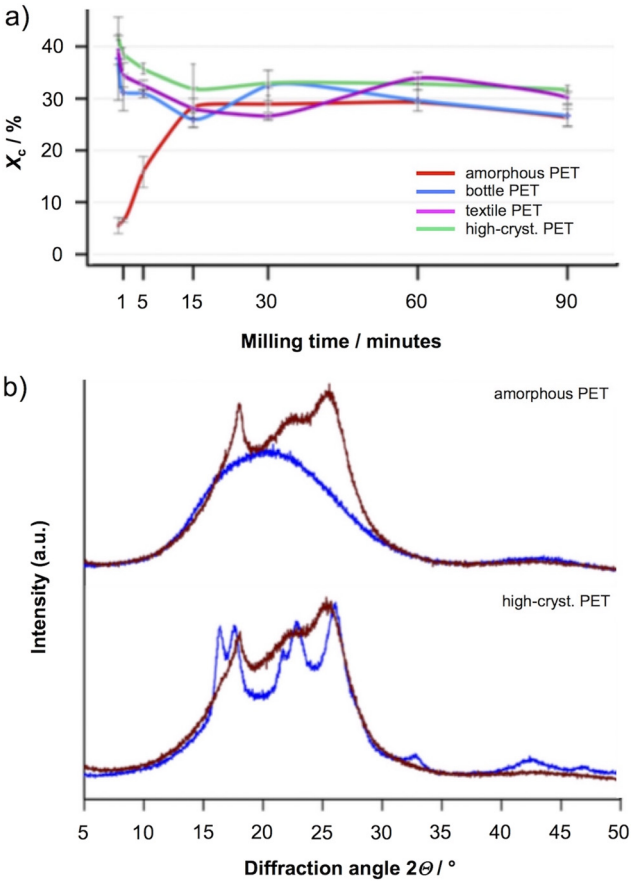

Fig. 6 (a) The effect of milling on percent crystallinity of different types of PET at 30 Hz frequency. (b) PXRD analysis of amorphous and high-crystallinity PET samples before (blue) and after (brown) 90 minutes of milling at 30 Hz. Adapted with permission from A. Zaker and K. Auclair, Impact of Ball Milling on the Microstructure of Polyethylene Terephthalate, *ChemSusChem*, 2025, **18**, e202401506.[33]

larger particles (87 μm) yielded 5% of TPA. However, for the PET samples with a particle size of *ca*. 130 μm, higher crystallinity PET (X_c = 42.5%) was poorly reactive (2% of TPA) and lower crystallinity (X_c = 32%) produced slightly better yield of TPA (6%). Although bulk temperatures did not exceed 55 °C in these experiments and were below the glass transition (T_g) and melting point (T_m) of PET, the results still indicate that competing processes of crystallization and amorphization of a PET polymer occur during ball milling until an equilibrium value of 30% crystallinity is reached. Local heating at points of collision between the balls and the vessel wall create an environment for a dynamic equilibrium of these opposing phenomena. The findings clearly show that ball milling of polymer substrates leads to particle size reduction and an increase in reactive surface area, but simultaneously induce microstructural changes that could account for the anomalous reactivity observed in mechanoenzymatic depolymerization where pre-amorphization was not required,[37] or the success of mechanochemical breakdown of PET polymer chains with NaOH in the solid state.

In the latest contribution to polyester recycling by mechanochemistry, Jain *et al.* reported on the alkaline depolymerization of bio-based poly(ethylene furanoate) (PEF) and poly(butylene furanoate) (PBF), as polymers derived from plant sugars that might replace PET synthesized from the fossil fuel feedstock.[38] Following the protocol published by our group, the authors performed the depolymerization of PEF (1.5 mmol, 0.25 g scale) with NaOH (3.0 mmol, 1 eq.) in the presence of NaCl as the inert grinding auxiliary, in a 10 mL SS jar charged with a single 10 mm ball. The optimization of several reaction parameters, including milling time, frequency, the jar/ball material, the type and amount of bases and solvents for LAG, revealed that ball milling at 30 Hz for 30 minutes gave 2,5-furandicarboxylic acid (FDCA) in the highest yield after an acidic workup (>98%). Without the NaCl additive, the PEF conversion (>92%) and the FDCA yield (91%) slightly dropped, due to unfavorable rheology that hindered a complete recovery of the reaction product. Consistent with previous studies, the authors also observed how the rheology of the reaction mixture with PEF and PBF polymers was affected by LAG (DMSO or water) or the choice of a base (*e.g.* KOH *vs.* NaOH) (Fig. 7a and b). In the case of PBF, the depolymerization to FDCA proceeded in a similar fashion with an almost quantitative isolated yield of 98%. Next, the reactions were scaled up to 2.5 g (PEF) and 1.94 g (PBF) by milling the polymer–NaOH–NaCl mixture in a 25 mL SS jar with two 15 mm balls at 30 Hz for 1 hour. The isolated yields of FDCA were 83% in the case of PEF and 90% starting from the PBF polymer.

In addition to the depolymerization of PEF and PBF by the alkaline hydrolysis reaction, the authors also tested conditions for the transesterification by methanolysis under ball milling conditions (Fig. 7c). The expected product of such a reaction is dimethyl furan-2,5-dicarboxylate ester (DMFDC), used in the polymerization process to produce the PEF polymer. While the reaction of PEF (1 mmol) with 10 eq. of methanol in the presence of NaOH did not afford the product, the addition of

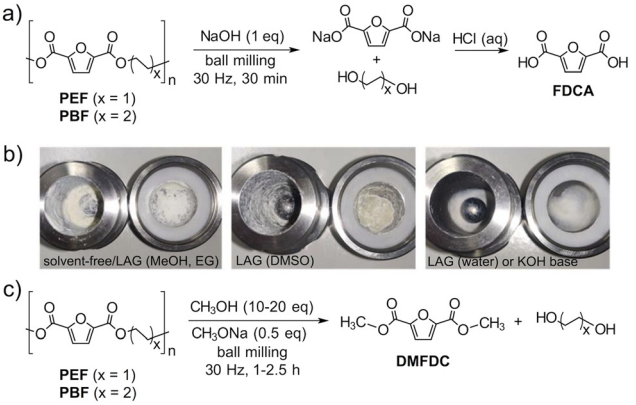

Fig. 7 (a) Mechanochemical alkaline hydrolysis of PEF and PBF polymers. (b) Rheology changes of the reaction mixture during PEF depolymerization under solvent-free or LAG conditions, or with KOH as the base. (c) Methanolysis of PEF and PBF to afford DMFDC products. Adapted with permission from D. Jain, F. Cramer, P. Shamraienko, H.-J. Drexler, B. Voit and T. Beweries, Highly efficient mechanochemical depolymerisation of bio-based polyethylene furanoate and polybutylene furanoate, *RSC sustain.*, 2025, **3**, DOI: 10.1039/d5su00428d.[38]

sodium methoxide (0.5 eq.) resulted in quantitative PEF conversion and 74% isolated yield of DMFDC after ball milling at 30 Hz for 1 hour, followed by an acidic workup and recrystallization at 5 °C. The mechanochemical methanolysis of PBF required 2.5 hours of milling with 20 eq. of methanol to reach 39% isolated yield of DMFDC. An attempt was also made to perform the methanolysis on a 10 mmol scale of PEF, which led to 65% of the dimethyl ester product employing the same workup procedure.

The idea of mechanochemical recycling of condensation polymers was further pursued by Borchardt and Kim who published the ball milling-induced methanolysis of poly(bisphenol-A carbonate) (BPA-PC) as a representative of polycarbonate esters, also including the polyesters poly(lactic acid) (PLA) and PET.[39] The monomeric products of these reactions were bisphenol A (BPA)/dimethyl carbonate (DMC), methyl lactate and DMT/EG, respectively (Scheme 2).

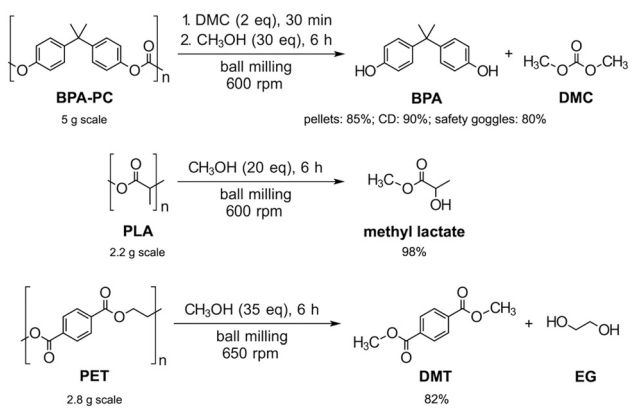

Scheme 2 Direct methanolysis of polycarbonate BPA-PC and polyesters PLA and PET.[39]

Their approach was based on solvent- and catalyst-free depolymerization through high-intensity ball milling in a planetary ball mill, which provided the energy for the process. The experiments were carried out in 25 or 125 mL stainless steel jars, charged with 50–500 stainless steel balls of 5 mm diameter, depending on the scale (0.25–5.0 g). Typically, the reactions were run for up to 6 hours at 600 rpm frequency with an excess of methanol of 30 eq. for BPA-PC and PLA substrates, and 35 eq. in the case of PET methanolysis. The crude mixtures were acidified with 1 M hydrochloric acid, and the products BPA, methyl lactate, and DMT were separated by extraction with dichloromethane and filtration through a short silica plug. Initial tests with 1.0 mmol of BPA-PC analogue diphenyl carbonate (DPC) revealed that the catalyst-free solution reaction in methanol (35 eq.) required heating to 100 °C in a closed vial, whereby 55% of the intermediate methyl phenyl carbonate (MPC) was still present after 9 hours and near quantitative conversion of DPC. A corresponding mechanochemical reaction at 600 rpm was shown to be faster, reaching quantitative DPC conversion after 3 hours of ball milling, and complete consumption of MPC after 5 hours (Fig. 8).

To exclude the possibility of metal catalysis from the milling media, the solution reaction at 100 °C was carried out in the presence of stainless steel (SUS304) fine powder, only to find that no appreciable rate enhancement was observed. When commercial BPA-PC powder was heated at 100 °C in methanol (70 eq.), no depolymerization occurred, as evidenced by size exclusion chromatography (SEC) analysis of the residue, which retained its unimodal dispersity ($Đ_0$ = 2.15 *vs.* $Đ$ = 2.04). However, ball milling the same mixture at 600 rpm with 50 balls in a 12 mL jar resulted in 97% conversion of BPA-PC to BPA (78%), BPA-monomethyl carbonate (18%) and BPA-dimethyl carbonate (1%) after 6 hours based on ^{1}H NMR analysis. Quantitative depolymerization to BPA (99%) and DMC was achieved in a 25 mL jar due to more efficient mixing and easier ball movement, while the amount of methanol was reduced from 70 to 30 eq. In the complete absence of methanol, the number-average molecular weight (M_n) of BPA-PC decreased only by 2% proving that polymer chains kept their integrity under high-intensity mechanical stress exerted by ball milling. Interestingly, the authors reported that as the methanolysis reaction proceeded, the M_n value of the unreacted BPA-PC slowly changed, despite detection and isolation of monomeric BPA species. We note here that the observed reactivity might also be described by the shrinking core model sharing similarities with the PET/NaOH system and possibly suggesting a general mechanism of mechanochemical depolymerization independent of the type of condensation polymer being chemically degraded.

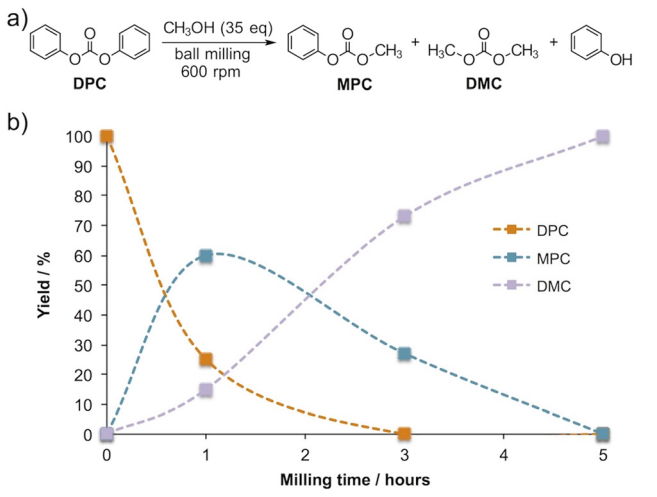

Fig. 8 (a) Mechanochemical methanolysis of diphenyl carbonate (DPC). (b) Concentration profiles during methanolysis of DPC at 600 rpm on a 1 mmol scale.[39]

Since the BPA-PC plastic is known for its high impact strength, the authors next explored the behaviour of BPA-PC pellets under ball milling methanolysis. Unlike the powdered substrate, the pellet shape was completely unreactive even after 6 hours. The addition of 2 eq. of DMC as a good solvent that caused BPA-PC to swell, allowed the transformation of pellets to powder after 30 minutes of ball milling. In the second step, 30 eq. of methanol were added and milling resumed for 6 hours to afford 99% yield of BPA and complete depolymerization of polycarbonate according to ^{1}H NMR. This strategy finally enabled scale up to 5.0 g of BPA-PC pellets in a 125 mL jar with 500 balls. The two-step sequence gave pure BPA (85%) after extraction from dichloromethane and isolation on a silica column. In the case of waste CD and safety goggles, the procedure afforded pure BPA in isolated yields of 90% and 80%, respectively. With PLA cups (2.2 g scale) and 20 eq. of methanol, the monomer methyl lactate was isolated in excellent 98% yield, while PET beverage cups (pre-milled, 2.8 g scale) required 35 eq. of methanol and higher frequency of 650 rpm for 6 hours to produce 82% of pure DMT after work up. Similarly to BPA-PC pellets, bulk PET chips displayed no reactivity.

Another way to go around the waste plastic management by mechanochemistry is to incorporate the monomer products into valuable functional materials. This upcycling approach led Gong and coworkers to consider coupling the mechanochemical alkaline PET hydrolysis with the synthesis of metal-organic frameworks (MOFs).[40] Although numerous MOFs have already been prepared by mechanochemical milling,[41] this route remained unexplored. In this way, the monomer TPA or preferably its sodium salt Na_2TPA is used directly as a 1,4-dicarboxylate ligand (BDC) in the structure of several MOFs comprising La^{3+}, Zr^{4+}, Ni^{2+}, Co^{2+}, Mn^{2+} and Ca^{2+} metal centers. The authors proposed a two-step mechanochemical sequence where PET powder or waste PET flakes (0.2 g scale) were first depolymerized with equimolar NaOH for 2 hours (or 4 hours with PET flakes) to produce Na_2TPA in quantitative yields following our procedure.[29] Then in the second step, the addition of stoichiometric amounts of metal nitrates (La^{3+}, Ni^{2+}, and Co^{2+}) or chlorides (Zr^{4+}, Mn^{2+}, and Ca^{2+}) gave MOFs after additional 2 hours of ball milling in a vibrational mill (Fig. 9a). The products were isolated by centrifugation,

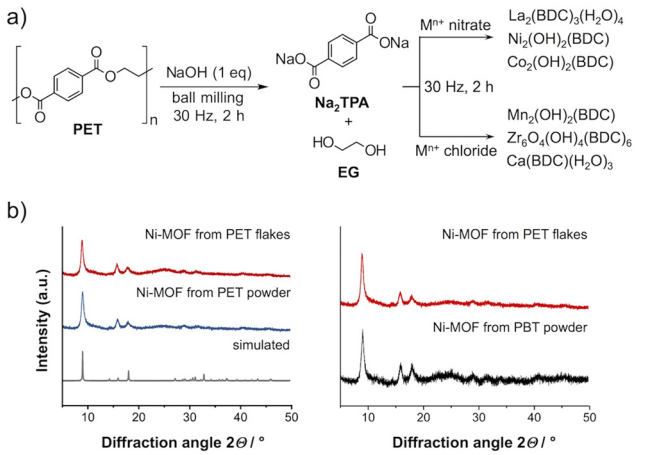

Fig. 9 (a) Mechanochemical upcycling of waste PET to MOFs. (b) PXRD patterns of the Ni-MOF synthesized from the PET flakes and powder (left), and comparison with the sample prepared from PBT as a source of 1,4-dicarboxylate ligand.[40]

washing with water and ethanol, and finally drying at 80 °C for 10 hours in good to excellent yields: $La_2(BDC)_3(H_2O)_4$ = 78%, $Zr_6O_4(OH)_4(BDC)_6$ = 56%, $Ni_2(OH)_2(BDC)$ = 90%, $Co_2(OH)_2(BDC)$ = 54%, $Mn_2(OH)_2(BDC)$ = 77% and $Ca(BDC)(H_2O)_3$ = 58%. The formation of desired MOFs was confirmed by PXRD and comparison of the measured data with simulated diffractograms, which also showed that the crystallinity of the prepared materials was low. Using the Ni-MOF as a model compound, the authors next used a waste PET bottle and polybutylene terephthalate (PBT) as sources of BDC ligands to demonstrate the effectiveness of the ball milling strategy for upcycling waste polyesters into advanced materials (Fig. 9b). The Ni-MOF mechanosynthesis from PET powder was successfully scaled up to 12.0 g of PET in a 1.5 L stainless steel jar with 12 balls of different sizes (d = 0.8, 1.2 and 1.5 cm) on a planetary ball mill operating at 400 rpm frequency. Four jars were simultaneously charged, producing 60.1 g of Ni-MOF in 93% isolated yield after milling for a total of 4 hours. PXRD analysis indicated the formation of low crystallinity $Ni_2(OH)_2(BDC)$ phase. The morphology of synthesized MOFs was investigated by SEM and transmission electron microscopy (TEM), which revealed the agglomeration of nanoparticles with uneven size distribution due to restricted size growth and different crystallization rates under ball milling conditions. Nitrogen adsorption–desorption measurements were in agreement with micro- and mesoporosity of MOFs, while X-ray photoelectron spectroscopy (XPS) further confirmed their chemical composition. Time-resolved *ex situ* PXRD analysis provided some insights into the mechanism of Ni-MOF formation from PET. The characteristic reflections of Na_2TPA disappeared after 30 minutes of milling with a nickel nitrate salt and gradual evolution of Ni-MOF and sodium nitrate reflections at 2θ angles 8.9° and 29.5° occurred as the reaction proceeded. An unknown intermediate phase with reflections at 2θ = 33.4° and a broad reflection at 2θ = 17°–26° was visible at an early stage of the reaction but eventually transformed into the Ni-MOF phase.

Polyurethanes. Polyurethanes (PU) comprise another group of technically important synthetic polymers. Formed by a polycondensation reaction between different diisocyanates and polyols in the presence of metal and amine catalysts, silicone surfactants and blowing agents, these materials are characterized by their outstanding properties such as strength, durability, flexibility and thermal stability with application in many industries, *e.g.* construction, automotive, production of footwear, adhesives and coatings.[42] Industrially important diisocyanates are toluene-2,4-diisocyanate (TDI), methylene diphenyl diisocyanate (MDI), hexamethylene diisocyanate (HDI) and isophorone diisocyanate (IPDI), while polyols are selected from a range of synthetic and bio-derived polyether or polyester derivatives.[43] Depending on the combination and mixing ratios of isocyanates and polyols, flexible, rigid and semi-rigid PU foams are produced.[44] The characteristic functional group in PU polymers is the carbamate (urethane) group, which is susceptible to nucleophilic attack by hydrolysis, glycolysis or aminolysis, and is therefore set as the target for chemical recycling of waste PU materials.[45] The valuable products of such reactions are diamines derived from the isocyanate part and various polyols that are repurposed to make the original PU.[46] Much of the work published has focused on the glycolysis routes under conditions that require high temperatures and pressures,[47] and the application of mechanical ball milling was limited to pulverization to facilitate physical recycling.[48] However, thermoset PU materials with their cross-linked structures still present an obstacle for purely mechanical recycling.[49] Schunk and Schüth have only recently reported the first example of mechanochemical degradation of base-impregnated PU by a synergistic methanolysis/hydrolysis approach to cleave the carbamate –NH–C(=O)– group (Scheme 3).[50]

As the PU substrate, a yellow portion of the kitchen sponge was selected and pre-milled in a planetary ball mill at 600 rpm in six 1 hour cycles, with an intermittent 10 minute pause to allow cooling. The milling was done at room temperature in an argon atmosphere to avoid potential oxidation under harsh conditions, producing PU as a fine powder, which was in the next step impregnated with a 10% NaOH solution. After removal of water and drying in a vacuum oven at 50 °C, the

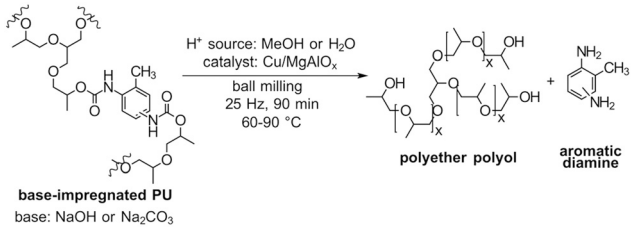

Scheme 3 Ball milling promoted degradation of a base-impregnated polyurethane in the presence of a $Cu/MgAlO_x$ catalyst at elevated temperatures.[50]

impregnated PU substrate (PU-NaOH) was kept under argon to prevent adsorption of water and CO_2. In a typical mechanochemical depolymerization reaction, 220 mg of PU-NaOH was milled with three 10 mm stainless steel balls at 25 Hz, using methanol (200 μL) or water : methanol (1 : 1) mixture (100 μL) as the proton source and a copper catalyst, Cu/$MgAlO_x$, with different Cu loadings (10, 20 or 30 wt%). The jar was heated during milling with a home-built ceramic heating box that allowed temperature control and monitoring. The final polyol product and residual solids were isolated by extraction with ethyl acetate, centrifugation and solvent evaporation. The authors noted that catalyst-free methanolysis milling at room temperature for 1 hour resulted in 11% yield of polyol, while in the presence of 30 wt% Cu/$MgAlO_x$ the yield was slightly better at 16%. Increasing the temperature during milling to 60 °C led to much better conversions of 58% and 68%, respectively. When methanol was replaced with water, the polyol recoveries dropped to 12% at 60 °C due to the stronger interaction of water molecules with Cu active sites in the catalyst. A further increase in temperature to 90 °C restored the 68% level with water, suggesting the adsorption/desorption equilibrium between water and the Cu catalyst. The optimization of Cu loading revealed that 20 wt% Cu/$MgAlO_x$ and ball milling for 90 minutes at 90 °C afforded polyols in high 86% recovery. Attempts to reduce the amount of NaOH to 1% for impregnation gave only 44% polyol under the same conditions.

Since NaOH adsorbs atmospheric CO_2 and gets converted into Na_2CO_3, the experiments were also carried out with Na_2CO_3 as the base. Expectedly, the polyol yield was lower since the carbonate is a weaker base, and led to 65% recovery under optimal conditions. The spent catalyst is deactivated with carbon and amine residues originating from the PU matrix, but calcination in air at 550 °C for several hours restores its activity. The mechanochemical approach was shown to be superior to hydrolysis in a NaOH solution, where only 6% of the polyol component could be recovered. The composition of the polyol fraction was analysed by NMR, GPC, mass spectrometry and FTIR-ATR spectroscopy, all of which indicated a high degree of structural similarity with the commercial polyol polyetherol (Lupranol® 2074). In terms of potential reuse of the obtained polyols, low nitrogen content (0.8%–2.7 wt%) and free hydroxyl groups allowed a successful preparation of a PU sample from toluene-2,4-diisocyanate in DMF at room temperature.

2.2. Addition polymers

Functional groups such as ester, carbonate or carbamate groups are prone to nucleophilic substitution reactions, a property which is extensively used in the chemical recycling of condensation polymers. However, commercially relevant addition polymers like low- and high-density polyethylene (LDPE, HDPE), polypropylene (PP), polystyrene (PS), polyvinyl chloride (PVC) and polyfluoroalkyl polymers lack the usual C–O or C–N heteroatom bonds that are easily broken, but consist of strong covalent bonds such as C–C, C–H, C–Cl and C–F. Polyolefins are typically characterized by low glass transition temperature (T_g) and high ceiling temperature (T_c) values, a combination that makes them less susceptible to depolymerization.[51,52] Additionally, they tend to degrade only to a certain degree without fully reaching the monomer stage.[53] Thus, it is not surprising that mechanochemical treatment of polyolefins is mostly reported with the purpose of polymer particle size reduction for use in composite materials.[54,55] With all this in mind, the task of breaking them apart is what makes chemical recycling of addition polymers even more challenging.[56] In this sense, high temperatures in combination with high pressures or catalysts in the absence of oxygen are often employed.[57] The resulting products are often referred to as the pyrolysis oil and are composed of a mixture of hydrocarbons with chain length from C_5 to C_{40} that typically resemble diesel fuel in chemical composition, rendering their use for blending with fossil fuels or in the co-processing in oil refineries.[58] Still, the presence of various additives and chemical species that poison catalysts or cause corrosion of the equipment in the upstream processing needs to be addressed, reflecting the problems related to the quality of the waste plastics.[59] Despite these technical challenges, chemical transformation into pyrolysis oil of mixed plastic waste, which is difficult to treat by mechanical recycling, is feasible, and currently, there are pilot-scale plants in the testing phase with potential for full industrial-scale operation.[60] Technologies such as gasification,[61] hydrothermal liquefaction (*e.g.* patented CAT-HTR technology)[62] or conversion to hydrogen[63] are also being extensively pursued. In the context of this review, recent developments in mechanochemical depolymerization have initiated intensive research on the application of ball milling for chemical recycling of addition polymers.

Polyethylene and polypropylene. Sievers and co-workers employed the Fenton reaction in the mechanochemical depolymerization of medium-density polyethylene (MDPE).[64] A mixture of MDPE, Fe_2O_3, and an aqueous 30% H_2O_2 solution was ball milled inside a stainless steel vessel (Scheme 4a).

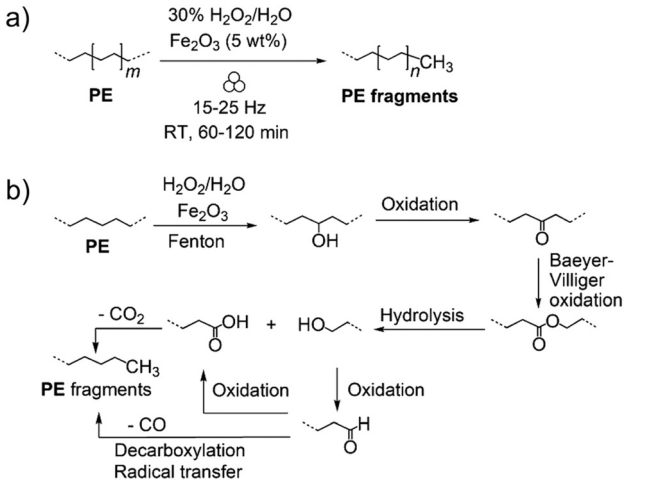

Scheme 4 (a) Depolymerization of MDPE by the Fenton process under ball milling conditions. (b) Proposed mechanism for the mechanocatalytic Fenton-type depolymerization of MDPE by ball milling.[64]

The efficiency of mechanochemical cracking of MDPE was ascertained by the measurements of weight-average (M_w) and number-average molar mass (M_n), and the corresponding polydispersity index PDI. High PDI values of samples showed a high degree of heterogeneity in the polymer after ball milling, indicating that the material was partially converted to small molecules, and the remaining was a polymeric residue. This mechanocatalytic PE depolymerization by the Fenton reaction is believed to start by random oxidation of carbon atoms in the PE chain, which activates the polymer for cracking, and formation of straight-chain oxygenates with significantly lower molecular weights through pathways including Bayer–Villiger oxidation, hydrolysis and decarboxylation radical transfers (Scheme 4b).

Another contribution from Schüth *et al.*[65] is their work on the development of the depolymerization process that proceeds at low temperatures and avoids harsh conditions of other methods, such as heating polymers to high temperatures (typically >500 °C) to transform them to pyrolysis oil. The novel mechanochemical depolymerization utilized the combination of solid and gaseous reactants. A planetary ball mill stainless steel jar equipped with gas inlets was loaded with a PE polymer, γ-Al_2O_3/Fe powder catalysts and gaseous hydrogen, and the reaction mixture was milled with ten 10 mm balls at 450 rpm for 21 hours under H_2 pressure of 170 bar. Before the introduction of H_2 gas, the jar was filled with argon and evacuated in three cycles. Among several carbon materials subjected to mechanochemical treatment were also commodity plastics polyethylene (PE) and PET in the powder form, which by solid-gas ball milling hydrogenation at room temperature provided gaseous light hydrocarbons (C_1–C_4). While the depolymerization reaction after 7 hours was modest, prolonged milling improved efficiency with PE to 27%, while PET afforded excellent conversion (97%) after 21 hours. Gas chromatography analysis (GC) revealed that methane gas (CH_4) was the major product of plastic gasification by milling (>90%–95% selectivity). The low conversion of PE was attributed to a combination of physical resistance to abrasion and impacts, its relative softness and tendency for plastic deformation, a more efficient dissipation of the mechanical energy compared to other substrates, as well as chemical inertness of the strong covalent C–C bonds. The reaction was postulated to proceed through a radical mechanism (Scheme 5), which was demonstrated by a significant decrease in conversion in the presence of TEMPO radical scavengers.

An attractive method for the depolymerization of PE by cracking with water has also been recently developed by the same group.[66] PE recycling *via* mechanochemical activation with water in the presence of γ-Al_2O_3, which likely acts as a dispersant, provided alkanes, alkenes, alcohols and ketones up to C_{50} in *ca.* 80% carbon conversion (Scheme 6a). This methodology does not require high temperatures, noble metal catalysts or handling gases under high pressures as it affords hydrocarbon mixtures mainly composed of wax and some solid fraction by milling at ambient temperature. Standard reactions were performed in a home-built zirconia jar with ten

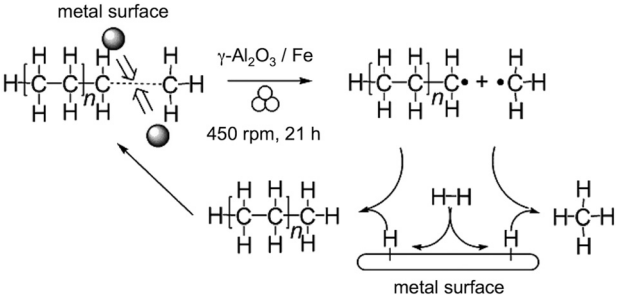

Scheme 5 Mechanochemical gasification of the PE and PET substrates with hydrogen gas in the presence of γ-Al_2O_3/Fe catalysts. The reaction proceeds by a radical mechanism.[65]

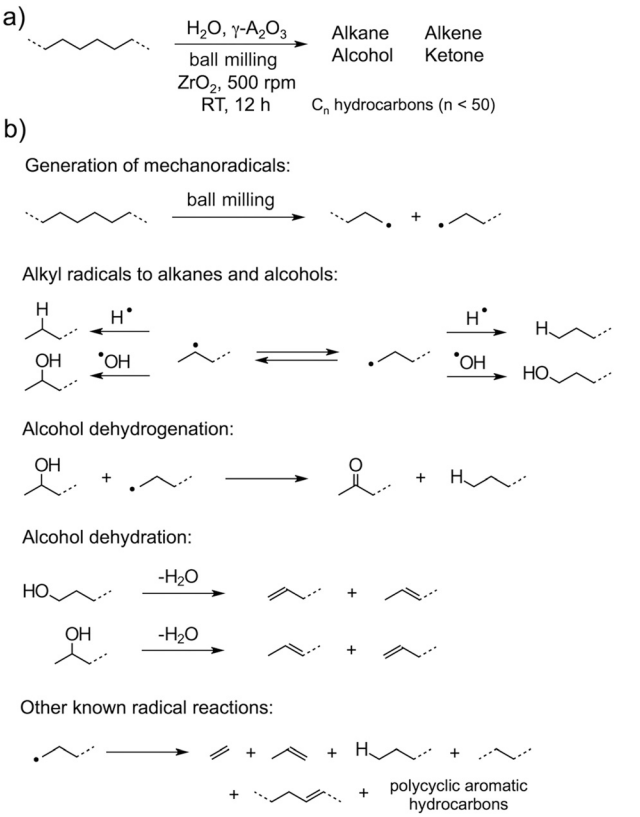

Scheme 6 (a) Mechanochemical degradation of PE by water activation in the presence of γ-Al_2O_3 dispersants. (b) Proposed reaction mechanism involves the generation of alkyl radicals by ball milling and subsequent homolytic water splitting to produce alkanes, alcohols, alkenes and ketones.[66]

10 mm ZrO_2 balls, which was placed inside an outer stainless steel casing. The jar was charged with 50 mg of PE, 300 mg pre-dried γ-Al_2O_3 and different amounts of water (5, 7.5, 10 and 12.5 μL) under an argon atmosphere, and the mixture was milled at 500 rpm speed for 12 hours. Following the reaction, GC and ^{1}H NMR analyses were performed to reveal the chemical composition of the hydrocarbon mixtures and the effect of milling parameters and water content on the efficiency of PE

depolymerization. In this way, the presence of a range of *n*-alkanes, i-alkanes, alkenes, alcohols and ketones in chemically complex reaction mixtures was confirmed. Most notably, as the amount of added water was decreased from 12.5 to 7.5 μL, the concentration of short-chain compounds in the mixture went up. Without water or with 5 μL, dark grey discoloration of the milling residue indicated coke formation, which was also pronounced in the absence of γ-Al_2O_3 dispersants.

It is proposed that alkyl radicals are initially generated by milling, which further react with water to form alkanes and alcohols. The formation of alkyl radicals was confirmed by trapping them with TEMPO scavengers and the detection of alkyl-TEMPO species, while homolytic water splitting to H$^{\bullet}$ and OH$^{\bullet}$ radicals under ball milling conditions was demonstrated by capturing OH$^{\bullet}$ with 5,5-dimethyl-1-pyrrolyine *N*-oxide (DMPO) to form the DMPO-OH adduct. Alcohols are dehydrated to alkenes, probably facilitated by Lewis acid sites on the surface of γ-Al_2O_3, and dehydrogenated to provide ketone derivatives. Other reactions characteristic of radicals (*e.g.* β-scission, disproportionation, recombination) occurred during water-assisted PE depolymerization and contributed to the chemical diversity of the degradation products (Scheme 6b).

Huang and coworkers have reported an efficient method for hydrogen generation by the gasification of ball-milled polyethylene with $Ca(OH)_2$ and $Ni(OH)_2$.[67] Although PE degradation itself was not achieved by mechanochemistry, this method involved pre-milling of PE substrate in a planetary mill to facilitate the gasification reaction at elevated temperatures (300 °C–500 °C) to produce H_2 and carbonate. The molar ratio of PE : $Ca(OH)_2$: $Ni(OH)_2$ = 6 : 12 : 1 provided the best selectivity for hydrogen. A different approach to mechanochemical upcycling of HDPE waste to hydrogen gas was developed by Jiang *et al.*, who applied manganese and chromium metal granules as catalysts.[68] Almost quantitative yield of hydrogen was achieved at 400 rpm milling speed after 36 hours with a recovery ratio of 98.5%, which was 6 times greater than the thermocatalytic method in the presence of Mn metal catalyst (Fig. 10a).

Ball milling reactions were carried out under argon atmosphere, although the process seemed to tolerate the presence of air. The most prominent feature of the mechanocatalytic method is that the initiation temperature for the process was lowered from 160 °C in the thermocatalytic method to only 45 °C by milling, making the process much more sustainable and energy-efficient. In addition, the purity of the H_2 gas evolved was outstanding at 99.4 vol% selectivity with only traces of hydrocarbons. In contrast, the thermocatalytic approach favoured the generation of C_1–C_4 hydrocarbons (mostly CH_4) over H_2 production with H_2 yields reaching only 10%. Some other metals with the potential to form carbides and drive the HDPE degradation reaction towards hydrogen generation were also screened (Cr, Mo, W and Fe), which revealed that the carbide formation energy was correlated with the PE decomposition rate. Better H_2 selectivity and recovery

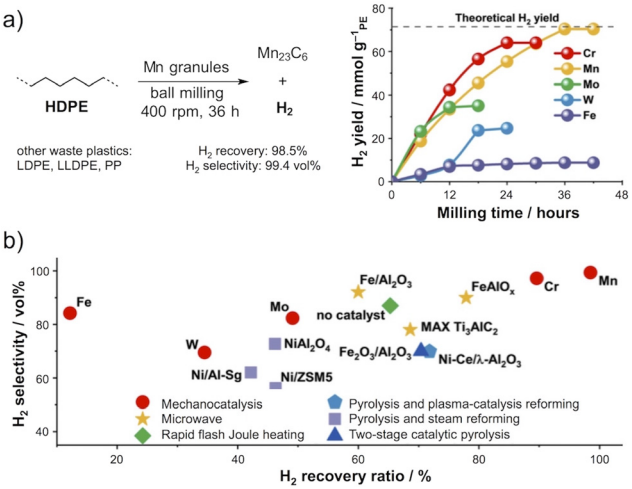

Fig. 10 (a) Upcycling of HDPE to high-purity hydrogen gas and metal carbide by ball milling with different metals. (b) Efficiency of various methods for hydrogen generation from polyethylene. Mechanocatalysis with Mn or Cr granules provides the best recoveries and selectivity. Adapted with permission from R. Gu, T. Wang, Y. Ma, T.-X. Wang, R.-Q. Yao, Y. Zhao, Z. Wen, G.-F. Han, X.-Y. Lang and Q. Jiang, Upcycling Polyethylene to High-Purity Hydrogen under Ambient Conditions *via* Mechanocatalysis, *Angew. Chem. Int. Ed.*, 2025, **64**, e202417644.[68]

rates were obtained for more stable carbides such as Mn and Cr ones, and the results were compared with alternative approaches to demonstrate the superiority of mechanochemistry (Fig. 10b). Furthermore, the formation of metal carbides $Mn_{23}C_6$ and Cr_2C, which extracted the carbon content from PE waste, was confirmed by PXRD, XPS and high-resolution TEM analyses. The authors noted that compounds such as $Mn_{23}C_6$ or Cr_2C formed as by-products could have application in materials science due to their hardness, high melting points and corrosion resistance, while 99.4 vol% selectivity for H_2 ensures practically zero carbon emission of the reaction. The authors tested their method on other types of waste plastics like LDPE, linear low-density polyethylene (LLDPE) and PP, and were able to show similar H_2 yield rates and selectivities.

In an interesting application of ball milling to produce radicals from polyolefins and couple this type of reactivity with organic synthesis, Ito *et al.* showed that azo compounds and organic peroxides could be replaced with plastic materials as safe radical initiators for the dehalogenation of organic halides with tris(trimethylsilyl) silane.[69] These reactions were induced with the mechanochemical generation of macroradicals from polymers, followed by hydrogen atom transfer (HAT) and radical chain dehalogenation (Fig. 11a).

Polyvinyl acetate (PVA) exhibited the highest activity after 1 hour of milling at 30 Hz at room temperature. PE required gentle heating of the jar to 60 °C with a heat gun for the best performance, whereas other polymers such as PS, PP, polypropylene sulfide, polysulfone, and poly(methyl methacrylate) (PMMA) were significantly less active. Without the polymer or in a solution environment, no reactivity was observed. GPC analysis of ball-milled PE and PVA showed reduction of M_n

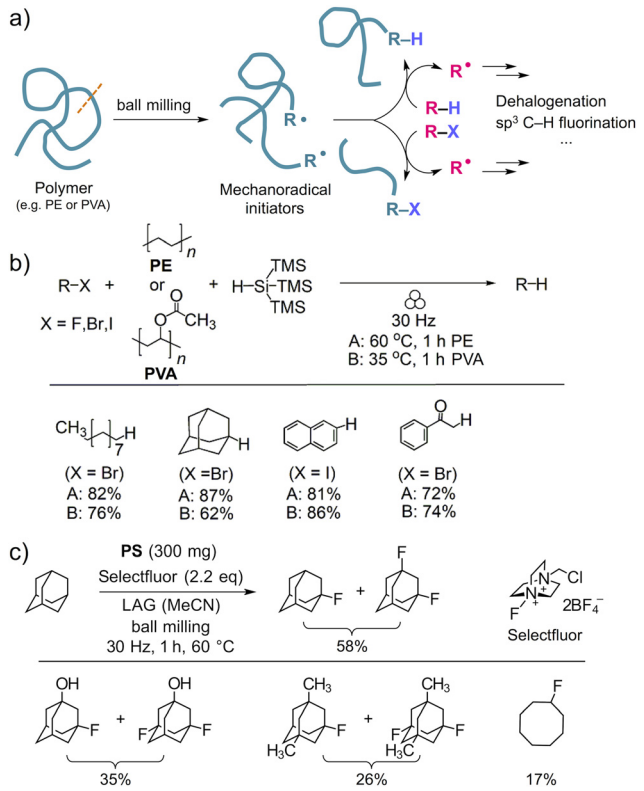

Fig. 11 (a) Mechanoradicals generated by ball milling as initiators of dehalogenation of organic halides with tris(trimethylsilyl) silane. (b) Selected examples of different substrates yielding dehalogenated products with PE (method A) and PVA polymers (method B) as radical initiators. (c) Use of polystyrene as the radical initiator for sp^3 C–F fluorination reactions.[69]

values, corroborating the hypothesis that mechanoradicals were formed during the reaction. Good to excellent yields were achieved with different alkyl and aromatic bromides and iodides, while chlorides reacted poorly (Fig. 11b). A scale-up experiment from 300 mg of PE to a gram scale (3.75 g) provided adamantane from 1-bromoadamantane in 85% yield, accompanied by a temperature increase to 80 °C. It was demonstrated that even plastic waste (*e.g.* PE plastic bags) could be used to convert 1-iodonaphthalene to naphthalene in 69% yield. Furthermore, synthetically useful radical cyclization reactions and fluorination reactions with 1-(chloromethyl)-4-fluoro-1,4-diazabicyclo[2.2.2]octane-1,4-diium ditetrafluoroborate reagent (known in organic synthesis as Selectfluor) in combination with polystyrene polymer as the radical initiator for sp^3 C–F fluorinations were also successfully mediated by mechanochemically generated macroradicals, demonstrating the broad utility of this methodology in organic chemistry (Fig. 11c).

Polypropylene depolymerization was the subject of research by Vollmer *et al.*[70] who developed a mechanocatalytic strategy for PP degradation into small hydrocarbons at temperatures <50 °C and ambient pressure, which is in contrast to traditional thermal cracking of PP that requires temperatures above 275 °C. The 2 gram scale reactions were carried out in a mixer mill with five 10 mm ZrO_2 balls at 30 or 35 Hz at room temperature for 1 hour. Mechanocatalysis was realized by surface activation of ZrO_2 balls to produce two types of catalytically active sites in sulfated (SZ) or tungstated (WZ) ceramic balls. In the case of SZ balls, the surface of pristine ZrO_2 balls was etched with concentrated sulfuric acid, washed and calcined, whereas the WZ balls were obtained by etching in molten NaOH and impregnation of tungstate species from an aqueous solution, followed by calcination and reduction with hydrogen. Such a mechanocatalytic approach is different from the conventional addition of a catalyst powder or using milling media as a catalyst[71] and is termed the "surface-activated mechanocatalysis" or SAM. The composition of the evolved gases and volatiles was monitored by online GC, which revealed the presence of the monomer propene, but also other gases such as methane, ethane, ethene, propane, and volatile C_5–C_{10} short-chain hydrocarbons as major products with cumulative yields up to 46% with SZ ceramic balls at 35 Hz milling frequency (Fig. 12a). In the case of non-treated ZrO_2 balls, the cumulative yield of 33% was achieved under the same milling conditions. Interestingly, the SAM catalysts in

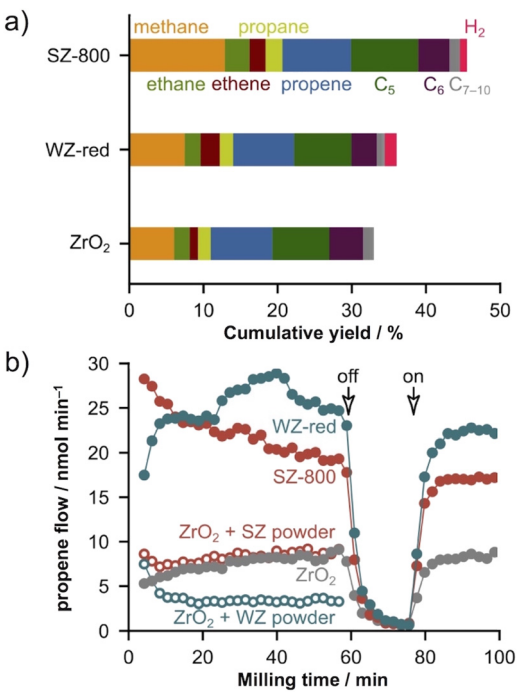

Fig. 12 (a) Cumulative yields after milling model PP for 1 h at 35 Hz with sulfated (SZ), tungstated (WZ) and non-treated ZrO_2 balls. (b) Propene flow during milling model PP with ZrO_2 or SZ and WZ-modified ceramic balls or powders at 30 Hz. When milling was stopped (off), the propene flow immediately dropped. The yield increased again when milling was resumed (on). Reprinted with permission from A. H. Hergesell, R. J. Baarslag, C. L. Seitzinger, R. Meena, P. Schara, Ž. Tomović, G. Li, B. M. Weckhuysen, I. Vollmer, Surface-Activated Mechano-Catalysis for Ambient Conversion of Plastic Waste, *J. Am. Chem. Soc.*, 2024, **146**, 26139–26147. Copyright 2024, American Chemical Society.[70]

powder form gave lower yields, implying that the high concentration of catalytic sites at the impact zone between the balls and PP substrate facilitates more efficient transfer of mechanical energy. When the ball milling was stopped, the yield of propene monomer immediately dropped and was only restored when the mill operation was resumed (Fig. 12b). The authors also showed that other types of plastics, such as high molecular weight PP, waste PP, PE and PS could be subjected to the SAM process. An important observation was that prolonged milling led to a decrease in depolymerization yields due to the destruction of the catalytically active surface layer of SZ- or WZ-modified ceramic balls. As in previous mechanistic considerations, the mechanochemical ball milling-induced homolytic chain scission to generate mechanoradicals was proposed as the initial step. These carbon-centred radical intermediates were observed by electron spin resonance (ESR) with nitrosobenzene and trapped with a radical scavenger, which completely quenched the propene monomer formation. The mechanocatalytic activity of SZ and WZ ceramic balls was reflected in the stabilization of macroradicals through reversible formation of adducts with polymer chain ends, allowing for longer radical lifetimes and better control of their reactivity and selectivity.

Polystyrene. There has been an ongoing research on the effects of milling on the physical properties of poly(styrene) (PS) as a typical representative of vinyl polymers for many decades,[72,73] but intriguingly the investigations focusing on changes towards chemical recycling upon milling began only in 2021 when Balema *et al.* reported the first mechanochemical partial depolymerization of PS to its monomer styrene under ambient conditions in air.[74] The ball milling was performed using a mixer mill in hardened steel (HS), tungsten carbide (WC) or silicon nitride (Si_3N_4) media during 12 hours with BPR between 10/1 and 13/1 in an air or argon atmosphere. Molecular weights M_n and M_w were calculated from GPC measurements, and the progress of depolymerization was evaluated by ^{1}H NMR and thermogravimetric analysis (TGA). In the case of milling in WC and HS media, ^{1}H NMR suggested that the breakdown of commercial PS to monomer was more efficient in WC as judged by a higher intensity of the vinyl protons in styrene. For experiments in HS, TGA showed *ca.* 8% weight loss below 170 °C, corresponding to a volatile monomer, while GC-MS analysis of the methanol extract of milled powder confirmed the formation of styrene in *ca.* 7 wt%. When ball milling was carried out in HS in an argon atmosphere, only traces of styrene monomer were detected. Furthermore, significant reduction in M_n and M_w values with respect to initial PS sample clearly revealed that mechanochemical ball milling caused scission of polymer chains and at least some degree of depolymerization through cleavage of C–C bonds in the polymer backbone. Similarly to chain scission in PET powder under ball milling in stainless steel that resulted in the formation of macroradicals,[35] the authors postulated the same type of reactivity in this case. Electron paramagnetic resonance (EPR) spectroscopy confirmed the presence of radical species in the sample milled in HS under air at room temperature, with two signals corresponding to oxygen-centred and carbon-centred radicals. In the presence of water or when using metal-free media (Si_3N_4), the depolymerization pathway to styrene monomer was practically switched off, but still polymer chain scission occurred as evidenced by a decrease in M_n and M_w values. The contribution of the thermal decomposition mechanism was excluded by milling a 2 : 1 mixture of PS and ammonium carbonate ($(NH_4)_2CO_3$) for 12 hours in air. Since *ca.* 10% weight loss was found by TGA, it was evident that the temperature during such a long milling did not exceed 60 °C, a limit at which $(NH_4)_2CO_3$ thermally decomposes into NH_3, CO_2 and H_2O. However, the small amount of water that was released was enough to prevent depolymerization and the formation of styrene monomer during milling. Based on these observations, the authors proposed a possible reaction mechanism (Scheme 7). In the first step, mechanochemical ball milling induces chain scission of PS molecules and generates carbon-centred macroradicals. These free radicals can react with oxygen from the air to form oxygen-centred radicals and peroxide intermediates. Collisions with metal balls and jar walls facilitate interactions of peroxide species with metal particles, which can coordinate to the polymer backbone and further catalyze the depolymerization reaction to styrene. If oxygen is not present, carbon-centred radicals can undergo recombination and chain termination, resulting in a reduction in the average molecular weight without the formation of any monomer.

Investigation of PS derivative poly(α-methylstyrene) (PMS) by Jung *et al.* provided more evidence for mechanochemically induced depolymerization.[75] It was shown by SEC analysis that ball milling PMS on a small scale (3 mg) with two 7 mm stainless steel balls in a 5 mL jar at 30 Hz decreased the M_n value from 137 kDa to 3.2 kDa after only 8 minutes. In parallel, ^{1}H NMR revealed 55% of the monomer α-methylstyrene (MS) present in the crude mixture, accompanied by *ca.* 1% of acetophenone as the oxygenated side product (Fig. 13a).

By changing the sample mass (*i.e.* BPR), it was observed that M_n decreased at a higher BPR and increased with the

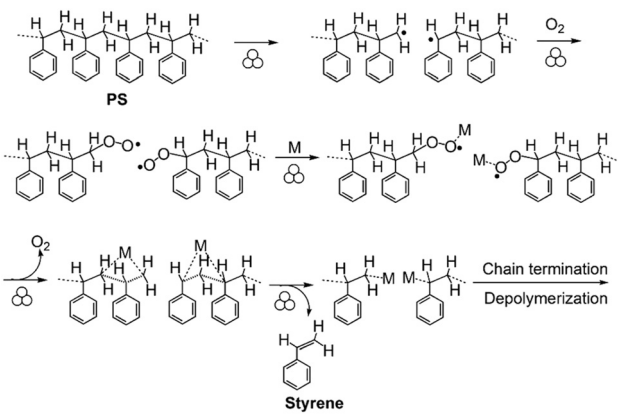

Scheme 7 Proposed mechanism of ball milling-promoted depolymerization of polystyrene.[74]

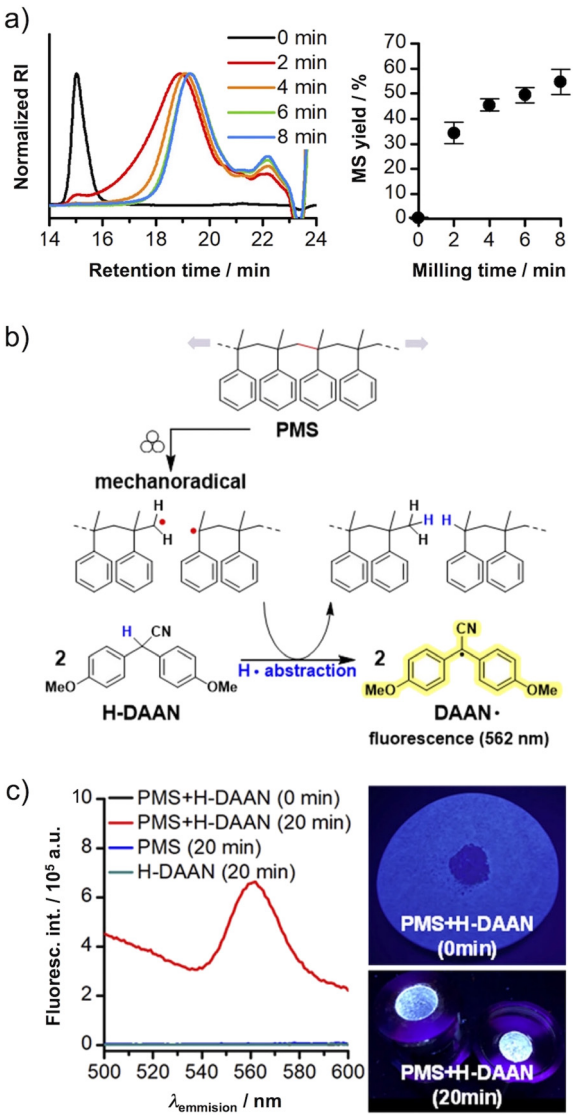

Fig. 13 (a) SEC traces showing a shift in the elution time due to a decrease in M_n value (left) and the yield of α-methylstyrene with milling time (right). (b) Formation of mechanoradicals from PMS under ball milling and their trapping with the H-DAAN probe. (c) Fluorescence spectra before and after milling PMS in the presence of the H-DAAN probe (left) and the reaction mixture in the jar under 365 nm UV light. Adapted with permission from E. Jung, D. Yim, H. Kim, G. I. Peterson and T. L. Choi, Depolymerization of poly(α-methyl styrene) with ball-mill grinding, *J. Polym. Sci.*, 2023, **61**, 553–560.[75]

sample size, but the MS recovery was found to be optimal at around 3 mg of PMS. Experiments at −10 °C and 48 °C produced MS in 39% and 64%, respectively. At a lower milling frequency, the rate of depolymerization was slow with MS yields of 4% (10 Hz) and 28% (20 Hz) after 8 minutes. Lower mechanical energy input also affected the extent of chain scission as M_n values of 23.5 kDa (10 Hz) and 4.4 kDa (20 Hz) indicated. Interestingly, when milling of PMS was carried out in an argon atmosphere, 60% of the monomer was detected with similar molecular weight distribution as in air, which is opposite to what Balema reported for PS depolymerization.[74] Moreover, the oxygenated acetophenone side product was not observed. The authors concluded that PMS depolymerization was initiated by mechanochemical homolytic polymer chain scission to form macroradicals, which in turn decomposed to MS monomer by a free radical mechanism (Fig. 13b). To support the hypothesis, macroradicals formed during ball milling were trapped with diarylacetonitrile-based fluorescent probe H-DAAN, which was shown to be an efficient radical scavenger for fluorescence detection of mechanochemically generated radical species.[76] Characteristic fluorescence under UV light (λ_{ex} = 365 nm) and coloration of the air-stable DAAN$^{\bullet}$ radicals was observed when PMS and H-DAAN were ball milled for 20 minutes. However, the fluorescence emission was not detected in the PMS/H–DAAN mixture before milling or when pure reagents alone were treated (Fig. 13c). Importantly, the yield of MS monomer in the presence of H-DAAN was reduced from 55% to 44% after 8 minutes of milling due to trapping of macroradicals, further supporting the homolytic chain scission mechanism. The authors also performed reactions with PS and PMMA and demonstrated that higher ceiling temperature T_c (the temperature at which the rates of polymerization and depolymerization are equal) lowered the rate of mechanochemical depolymerization.

Kinetic aspects of PS depolymerization were studied in detail by Sievers *et al.*[77] In their extensive research, the findings support the PS depolymerization model proposed by Balema *et al.*[74] and also account for the reactivity of PMS established by Jung *et al.*[75] The reduction of polymer M_n and M_w values and depolymerization are recognized as distinct processes under ball milling conditions. Mechanochemically induced chain scission by homolytic bond cleavage generates primary carbon-centred macroradicals, which may undergo a plethora of radical reactions that eventually lead to microcracks and fracturing of polymer particles. At this point, the decrease in molecular weight levels off as the minimum particle size is reached under specific milling conditions. Further mechanisms like depropagation from chain end radicals explain the formation of styrene or α-methylstyrene even under an inert atmosphere, whereas hydrogen atom abstraction, hydrogen shift and branching by repropagation lead to other hydrocarbon species detected by GC-MS. The presence of air (oxygen) promotes the formation of peroxyl radicals, which abstract a hydrogen atom, release hydroxyl radicals and generate polymer chain-end oxy radicals as the site of depropagation. With respect to PMS depolymerization that proceeded efficiently even in the absence of oxygen, the more stable and sterically hindered secondary radical derived from α-methylstyrene and a much lower T_c value of PMS (61 °C) allow mechanochemical depolymerization to occur. With PMMA or PS polymers, the thermodynamically favoured process is polymerization due to high T_c (220 °C and 310 °C for pure monomers, respectively) and fast recombination of primary macroradicals prevails. The role of peroxy radicals is therefore stabilization of reactive carbon-centred radicals, allowing the depolymerization of PMMA and PS by ball milling

even at ambient temperatures. Iron and chromium metals from the milling media contribute to the activation of the depolymerizaton pathway; however, the effect of Fe is more pronounced since Cr forms a passivating oxide layer in an air atmosphere.

Golder *et al.* explored a different route to valorize waste PS material by utilizing the LAG methodology.[78] Instead of depolymerization to styrene or functionalization of chemically reactive groups already present in the aromatic part of PS such as 4-carboxaldehyde[79] or 4-chloromethyl,[80] the post-polymerization modification (PPM) of the aromatic rings on the polymer backbone by a direct C–H functionalization reaction enabled the upcycling of several types of post-consumer wastes such as expanded PS foam (EPS), dyed PS coffee cup lid and commercial PS granules into potentially useful materials with a higher economic value. The electrophilic trifluoromethylation reaction that introduces fluorine functionality into the aromatic rings was selected to prepare PS grafted with CF_3 groups (TFM-PS) (Fig. 14a). However, since vinyl polymers have been shown to undergo both chain scission and depolymerization under ball milling conditions, the reaction time required to introduce functionalities on the polymer backbone by PPM may lead to undesired reduction of M_n and M_w values at the expense of losing targeted physical properties. In addition, the degradation process is faster for high molecular mass polymers and is also linearly correlated with the polymer glass transition temperature T_g.[51] The authors hypothesized that the addition of liquid during LAG could produce a plasticizing effect on the polymer by decreasing the T_g values, thus enhancing the rate of PPM over chain scission induced by ball milling. Standard reaction conditions included a 5 mL stainless steel jar with two 8 mm balls containing PS substrate (0.81 mmol), fluorination reagent $TMSCF_3$ (10 mol%), AgOTf (40 mol%), KF (40 mol%) and 1,2-dichloroethane (DCE) for LAG (η = 0.2 μL mg^{-1}). All reactants except for PS were added in a glovebox before the jar was sealed under nitrogen and milled for 4 hours at 30 Hz. The progress of the PPM reactions was conveniently followed by ^{19}F NMR using 4,4′-difluorobenzophenone as an internal standard, while molecular weights were retrieved from the GPC data. The optimization of reaction conditions on a model low molecular mass PS derivative (~9.0 kDa) revealed that a larger jar (25 mL) or more balls (3 or 4) reduced the CF_3-functionalization density from 1.2 to 0.76 mol%. With a higher molecular mass PS sample (~26.0 kDa), LAG screening showed that DCE at 0.2 μL mg^{-1} resulted in more chain scission and best CF_3 density (1.3 mol%) but the increase in η value had a positive impact on M_n by lowering T_g and suppressing the polymer backbone degradation in LAG-treated PS. Finally, commercial and post-consumer high-molecular-weight PS samples (113–132 kDa) were grafted with CF_3 groups under LAG conditions (0.8–1.0 μL mg^{-1}) in the presence of dioctyl terephthalate plasticizer (DOTP, 2 wt%) to keep the extent of polymer scission as low as possible, achieving functionalization densities in TFM-PS from 0.60 to 1.0 mol% (Fig. 14b).

In the most recent contribution by Kim *et al.*, the PPM ball milling approach to functionalize PS derivatives was extended to the Birch reduction reaction, which gave access to diene-containing PS.[81] In contrast to conventional solution reactions, the mechanochemical Birch reduction with lithium electride generated from ethylenediamine (EDA) in tetrahydrofuran (THF) proceeded efficiently with high PS conversion and diene yield, keeping the rates of polymer degradation *via* chain scission and cross-linking at low levels. Another advantage was that the reactions were simply conducted in air, thus avoiding air- and moisture-sensitive techniques typically involved when working with reactive metal species. Optimization and substrate scope screening experiments were conducted on a 20 mg scale in 10 mL SS jars using a single 10 mm SS ball at a ball milling frequency of 30 Hz. The Birch reduction was fast and in most cases required only 1 minute of milling (Scheme 8a). The initial experiments were done on a PS standard sample with an M_n value of 28.7 kDa and low dispersity ($Đ$ = 1.06), while ^{1}H NMR spectroscopy was used to determine the PS conversion, total diene content and diene ratio in the products, as well as the amount of monoene derivatives present due to over-reduction. While the reaction with 2.5 eq. of Li, 5 eq. of EDA and 1.5 eq. of *tert*-butanol (*t*-BuOH) as the proton source gave only 1.6% conversion in the absence of THF, the addition of 10 eq. of THF increased the conversion to 47% and total diene content to 43%. With more Li (10 eq.), EDA (12 eq.), THF (15 eq.) and *t*-BuOH (2 eq.), excellent 90% PS conversion was achieved, the amount of diene was only 68% and the monoene content increased to 21%. However, without *t*-BuOH, the conversion was even higher (96%) with better diene (81%) and lower monoene content (15%). This modification also improved the diene ratio to 12 : 1 in favor of the 1,4-diene ("skipped") *vs.* 1,3-diene ("conjugated"). The authors also tested other metals in the Birch reduction, *e.g.* sodium, calcium and magnesium, but Li showed the best performance.

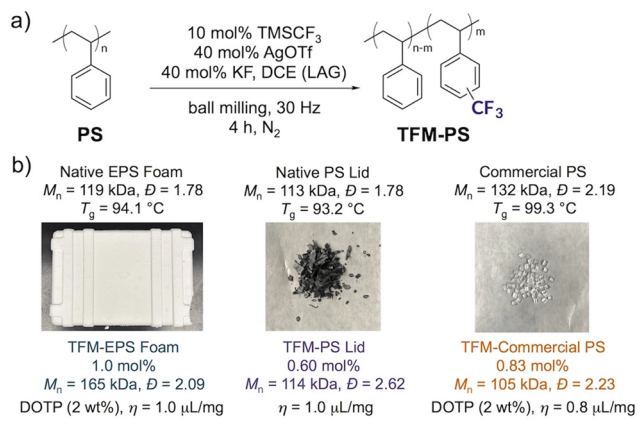

Fig. 14 (a) Electrophilic trifluoromethylation strategy for grafting polystyrene by ball milling. (b) Examples of post-consumer and commercial polystyrene samples functionalized with CF_3 groups under LAG conditions and in the presence of DOTP plasticizer. Adapted with permission from M. E. Skala, S. M. Zeitler and M. R. Golder, Liquid-assisted grinding enables a direct mechanochemical functionalization of polystyrene waste, *Chem. Sci.*, 2024, **15**, 10900–10907.[78]

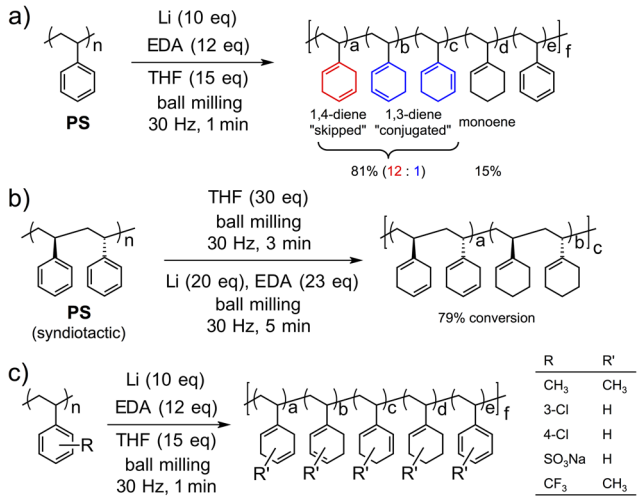

Scheme 8 (a) The mechanochemical Birch reduction of polystyrene using the Li/EDA system. (b) The Birch reduction of syndiotactic polystyrene. (c) Substrate scope of the Birch reduction by ball milling.[81]

The optimized Birch reduction of the standard PS sample led to only 3% of intermolecular cross-linking and minimal intramolecular linkage, with an M_n value of 28.3 kDa for the diene-functionalized PS, which was attributed to a very short reaction time and the presence of liquid reagents that lowered T_g through plasticizing effects, as earlier reported by Golder.[78] The addition of 1 or 2 eq. of water as the proton source only slightly lowered the conversion to 87–90%, revealing that adventitious water during open air manipulation was actually responsible for the high efficiency when *t*-BuOH was left out. Finally, the Birch reduction at 0 or 10 Hz milling frequency did not work at all with large pieces of unreacted Li metal still present in the jar. Since the reaction proceeded to 79% PS conversion at 20 Hz, it was obvious that mechanical treatment and mixing during ball milling played a crucial role in dissolving the Li metal and *in situ* generation of Li electride necessary for the arene reduction.

Except for low-molecular weight PS, samples with M_n of 115 kDa and 505 kDa were also tested and shown to react in a similar fashion. The problem of insolubility of syndiotactic PS in electrochemical Birch reduction was successfully overcome by ball milling, which provided the product in 79% conversion and a diene content of 59% after 5 minutes. Here, a short 3 minute pre-milling step was necessary to solubilize the substrate in THF before the Birch reduction occurred (Scheme 8b). 4-Methyl substituted PS and PMS underwent the Birch reduction in 92% and 77%, respectively. Furthermore, 3-chloro and 4-chloro-substituted PS led to simultaneous reduction and dechlorination reactions in an overall 96% conversion with 78% diene content and 1,4-diene as the major isomer. Similarly, polystyrene sodium sulfonate reacted smoothly in 89% conversion to afford 80% diene accompanied by desulfonation, while 4-trifluoromethyl substituted PS derivative gave dearomatized and defluorinated products (81% conversion with 1/1 ratio of 1,4- *vs.* 1,3-diene) (Scheme 8c).

When this mechanochemical strategy was applied to PS waste, *e.g.* clear, white and black coffee cup lids and an expanded PS foam food tray, conversion rates of 79%–94% were achieved on a 1.0 gram scale after 2 minutes of milling, whereby the amount of EDA was adjusted to 8 eq. with *t*-BuOH as the proton source (2 eq.). This modification was necessary to keep the level of monoene side product low and to improve the diene ratio in favor of the 1,4-isomer.

Mechanochemical grafting procedure to prepare polymer-functionalized graphene nanocomposites from graphite and polystyrene was employed by Chen and coworkers (Scheme 9).[82] A graphite suspension in the PS solution was subjected to a wet mechanochemical reaction in a vertically stirred mill at room temperature, using less common zirconia/yttria milling beads. In the process, graphite was exfoliated and subsequently reacted with *in situ* formed macroradicals, providing PS chains grafted onto graphene sheets. The composite obtained by this method exhibited improved electrical properties in comparison to graphene or carbon black. In a similar fashion, polyvinylpyrrolidone polymer (PVP) was grafted on graphene by the same group.[83]

More recently, Kubota, Ito *et al.* have developed direct introduction of a luminophore into polymers by applying mechanical milling (Scheme 10).[84] In addition to PS and PMMA, polyphenylene sulfide (PPS), polyethylene (PE), and polysulfone (PSF) were functionalized. A stainless steel milling vessel was used and coumarin-based luminophore was incorporated by short milling. A higher ball-milling frequency (15–30 Hz) resulted in lower M_n and better incorporation of the luminophore molecule, suggesting that a higher mechanical impact can generate more mechanoradicals, which are essential in the mechanochemical coupling of polymers with luminophores. The described PS upcycling procedure was simple and did not require a mechanophore or any sophisticated synthesis steps.

Polymethacrylates. A previous study on PMS reactivity under ball milling conditions has also included PMMA, where only 4% depolymerization was observed due to high T_c (220 °C for pure monomer methyl methacrylate, MMA).[75] In addition, it was shown in earlier works that ball milling of PMMA led to

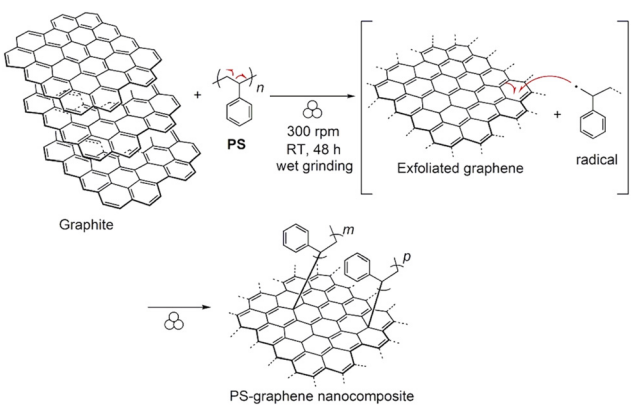

Scheme 9 Mechanochemical grafting of polystyrene with graphene by wet ball milling.[82]

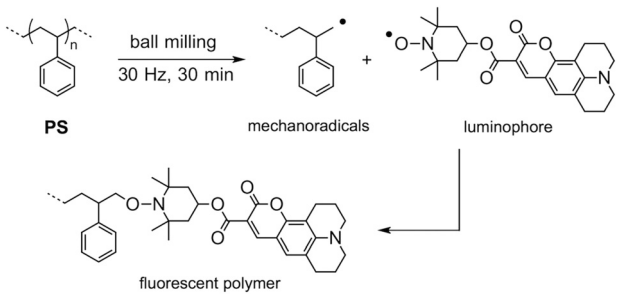

Scheme 10 Ball milling functionalization of PS with a luminophore molecule enabled by mechanochemically generated macroradicals.[84]

chain scission and formation of macroradicals until a limiting molecular weight was reached, usually in the range of 5–6 kDa and without depolymerization.[85,86] In continuation of the research on mechanochemical recycling of addition polymers, Jung *et al.* went on to explore the potential of ball milling to increase the depolymerization yield for a series of polymethacrylates as challenging targets (Scheme 11).[87] In their approach, the authors resorted to a combination of milling and heating to 43 °C where polymethacrylate samples in the form of a slurry were broken down to monomers in *ca*. 20%–40% depolymerization conversion. Initial screening tests were performed in a 5 mL SS jar with two 7 mm balls on PMMA samples (3 mg scale, M_n = 73 kDa), ball milled at 30 Hz for 8 minutes. The reactivity at room temperature was poor with only 2.6% conversion, while gentle heating to 43 °C increased it to *ca*. 8%. LAG using ethylacetate (η = 1 μL mg^{-1}) did not improve the yield; however, a larger volume of the solvent under slurry conditions (η = 3.3 μL mg^{-1}) increased the conversion to *ca*. 14%, presumably due to lower T_c in a more dilute environment. By switching to fifteen 5 mm balls, the depolymerization conversion increased significantly to 33.3% and using *t*-BuOH instead of ethylacetate gave 35.1% after 8 minutes of ball milling. Prolonging the milling time to 20 minutes with high-molecular-weight PMMA (M_n = 148 kDa) further improved the conversion to 41.1%. The authors noted that the residual polymer had M_n of 1.0 kDa, which was substantially lower than previously reported values of the limiting molecular weight.

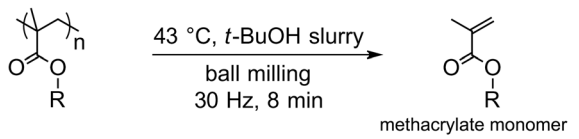

PMMA (R = methyl)	35.1%
PEMA (R = ethyl)	32.6%
PnBMA (R = *n*-butyl)	22.5%
PBnMA (R = benzyl)	19.7%
PPhMA (R = phenyl)	22.5%
PiPMA (R = *i*-propyl)	38.9%

Scheme 11 Mechanochemical depolymerization of different polymethacrylate derivatives under slurry conditions in *tert*-butanol with gentle heating at 43 °C.[87]

When the depolymerization was conducted on a 100 mg scale in a 10 mL SS jar with two 10 mm balls for 60 minutes, the 121 kDa PMMA sample underwent 16.8% conversion. The depolymerization equilibrium where a high T_c value for PMMA limits the extent of the MMA monomer production could be shifted to the product side by removing the monomer from the reaction mixture. Indeed, when ball milling was carried out at 2 minute intervals up to 30 minutes of total milling time, with intermittent heating of the opened jar content at 95 °C for 5 minutes to allow the MMA monomer to evaporate, the depolymerization yield was 26.4%. The authors also investigated mechanochemical depolymerization of other polymethacrylates, *e.g.* poly(ethyl methacrylate) (PEMA), poly(*n*-butyl methacrylate) (PnBMA), poly(benzyl methacrylate) (PBnMA), poly(phenyl methacrylate) (PPhMA) and poly(i-propyl methacrylate) (PiPMA). For example, milling PiPMA and PEMA under slurry conditions resulted in 38.9% and 32.6% conversion, respectively. Other polymethacrylates with sterically more demanding substituents reacted with *ca*. 20% depolymerization yield alongside the formation of side products. Interestingly, the observed reactivity trend in slurry experiments (PiPMA > PMMA > PEMA > PPhMA ≈ PnBMA > PBnMA) was opposite to the solvent-free analogues. Similarly to PS depolymerization by ball milling reported by Balema,[74] the reactivity of PMMA in an argon atmosphere was drastically reduced with only 4.7% conversion, suggesting that oxygen plays an important role in the PMMA depolymerization mechanism through the formation of peroxy radicals.

Polyvinyl chloride. Alongside PE and PP, PVC occupies the third place in the market share of industrial production of thermoplastic synthetic polymers. It is predominantly used in the construction sector, production of pipes and tubings, flexible films and sheets, as well as in packaging, automotive, medical devices *etc*. Waste PVC is mainly landfilled or incinerated, which has become an environmental issue due to toxic degradation products like HCl and dioxins arising from the thermal decomposition.[88] In general, the dehalogenation of materials such as persistent organic pollutants and halogen-containing polymers has been successfully targeted by mechanochemistry.[89] High-energy ball milling of such substrates provides an environment where several reaction pathways are operational following the initial dehalogenation step and formation of radicals. These reactions include dehydrogenation, hydrogenation, oligomerization, fragmentation and graphitization, yielding a mixture of amorphous and graphitic carbon or alkene residues as the products, rather than ending up with the corresponding halogenated vinyl monomer.[90] For example, mechanochemical dechlorination of waste PVC as an environmentally friendly alternative has been recently reviewed by Saito *et al.* listing various approaches to PVC treatment.[91] The same group investigated ball milling for waste PVC remediation and subjected equimolar amounts of PVC and calcium oxide (CaO) to planetary mill conditions in a 50 mL jar with seven 15 mm stainless steel balls at a rotational speed of 700 rpm for 5 hours and cooling intervals every 15 minutes (Scheme 12).[92]

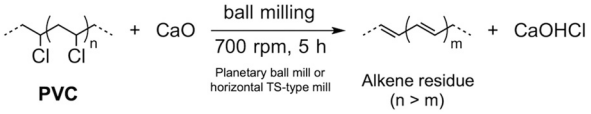

Scheme 12 Dechlorination of PVC under ball milling conditions using calcium oxide.[92]

The mechanochemical treatment decreased the degree of polymerization from 10 000 repeating units in the starting polymer to 800 after 8 hours of milling. The dechlorination rate increased with the addition of CaO excess (1 : 4) and reached 90% after 1.5 hours of reaction. FTIR analysis indicated the formation of C=C bonds in the residue, while PXRD revealed the formation of the CaOHCl phase in the crude mixture after 3.5 hours.

A detailed study of the effects of various inorganic powder additives (CaO, $CaCO_3$, SiO_2, Al_2O_3 or slag) in a planetary mill on the waste PVC dechlorination identified CaO, SiO_2, and Al_2O_3 as the most effective ones.[93] In a subsequent paper, Saito added quartz powder to the PVC–CaO mixture as the grinding aid to initiate the mechanochemical reaction and found that the rate of mechanochemical PVC dechlorination could be improved with the increase in the mill speed and the number of balls introduced into the mill.[94] Furthermore, co-grinding with various metal oxides (CaO, Fe_2O_3, SiO_2 and Al_2O_3) was carried out to show that CaO and Fe_2O_3 yielded the respective chlorides CaOHCl and $FeCl_3{\cdot}2H_2O$, whereas SiO_2 and Al_2O_3 caused the release of HCl gas.[95] Grinding PVC with La_2O_3 additive indicated that lanthanum oxide was a more effective additive than CaO in the decomposition of PVC, which led to the formation of C–O bonds in the milling residue. However, the insolubility of LaOCl in water was the reason why the chloride yield was poor at <50%.[96] The presence of polymeric impurities in PVC samples was shown to inhibit the dechlorination of PVC with NaOH in a planetary mill.[97] Eco-friendly hydrated and dehydrated calcium sulfates ($CaSO_4{\cdot}2H_2O$ and $CaSO_4$) were also used in the mechanochemical dechlorination of PVC, leading to dechlorinated hydrocarbons with C=C bonds in the residue and calcium chloride ($CaCl_2$) as the water-soluble chloride product. Within 4 hours of ball milling, 95% of the chlorine content was removed from PVC when unhydrated calcium sulfate was applied, whereas hydrated $CaSO_4$ was much less efficient.[98] The same group also reported that calcium carbonate additive can be effectively replaced by oyster-shell waste for the mechanochemical dechlorination of PVC.[99] Grinding of the PVC and oyster-shell mixture (with molar ratios PVC : oyster-shell = 1 : 4) in a planetary ball mill at 700 rpm, which provided the best results, was carried out for 4 hours. The PXRD and FTIR analyses showed that the complete extraction of chlorine was achieved. This milling procedure produced $CaCl_2$ and alkene-containing hydrocarbons, which could be used as fuel/energy sources. By using oyster-shell waste as a renewable source of $CaCO_3$, the environmental issues of two waste materials were addressed.

Chow *et al.* carried out solid-state ball milling of waste PVC with a slight excess of potassium permanganate ($KMnO_4$) to completely decompose the polymer by an oxidation process.[100] In a typical experiment, a mixture of PVC (0.5 g) and $KMnO_4$ (1.2 eq.) was loaded to a hardened steel jar with balls of different sizes (3, 5 and 10 mm), keeping the BPR value at 55 : 1. The jar was evacuated and milling was performed at 800 rpm for 12 to 48 hours. Gas-phase composition was analyzed by GC, which showed that gasification products included carbon monoxide as the major component, followed by hydrogen gas and a small amount of methane. A large proportion of the initial carbon content in PVC was transformed into carbonate salts, and all of the chlorine ended up in the form of chloride anions (Scheme 13). The black solid residue was also made up of manganese oxide (MnO_2) and organic polymers with C=C, C=O and O–H functionalities, as evidenced by FTIR analysis. A plausible reaction mechanism was proposed based on the experimental results and DFT calculations. The HAT reactions from the polymer backbone to $KMnO_4$ with the generation of diradical species that recombine to alkene units were postulated as the driving force for polymer decomposition. Polyethylene and polypropylene plastic wastes were gasified in the same manner.

The power of mechanochemistry for the degradation of PVC into biodegradable low-molecular-weight fragments has been recently described by the Kim group.[101] In their elegant approach, the dechlorinated alkene residues formed by ball milling PVC with 1,8-diazabicyclo[5.4.0]undec-7-ene (DBU) base were subjected to an epoxidation reaction with *m*-chloroperoxybenzoic acid (*m*-CPBA). The resulting epoxides underwent nucleophilic addition and ring-opening reactions followed by hydrolysis of the formed esters and acetals to yield water-soluble oligomers functionalized with carbonyl and hydroxyl groups. The strategy is based on the fact that three-membered oxirane rings, installed in the polymer backbone using *m*-CPBA, act as mechanophore units and produce carbonyl ylide intermediates by a force-induced heterolytic ring-opening reaction. The ylide intermediates are the sites where nucleophiles can attack the polymer backbone to generate acetals. Under basic conditions, these acetals are hydrolysed into aldehydes and alcohols with concomitant chain scission. In this way, the original chlorinated polymer chain in PVC is

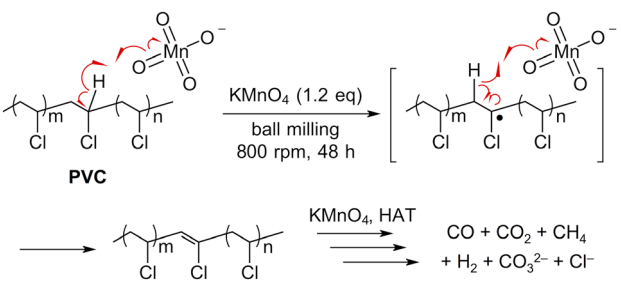

Scheme 13 Proposed mechanism for the potassium permanganate-promoted oxidation of waste PVC and its transformation to gaseous products.[100]

transformed into small fragments with hydroxyl and carbonyl groups attached.

The optimized process was envisaged as a step-wise mechanochemical transformation starting from a mixture of PVC (0.5 g scale, M_n = 70.7 kDa) and DBU (1.0 eq.), ball milled in a mixer mill in a 25 mL SS jar with three 12 mm SS balls at 30 Hz for 3 hours. The dark brown dechlorinated PVC product (DC-PVC) was isolated in 86% yield after washing with water and methanol. FTIR-ATR and cross-polarization magic angle spinning (CP-MAS) ^{13}C NMR analyses revealed almost complete dehlorination of PVC, as well as the presence of alkene residues and hydroxyl groups. The authors hypothesized that the –OH groups were formed due to reaction with adventitious water since PVC is a hydroscopic polymer. The epoxidation reaction with *m*-CPBA (1.0 eq.) was the next step, carried out with 200 mg of DC-PVC under the same milling conditions as in the dechlorination step (25 mL jar, 3 × 12 mm balls, 3 hours at 30 Hz) (Scheme 14a). The off-white epoxidized PVC product (EP-PVC) was isolated in 83%. Again, FTIR-ATR and CP-MAS ^{13}C NMR showed that the epoxidation of alkene moieties on the polymer backbone to oxirane occurred, alongside ester and hydroxyl group formation as a result of nucleophilic attack of *m*-chlorobenzoic acid (from *m*-CPBA) and oxirane ring-opening reaction (Scheme 14b). This also led to a slight increase in chlorine content from 1.2% in DC-PVC to 1.8% in EP-PVC due to the incorporation of the *m*-chlorobenzoyl group.

In the last step, a hydrolysis reaction in NaOH solution (1 mol dm^{-3}) for 30 minutes was performed on EP-PVC (0.5 g scale). Following the removal of excess NaOH by dialysis and lyophilization, a light brown hydrolyzed PVC (HY-PVC) was isolated in 80% yield (Scheme 14c). Most notably, FTIR-ATR confirmed the cleavage of ester groups and GPC analysis showed that HY-PVC had an M_n value of 4.1 kDa, which is 17 times less than that of the initial PVC sample. However, a PVC sample epoxidized with *m*-CPBA in a methanol solution was hydrolyzed under the same conditions and resulted in water-insoluble products. This discrepancy between ball mill- and solution-epoxidized PVC during hydrolysis was attributed to chain degradation at the acetal groups, which were only present in the mechanochemically treated sample. The acetal groups were generated by the nucleophilic addition of *m*-chlorobenzoic acid on carbonyl ylides, formed by the mechanochemical force-induced scission of the oxirane mechanophores (Scheme 14b). The formation of acetal groups was indirectly proven by ^{1}H NMR analysis of HY-PVC, where the characteristic peaks of the OH proton and vinylic protons of the enol form of aldehydes were identified, as the aldehyde functionality was expected in products. The authors also conducted cytotoxicity and phytotoxicity screening tests to demonstrate the biocompatibility of the water-soluble hydrolyzed PVC product, while the mechanochemical PVC dechlorination–epoxidation sequence was successfully applied to commercial materials such as hard PVC window frames or medium and soft PVC films.

Upcycling of waste PVC to porous carbon materials by ball milling was described in a paper by Wu *et al.*[102] Efficient dechlorination of PVC with potassium hydroxide and polyethylene glycol 800 (PEG-800) was carried out by ball milling in a zirconia jar and balls at ambient temperature and a speed of 900 rpm for 10 hours (Scheme 15). A high degree of dechlorination (94%) and simultaneous crosslinking was achieved in the dechlorinated PVC product (DPVC). In the following step, pore formation and carbonization were accomplished by mixing the dechlorinated product with an equal mass of K_2CO_3 and grinding in an agate mortar before carbonization at 700 °C –900 °C for 3 hours. The material obtained (C_{DPVC}) had a low degree of graphitization with micro- and mesoporosity developed, and this high-quality porous carbon material demonstrated exceptional electromagnetic wave absorption properties.

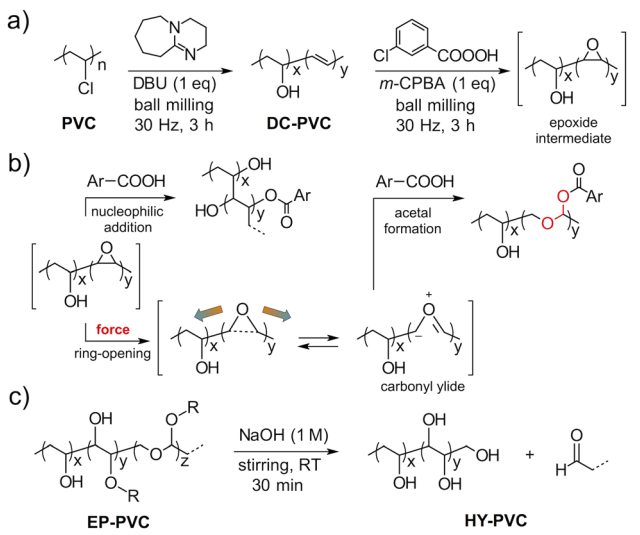

Scheme 14 (a) A mechanochemical PVC dechlorination/epoxidation sequence. (b) The epoxide intermediate undergoes simultaneous nucleophilic addition and force-induced ring-opening reactions with the formation of acetals. (c) Epoxidized product EP-PVC is hydrolyzed in a NaOH solution with the generation of water-soluble low-molecular-weight non-toxic products.[101]

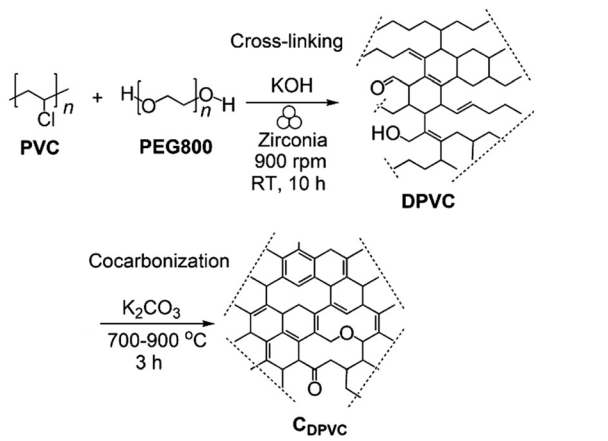

Scheme 15 Mechanochemical upcycling of waste PVC *via* KOH/PEG-800 promoted dechlorination and cocarbonization with K_2CO_3 at high temperatures.[102]

An interesting example of PVC modification by mechanochemistry for use as a carrier of azole-based drugs showing antifungal, antidiabetic and antiviral properties was published by Zyryanov *et al.* (Scheme 16).[103] The 2-mercaptobenzothiazole, 5-methyl-6-nitro-7-oxo-1,2,4-triazolo[1,5-*a*]pyrimidinide and 4-oxo-1,4-dihydropyrazolo[5,1-*c*]-1,2,4-triazine-3,8-dicarboxylic acid diethyl ester were grafted on PVC by reacting the sodium or potassium salts of these heterocycles under LAG conditions with DMF or cyclohexanone. For comparison, a solution reaction with 2-mercaptobenzothiazole and PVC was attempted, but required a longer reaction time and heating due to the low reactivity of heterocyclic salts.

Polyfluoroalkyl substances. Environmental and health concerns associated with per- and polyfluoroalkyl substances (PFAS) have been in the focus of worldwide media attention for many years. PFAS have been identified as persistent organic pollutants, also known in the popular culture as "forever chemicals". As such, their widespread use as water- and heat-resistant coatings in cookware, waterproof fabrics, personal care products, firefighting foam, food packaging and many others, has made modern life hard to imagine without PFAS. If a compound contains at least one fluorinated methylene (–CF_2–) or methyl group (–CF_3), it falls under the broad definition of PFAS.[104] PFAS are divided into non-polymers (*e.g.* perfluorooctanoic acid (PFOA), perfluorooctane sulfonate (PFOS), *etc.*) and polymeric compounds such as poly(tetrafluoro ethylene) (PTFE, Teflon), poly(vinylidene fluoride) (PVDF), ethylene tetrafluoroethylene (ETFE), fluorinated ethylene propylene (FEP) *etc.* (Scheme 17).[105] Intriguingly, while there is a body of research data on ball milling destruction of mostly non-polymeric PFAS molecules,[106–112] none have specifically focused on the chemical recycling of PFAS but instead looked into the potential of mechanochemistry for their environmental remediation. As such, we highlight here an intriguing example of a successful application of mechanochemical ball milling to cleave the "notorious" C–F bond and retrieve the fluoride content for PFAS upcycling to valuable fluorination reagents extensively used in the production of fluoroorganics.

Paton and Gouverneur have most recently described a mechanochemical strategy for upcycling of non-polymeric

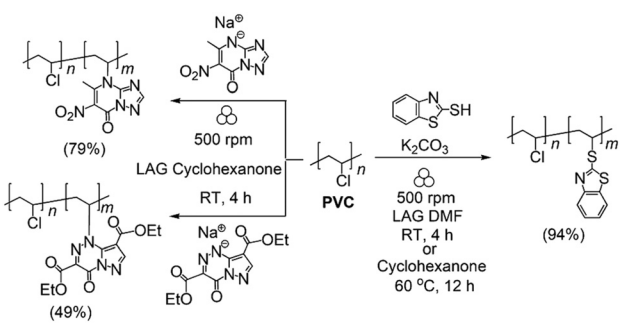

Scheme 16 Functionalization of waste PVC by grafting azole-containing drugs under LAG ball milling conditions.[103]

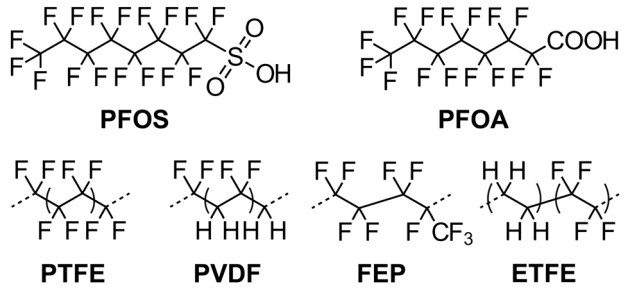

Scheme 17 Chemical structures of common non-polymeric and polymeric PFAS compounds.

PFAS and polyfluoroalkyl polymers to high-value fluorination reagents.[113] This interesting approach was based on the observation that ball milling calcium fluoride with dipotassium phosphate salt (K_2HPO_4) in stainless steel jars with PTFE seals gave higher yields of fluoride-containing salts, which implied that fluorine from PTFE leached into the product. When milling experiments were carried out in a mixer mill with a PTFE substrate and potassium phosphate (K_3PO_4, 1.25 eq. per F) in a 15 mL stainless steel jar with a rubber sealing ring and two hardened chrome steel balls (each 7 g) at 35 Hz, ^{19}F NMR spectroscopy revealed 99% fluorine recovery after 3 hours, distributed into fluoride (84%) and monofluorophosphate PO_3F^{2-} anions (15%). Interestingly, potassium pyrophosphate salt $K_4P_2O_7$ (0.625 eq. per F) reversed this distribution in favour of the PO_3F^{2-} form with outstanding 99% selectivity (Fig. 15, methods A and B, respectively).

Solution and solid-state NMR measurements indicated the presence of several forms of phosphorus (PO_4^{3-}, PO_3F^{2-},

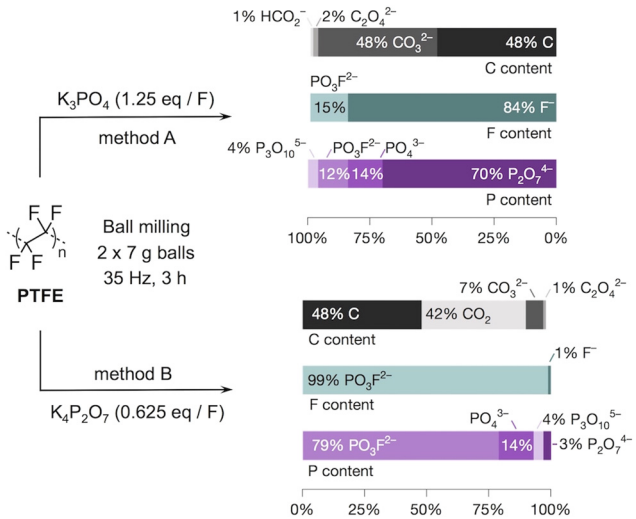

Fig. 15 The effect of K_3PO_4 and $K_4P_2O_7$ salts on the distribution of carbon, fluorine and phosphorus in the product after ball milling PTFE at 35 Hz for 3 hours. Adapted with permission from L. Yang, Z. Chen, C. A. Goult, T. Schlatzer, R. S. Paton and V. Gouverneur, Phosphate-enabled mechanochemical PFAS destruction for fluoride reuse, *Nature*, 2025, **640**, 100–106.[113]

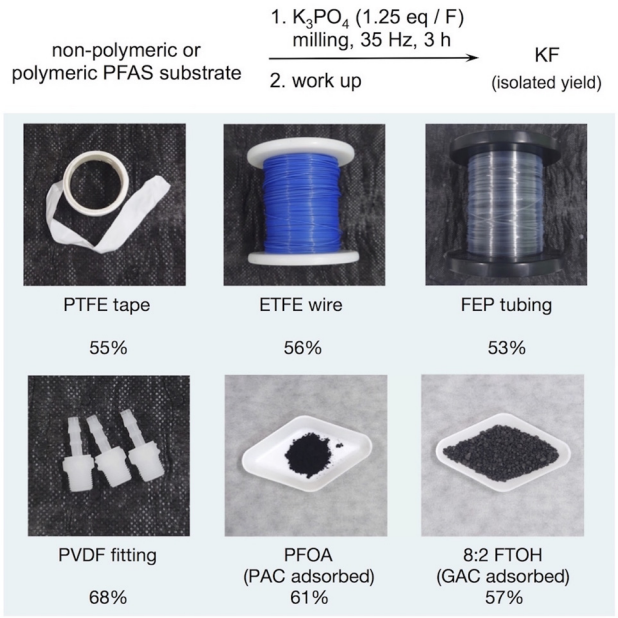

Fig. 16 Several examples of successful degradation of different commercial PFAS compounds by ball milling in the presence of K_3PO_4 salt (method A) after 3 hours. Adapted with permission from L. Yang, Z. Chen, C. A. Goult, T. Schlatzer, R. S. Paton and V. Gouverneur, Phosphate-enabled mechanochemical PFAS destruction for fluoride reuse, *Nature*, 2025, **640**, 100–106.[113]

$P_2O_7^{4-}$, and $P_3O_{10}^{5-}$) and carbon (CO_3^{2-} and $C_2O_4^{2-}$), while gas analysis showed CO_2 when $K_4P_2O_7$ salt was used. The remaining 48% of carbon content was traced down to graphitic-type residue. It was also found that water suppressed the PTFE degradation under these conditions. The methodology was tested on a number of long-chain non-polymeric and polymeric PFAS products such as PFOA, PFOS, Teflon seal and tape, FEP tubings and films, PVDF fittings and ETFE wires, perfluoroalkoxy alkane (PFA) tubing, poly(chlorotrifluoroethylene) (PCTFE), poly(vinylidene fluoride-*co*-hexafluoropropylene) (PVDF–HFP), polyvinyl fluoride (PVF) and ethylene-chlorotrifluoroethylene (ECTFE) films, with both methods performing successfully yielding high fluorine recovery (Fig. 16). Potassium fluoride could be isolated in 64% yield from a PTFE mix and utilized in the synthesis of several fluorochemicals. Similarly, PTFE degradation with $K_4P_2O_7$ salt, followed by reflux with tetramethyl- or tetrabutylammonium hydroxide/*tert*-butanol provided the corresponding tetramethylammonium fluoride (TMAF, 81%) and tetrabutylammonium fluoride (TBAF) complex with *t*-BuOH (50%). TMAF was quantitatively converted to its *tert*-amyl alcohol complex. The fluorination efficiency with reagents prepared in this way matched those obtained from conventional sources.

2.3. Mechanochemically assisted enzymatic depolymerization

The combination of mechanochemistry with enzymatic transformations, known as mechanoenzymatic reactions, has gained great interest in recent years.[114,115] All the above-mentioned benefits of mechanochemistry in combination with biocatalysts create a green paradigm for highly efficient enzyme catalysis in a non-conventional setting.[116] It is believed that conditions without bulk solvent, as in neat grinding or LAG, help enzymes perform better than in solution reactions by closely imitating their natural environment.[117] Hydrolases have mainly been used for mechanoenzymatic transformations, *e.g.* lipases, proteases, and glycosyl hydrolases, showing promising reaction rates, space-time-yields and conversions.[116,117] A further improvement in mechanoenzymatic transformations is achieved by conducting repeating cycles of ball milling and aging in the so-called RAging technique (**R**eactive milling + **Aging**).[118] Each milling cycle is followed by the incubation period for further enzymatic reaction (Fig. 17). In this way, the energy consumption associated with ball milling is reduced and the denaturation of the enzymes is also decreased. Friščić and Auclair introduced the RAging technique for the mechanoenzymatic hydrolysis of cellulose to glucose. The optimization of the RAging conditions to 12 cycles consisted of 5 minutes grinding followed by 55 minutes of aging at 55 °C with *Trichoderma longibrachiatum* cellulases (3% w/w), resulting in a conversion of 50% of the microcrystalline cellulose without chemical pretreatment yielding about three times more glucose (3.2 M) compared to conventional methods (0.9 M) and also producing valuable cellulose nanocrystals.[118]

The mechanoenzymatic reaction has also been successfully used for plastic depolymerization. Kaabel *et al.* used RAging for the depolymerization of commercially available PET powder of 36% crystallinity in the presence of *Humicola insolens* cutinase (HiC, Novozym 51032) (0.6 wt%).[37] Milling under LAG conditions (liquid-to-solid ratio η = 1.5 μL mg^{-1}, *i.e.*, 667 mg mL^{-1}) and aging the highly crystalline PET at 55 °C for 7 days resulted in 20% TPA, a 20-fold selectivity for TPA over MHET without detection of BHET compared to the conventional reaction in solution, which resulted in 10% yield with only 2.8-fold selectivity for TPA over MHET (Fig. 18). A further advantage of HiC-catalyzed depolymerization in a mechanoenzymatic reaction compared to the conventional reaction in solution was the ability of the cutinase to directly depolymerize

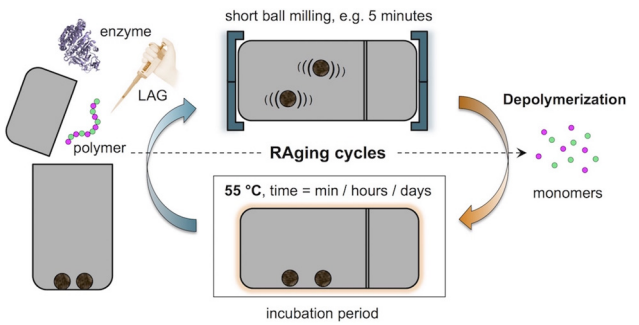

Fig. 17 Schematic representation of the RAging technique for the hydrolysis of biopolymers and synthetic polymers.[118]

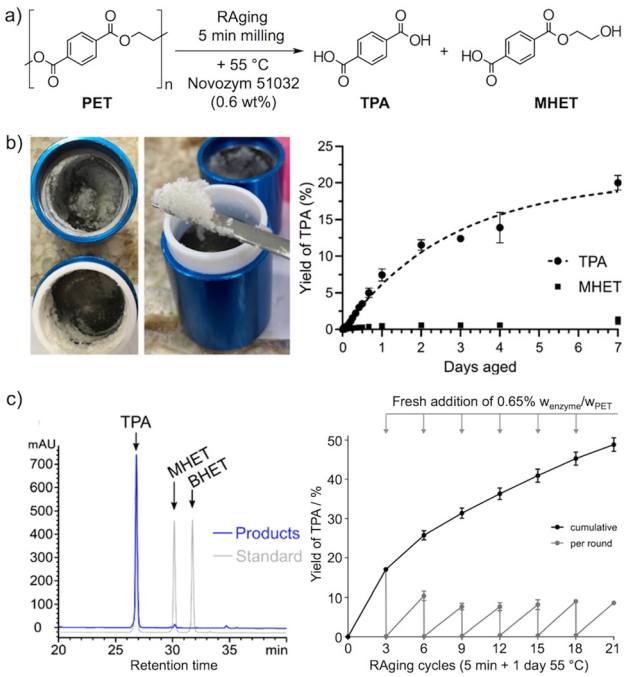

Fig. 18 (a) Mechanoenzymatic depolymerization of PET to TPA and MHET by RAging technique. (b) The appearance of the crude reaction mixture after 5 minutes of ball milling (left) and the cumulative yield of TPA and MHET after 7 days of RAging (right). (c) HPLC analysis of the crude reaction mixture (left) and per-round and cumulative TPA yields in multi-round RAging depolymerization of PET with the addition of fresh enzyme every 3 cycles for 7 rounds (right). Adapted with permission from S. Kaabel, J. P. D. Therien, C. E. Deschênes, D. Duncan, T. Friščić and K. Auclair, Enzymatic depolymerization of highly crystalline polyethylene terephthalate enabled in moist-solid reaction mixtures, *Proc. Natl. Acad. Sci. U. S. A.*, 2021, **118**, e2026452118.[37]

both amorphous and crystalline regions of PET, without pretreatment. The authors applied the optimized mechanoenzymatic reaction to other PET types (X_c = 30% to 35%, transparent, green, and light blue), powdered black post-consumer PET container (labeled as 80% recycled) and to PET with the addition of microcrystalline cellulose or PS, all of which provided TPA in *ca.* 15%. In addition, the same method also worked for other types of plastics such as PBT and PC. The yield of TPA monomers was slightly improved with three RAging cycles, consisting of 5 minute milling followed by a 24 hour aging at 55 °C. Under these conditions, the depolymerization of PET gave TPA in 25% yield. A mechanistic investigation led to the conclusion that a further improvement of reaction efficiency was not possible due to HiC denaturation. To avoid this, the enzyme was added in batches every three days for 7 rounds. After the first RAging cycle, which resulted in 17% TPA, each subsequent cycle resulted in about 10%, so that a total of almost 50% TPA was achieved with 3 wt% enzyme (Fig. 18c). The effectiveness of mechanoenzymatic hydrolysis of mixed PET/cotton textiles was also demonstrated by the same group.[119] Pre- and post-consumer PET and PET/cotton textiles with different ratios of PET and cotton (65%–100% PET, 0%–35% cotton) were depolymerized by simultaneous or sequential application of commercial HiC for PET hydrolysis and the Cellic CTec2® cellulases mixture for cotton hydrolysis. Under LAG reaction conditions using the multi-round RAging technique, the authors reported TPA yields up to 30% from the PET component and glucose yields up to 83% as a result of cellulose breakdown from the cotton fibers.

Hailes *et al.* next investigated the use of whole-cell PETase enzymes for the mechanoenzymatic hydrolysis of PET, where ball milling can open the cells *in situ*, avoiding the extraction and purification of the enzymes.[120] The authors first investigated the mechanoenzymatic hydrolysis of BHET as a model substrate with Is-PETase S238F/W159H, *Polyangium brachysporum* PETase (Pb-PETase), short *Burkholderiales bacterium* PETase (short Bb-PETase, subcloned gene with 141 aminoacid residues removed from the N-terminus) and PET2 from a non-cultured organism and compared it with the traditional solution reaction. In KPi buffer using lyophilized whole-cell PETase at 30 °C and pH 7.5, Is-PETase S238F/W159H showed the highest activity, followed by short Bb-PETase and Pb-PETase, while PET2 showed very low activity. MHET was the main product for all enzymes used. Eight RAging cycles of 20 minutes milling and 40 minutes aging showed the same trend for enzyme activity in the mechanoenzymatic reactions, but with a much lower level of BHET hydrolysis compared to the solution reactions due to denaturation of the enzymes. For the mechanoenzymatic hydrolysis of PET, different RAging cycles were also tested, consisting of 5, 10, 20 or 30 minutes of milling followed by 55, 50, 40 or 30 minutes of aging, each repeated 8 times using 200 mg of PET powder and 50 mg of lyophilized whole-cell PETase. The best degradation was again obtained with Is-PETase S238F/W159H, followed by Pb-PETase and short Bb-PETase, while PET2 showed no degradation. Here, TPA was the main product for all enzymes and also the only product when milled for 5 minutes and for all different RAging cycles when short Bb-PETase was used. When performing equivalent reactions in solution with both whole cell and lysate, no degradation of PET occurred, confirming the advantages of milling in the mechanoenzymatic hydrolysis of PET. The optimized mechanoenzymatic reaction was tested on other PET forms: PET film (0.25 mm thickness, X_c = 40%–60%), a sample of a postconsumer PET beverage bottle (0.15 mm thickness) and recycled PET (0.30 mm thickness) as well as the recycled PET fabric. In all cases, the mechanoenzymatic hydrolysis of PET to TPA was compatible with the tested PETases and resulted in higher efficiency than the reactions in solutions (Fig. 19).

In the context of mechanoenzymatic PET depolymerization and previous attempts at chemo-microbial polyester degradation,[121] Mellies and Loya performed an important study on the relationship between polymorphism and microbial degradation of BHET, as one of the PET degradation products.[122] BHET exists in four different polymorphs, of which only two, the α- and δ-forms, are stable in water and thus suitable for microbial degradation. The authors employed ball milling at 25 Hz in a mixer mill to selectively generate one of two forms of BHET and also reversibly interconvert them, starting from

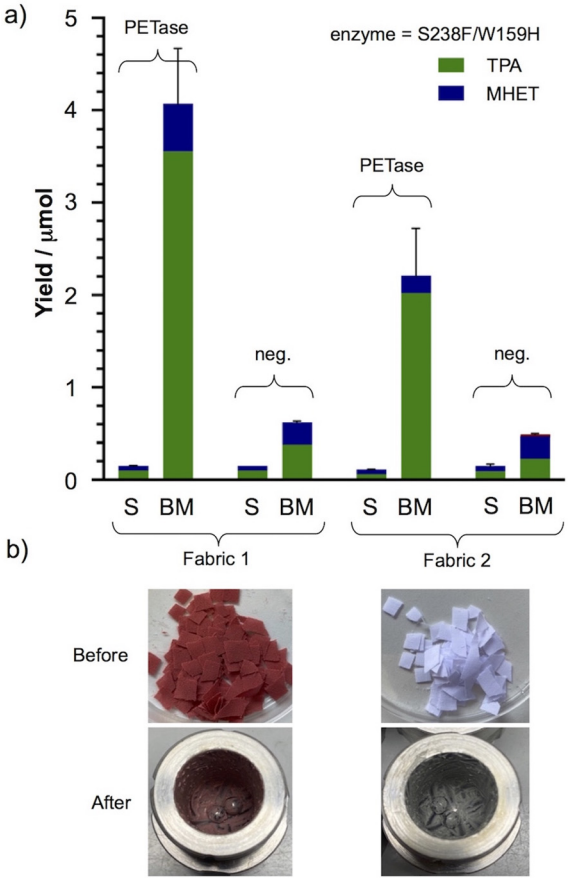

Fig. 19 (a) Enzymatic depolymerization of two samples of PET fabric in solution (S) and under ball milling (BM). (b) PET fabric samples before and after mechanoenzymatic hydrolysis. Adapted with permission from E. Ambrose-Dempster, L. Leipold, D. Dobrijevic, M. Bawn, E. M. Carter, G. Stojanovski, T. D. Sheppard, J. W. E. Jeffries, J. M. Ward and H. C. Hailes, Mechanoenzymatic reactions for the hydrolysis of PET, *RSC Adv.*, 2023, **13**, 9954–9962.[120]

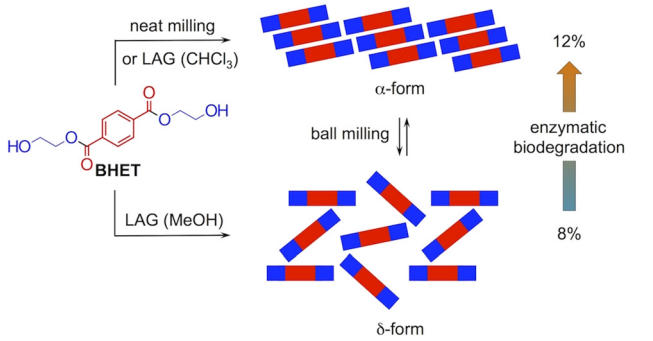

Fig. 20 Two stable polymorphs of BHET form selectively and interconvert under neat or LAG ball milling conditions. The thermodynamically more stable α-form is enzymatically hydrolyzed at a faster rate than the δ-form.[122]

commercially available BHET or the crude product of PET glycolysis,[121] which contained both forms. Based on PXRD analysis, neat milling for 90 minutes and LAG with chloroform for 60 minutes led exclusively to the thermodynamically more stable α-form. However, LAG with methanol for 120 minutes resulted in the δ-form. Moreover, LAG of the pure δ-form or glycolysis polymorph mixture with chloroform for 60 minutes resulted in conversion to the α-form, while the corresponding LAG experiments with methanol for up to 210 minutes selectively yielded the δ-form from the α-form. The authors also demonstrated that inoculation of both the α-and δ-forms of BHET with the full microbial consortium after one month resulted in faster degradation of the α-polymorph, reaching almost 12% biodegradation level, compared to *ca.* 8% for the δ-form (Fig. 20). When non-microbial hydrolysis was factored in, total BHET degradation increased to 25% and 22%, respectively.

In addition to PET, there are also literature examples of efficient mechanoenzymatic depolymerization of other types of plastic waste. For instance, Friščić and Auclair reported a modification of the RAging technique where the initial mixture was ball milled only once for several minutes, and then left aging in a humid environment for the desired duration (minutes or hours), instead of doing repeating cycles. This so-called MAging process (**M**illing + **Aging**) was used for the depolymerization of bio-degradable polymer polylactic acid (PLA).[123] The authors were successful in quantitatively depolymerizing PLA to lactic acid under moist-solid conditions with a HiC enzyme loading of 0.65 wt%, 3 M Tris buffer at pH 9 (η = 4.5 µL mg^{-1}) and milling for 15 minutes at 30 Hz in a PTFE jar with a single 10 mm ZrO_2 ball, followed by incubation at 55 °C. A second batch of buffer after 2 days of incubation was added to reach the final η-value of 6 µL mg^{-1}. The addition of the second batch of buffer to neutralize the acid proved to be an important step to ensure that the HiC-catalyzed depolymerization of PLA was quantitative. When an equivalent conventional hydrolysis reaction was performed in a slurry at an η-value of 10 µL mg^{-1}, quantitative conversion was achieved after 9 days. Interestingly, a small fraction of PLA also underwent aminolysis reactions with glycine and Tris buffers, yielding the respective amide products. Furthermore, the lactic acid recovered during mechanoenzymatic depolymerization was clean enough to be used for the synthesis of a benzimidazole-based drug precursor.

Xia and Auclair have recently carried out a mechanoenzymatic hydrolysis reaction of polyethylene naphthalate (PEN) to its monomer 2,6-naphthalenedicarboxylic acid (2,6-NDA).[124] To optimize the MAging process, the authors tested various conditions: milling time from 5 to 60 minutes at 30 Hz, η-values from 0.5 to 4 µL mg^{-1}, adjusted with 0.1 M NaPi buffer at pH 8.0, BPR from 3 to 23, aging temperature from 45 °C to 70 °C and enzyme loading from 0.43 to 4.55 wt% (*Humicola insolens* cutinase HiC). The optimal conditions were 30 minutes milling with η = 1.5 µL mg^{-1} and BPR = 7 at an incubation temperature of 55 °C in the presence of 2 wt% enzyme (Fig. 21a). These conditions produced about 16% of 2,6-NDA with 16-fold selectivity over the mono(2-hydroxyethyl)-2,6-naphthalene-dicarboxylic acid (MHENDA) after 30 days of

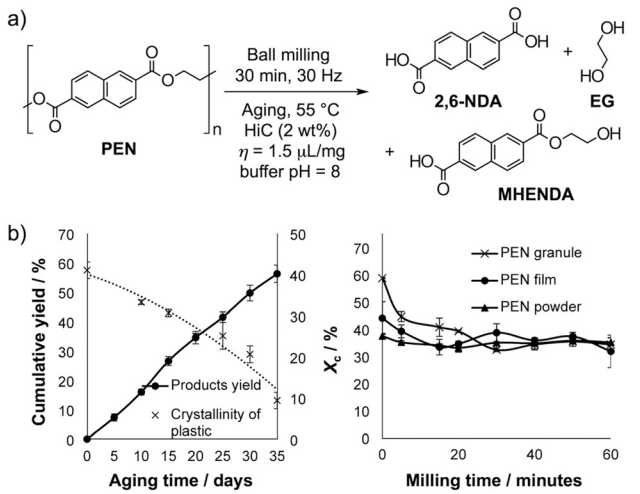

Fig. 21 (a) Mechanoenzymatic depolymerization of PEN by MAging in moist-solid mixtures for 30 days. (b) The cumulative yield of 2,6-NDA and MHENDA products (left) and the change in crystallinity of PEN during a reaction under RAging conditions (right). Reprinted with permission from Y. Xia and K. Auclair, Mechanoenzymatic Depolymerization of Highly Crystalline Polyethylene Naphthalate under Moist-Solid Conditions, *ACS Sustainable Chem. Eng.*, 2024, **12**, 14832–14840. Copyright 2024 American Chemical Society.[124]

aging. A further improvement in the cumulative yield was achieved with RAging strategy by adding the enzyme in batches every five days for seven rounds. Each round resulted in a yield of about 9%, so that after 7 rounds and 35 days reaction time, a total yield of 56% of 2,6-NDA from highly crystalline PEN (X_c = 41%) was obtained (Fig. 21b).

As with the above-mentioned PET, both the amorphous and crystalline regions of the PEN were depolymerized. When an equivalent conventional reaction was performed in aqueous conditions, 30 times less product was obtained. The authors carried out further experiments to gain more insights into the mechanoenzymatic depolymerization reactions. It was found that enzymatic depolymerization led to a decrease in the crystallinity of the material, the enzyme adsorbed quickly to the plastic substrate during milling and retained its activity even after 60 minutes of milling, and that adsorbed enzymes were more stable than free ones.

It is clear from the cited examples that the mechanoenzymatic depolymerization of plastic waste, although at an early stage of development, shows promising results compared to conventional reactions under aqueous conditions. Further improvements in the field are expected to be achieved by a combination of mechanochemical reactivity with computer-aided enzyme engineering and application of genetic tools for specific design of plastic degradation enzymes, which could also tolerate elevated temperatures and high crystallinity regions in polymer substrates.[125] Another important consideration is the issue of reusability and scalability of enzymes in mechanoenzymatic reactions, which are prerequisites for potential industrial applications.

2.4. Reactive extrusion and scale up

Mechanochemical treatment of polymers is mainly carried out on a small laboratory scale, which is typically 10–500 mg, and scaling up to grams and even further to kilogram quantities to be of industrial importance still represents a technological challenge.[126] However, there are several notable examples in the literature that demonstrate how the mechanochemistry of waste polymer degradation could be successfully scaled up and turned into a continuous process using equipment other than standard vibration or planetary ball mills.

Scholl *et al.* reported the results of a mechanochemical depolymerization in a quasi-solid-solid kneading reaction, by recycling PET waste to its monomer building blocks TPA and EG.[127] The use of larger gram-scale quantities of PET flakes (30 g), NaOH (13 g) and ethylene glycol (15 g) was realized in a laboratory kneader (Fig. 22a). The effects of several parameters, such as temperature range, size of NaOH particles and speed of the rotor inside the kneading chamber, were tested. The optimum conditions for the PET depolymerization reaction were a barrel temperature of 160 °C at a rotational speed of 40 rpm for 5 minutes. The crude mixture was suspended in water, and after filtration to remove unreacted material and acidification with sulfuric acid, TPA monomers in a yield of >90% were obtained. In general, converting batch to continuous processing is challenging from the chemical engineering point of view, with the application of extruders for mechanochemical depolymerization reactions on a larger scale still being largely underdeveloped. For instance, back in 2000 Kamal *et al.* investigated the continuous hydrolytic depolymerization of PET by reactive extrusion.[128] In addition to several technical parameters relevant for the reactive extrusion equipment, such as temperature, rotational speed, residence time and feed rate, the screw configuration was found to be important and had a significant effect on the final effectiveness of the process. With a screw configuration consisting of standard and reverse conveying and kneading block elements, the best conversion of 33.6% was achieved at a H_2O/PET ratio of 0.68 : 1, a reaction temperature of 300 °C, a screw speed of 10 min^{-1}, a feed rate of 1.11 kg h^{-1} for PET and a feed rate of 0.75 kg h^{-1} for H_2O, a reaction pressure of 4757 kPa, and a residence time of 9 min. In another recent contribution by Scholl, it was demonstrated that the mechanochemical batch process of PET depolymerization with NaOH described earlier can be successfully upscaled by switching to a continuous

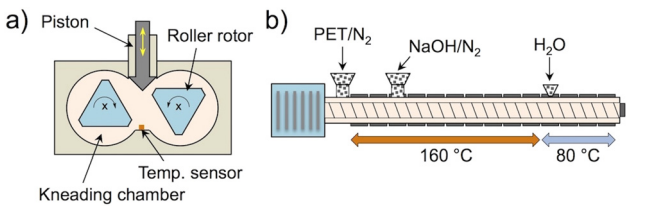

Fig. 22 (a) Schematic diagram of a laboratory kneader used by Scholl to depolymerize PET with NaOH on a 30 gram scale.[127] (b) Scheme of continuous alkaline depolymerization of PET by reactive extrusion.[129]

process through implementation of the twin-screw extruder (Fig. 22b).[129] For alkaline PET depolymerization by reactive extrusion, the temperature was kept constant at 160 °C in all barrels except for barrels 1 just after the PET feed and 11–15, where the water was dispersed at 80 °C. The screw configuration with mixing, holding and kneading elements was crucial for achieving high shear stress rates and long-enough residence times to allow breakdown of PET polymers to its monomers. During the reaction, a constant total feed rate of 20 kg h^{-1} with a rotational speed of 200 min^{-1} was maintained, while the average residence time of the product was adjusted by controlling the screw speed between 200 and 400 min^{-1}. Under such conditions, a high degree of depolymerization and high TPA yields were achieved (97%–98.3%).

In the work by Saito *et al.*,[92] PVC dechlorination by CaO was scaled up from a planetary ball mill to a custom-made larger horizontal TS-type mechanochemical reactor consisting of inner and outer cylinders that rotate simultaneously in opposite directions. The TS reactor was charged with 10 mm steel balls in diameter to a total mass of 172 kg and a 50% fill rate, and 1 kg of the PVC–CaO (1 : 4) powder mixture. The inner cylinder was rotated at 300 rpm and the outer cylinder at 70 rpm, producing shear forces that induced PVC dechlorination in yields up to 90% after 10 hours of treatment. Despite slower reaction, the TS-type reactor was about 15 times more energy efficient than a small planetary mill, consuming about 34 kWh kg^{-1} in comparison to 500 kWh kg^{-1}.

Kumagai *et al.* have carried out dechlorination of waste PVC sealing strips and cable coverings at a 100–200 g scale in a large horizontal ball mill reactor, using 0.5–1.0 M NaOH solution in ethylene glycol (5 L) and heating the mixture to 190 °C (Fig. 23a).[130] The up-scale ball mill reactor was charged with stainless steel milling balls (200–3200 pieces) and equipped with an inlet for N_2 gas, a heater, and operated at rotational speeds of 15–60 rpm (Fig. 23b). The chloride content was determined by ion chromatography and elemental analysis, and it was shown that overall alkaline PVC dechlorination can reach up to 99%. Kinetic data and DEM simulations revealed a linear correlation between the apparent rate constant of the PVC dechlorination and specific impact energy, which in combination with FTIR and SEM analysis of the depolymerization residue enabled the authors to propose the PVC dechlorination reaction mechanism based on the shrinking core model. In a more recent contribution, the life-cycle assessment (LCA) study of the described mechanochemical PVC waste treatment including the chloride recovery process based on electrodialysis was performed.[131] The recycled NaCl could be sourced by the chlor-alkali industry, while regenerated EG could be reused in the PVC degradation. The main contributors that have the potential to substantially reduce the greenhouse gas emissions associated with PVC were determined, and the effectiveness of the dechlorination process for various throughputs of PVC waste (from 100 to 1000 g) was shown.

The Baláž group successfully upscaled their previous work on PVC dechlorination to soluble calcium chloride with eggshells as the $CaCO_3$ source (Fig. 24).[132] Similarly to the work by

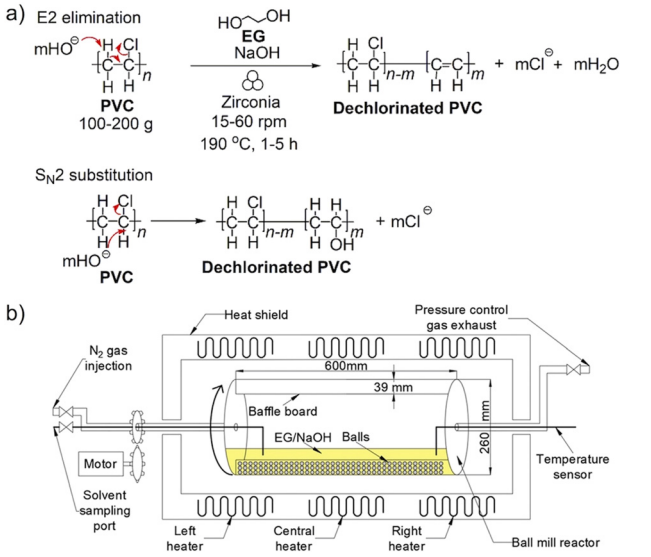

Fig. 23 (a) NaOH/EG-promoted mechanochemical dechlorination of waste PVC proceeds through E2 elimination and S_N2 substitution mechanisms. (b) Diagram of the horizontal ball mill reactor used for the PVC dechlorination on a 100–200 gram scale. Adapted with permission from J. Lu, S. Borjigin, S. Kumagai, T. Kameda, Y. Saito and T. Yoshioka, Practical dechlorination of polyvinyl chloride wastes in NaOH/ethylene glycol using an up-scale ball mill reactor and validation by discrete element method simulations, *Waste Manag.*, 2019, **99**, 31–41.[130]

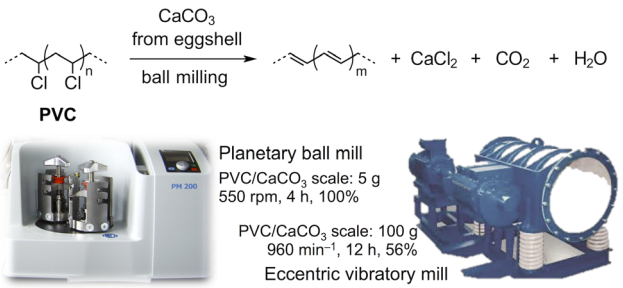

Fig. 24 Upcycling of waste PVC and biowaste eggshells as a source of $CaCO_3$ for mechanochemical dechlorination on a laboratory and semi-industrial scale reported by Baláž *et al.*[132]

Tongamp *et al.*,[99] an interesting aspect of this research was that two types of waste materials (plastic and biowaste) were treated mechanochemically on a large scale to convert them into valuable products. The laboratory-scale planetary ball milling of 1 gram of PVC and 4 g of eggshell with fibrous membranes removed (total mass 5 g) in WC media at 550 rpm milling speed for 4 hours led to 100% dechlorination. On a semi-industrial scale of 100 g PVC and 200 g eggshell (300 g in total), 12 hours of milling in an air atmosphere provided 56% of PVC dechlorination. For this purpose, an eccentric vibratory ball mill was employed with a 5 L steel milling chamber attached to the main corpus of the mill, WC balls with a diameter of 35 mm (total mass 30 kg) at 80% ball filling and rotational speed of the motor 960 min^{-1}. PXRD and FTIR con-

firmed the formation of calcium chloride during the process, which was shown to be feasible at scales 20 times higher than that of ordinary laboratory milling.

3. Conclusions

The highlighted research in this review clearly demonstrates how the synergy between mechanochemistry and principles of chemical recycling of polymers has resulted in many discoveries and exciting new opportunities for waste plastics management that fit into the circular economy scheme. The relevance of such investigations in modern society is further supported by IUPAC in a worldwide recognition of mechanochemistry and reactive extrusion together with plastic depolymerization to monomers, as technologies that have the potential to make a lasting impact on our efforts to embrace sustainability in the production and consumption of goods.[133] A unique environment of solid-state ball milling where reactivity goes beyond limitations imposed by interactions in bulk solvents enables the recovery of monomers from commodity condensation polymers with high conversions and selectivities. Despite certain similarities between thermochemical and mechanochemical processes for vinyl polymers, the efficiency of waste polyolefin depolymerization under reaction conditions close to ambient temperatures and pressures is likely due to the specific nature of mechanochemical mechanisms. These effects are also translated into the arena of enzymatic catalysis where mechanoenzymology is emerging as a powerful technology to break down plastics, as well as for the remediation of environmental pollutants from the family of fluorinated polymers. Most certainly, a deeper understanding of the mechanochemical mechanisms through an interplay of experiments with theoretical description[134] and quantum chemical calculations[135] will enable the design of more effective reaction strategies that surpass a purely phenomenological approach, and aid in the optimization and transition of ball milling waste plastics from the laboratory setting to an industrial scale for commercial exploitation.

Conflicts of interest

There are no conflicts to declare.

Abbreviations

Al_2O_3	Aluminum oxide
BDC	1,4-Dicarboxylate ligand
BHET	Bis(2-hydroxyethyl) terephthalate
BPA	Bisphenol A
BPA-PC	Poly(bisphenol-A carbonate)
BPR	Ball-to-powder ratio
CAT-HTR	Catalytic hydrothermal reactor
CO_2	Carbon dioxide
CP-MAS	Cross-polarization magic angle spinning
DBU	1,8-Diazabicyclo[5.4.0]undec-7-ene
DEM	Discrete element method
DFT	Density functional theory
DMC	Dimethyl carbonate
DMF	*N*,*N*-Dimethylformamide
DMPO	5,5-Dimethyl-1-pyrrolyine *N*-oxide
DMSO	Dimethyl sulfoxide
DMT	Dimethyl terephthalate
DOTP	Dioctyl terephthalate
DPC	Diphenyl carbonate
DPVC	Dechlorinated poly(vinyl chloride)
DC-PVC	Dechlorinated poly(vinyl chloride) as a substrate for epoxidation
DSC	Differential scanning calorimetry
Đ	Dispersity
ECTFE	Ethylene-chlorotrifluoroethylene
EDA	Ethylenediamine
EG	Ethylene glycol
EP-PVC	Epoxidized poly(vinyl chloride)
EPR	Electron paramagnetic resonance
EPS	Expanded polystyrene foam
ESR	Electron spin resonance
ETFE	Ethylene tetrafluoroethylene
FEP	Fluorinated ethylene propylene
FTIR-ATR	Fourier transform infrared attenuated total reflection infrared spectroscopy
GC	Gas chromatography
GC-MS	Gas chromatography-mass spectrometry
GPC	Gel permeation chromatography
HAT	Hydrogen atom transfer
HCl	Hydrochloric acid
HDI	Hexamethylene diisocyanate
HDPE	High-density polyethylene
HiC	*Humicola insolens* cutinase
H_2O	Water
HS	Hardened steel
HY-PVC	Hydrolyzed poly(vinyl chloride)
ILAG	Ion and liquid-assisted grinding
IL-AG	Ionic liquid-assisted grinding
IPDI	Isophorone diisocyanate
IUPAC	International union of pure and applied chemistry
K_3PO_4	Potassium phosphate
$K_4P_2O_7$	Potassium pyrophosphate
LAG	Liquid-assisted grinding
LCA	Life-cycle assessment
LDPE	Low-density polyethylene
LLDPE	Linear low-density polyethylene
MAging	Milling + aging
m-CPBA	*m*-Chloroperoxybenzoic acid
MeCN	Acetonitrile
MeOH	Methanol
MDI	Methylene diphenyl diisocyanate
MDPE	Medium-density polyethylene
MHENDA	Mono(2-hydroxyethyl)-2,6-naphthalenedicarboxylic acid
MMA	Methyl methacrylate

MMT	Mono-methyl terephthalate
M_n	Number-average molecular weight
MPC	Methylphenyl carbonate
MOF	Metal-organic framework
MS	α-Methylstyrene
M_w	Weight-average molecular weight
MHET	Mono(2-hydroxyethyl) terephthalate
NaCl	Sodium chloride
NaMHET	Sodium mono(2-hydroxyethyl) terephthalate
NaOH	Sodium hydroxide
Na_2TPA	Sodium terephthalate
2,6-NDA	2,6-Naphthalenedicarboxylic acid
NMR	Nuclear magnetic resonance
PBF	Poly(butylene furanoate)
PBnMA	Poly(benzyl methacrylate)
PnBMA	Poly(*n*-butyl methacrylate)
PBT	Poly(butylene terephthalate)
PC	Polycarbonate
PCTFE	Poly(chlorotrifluoroethylene)
PDI	Polydispersity index
PEG-800	Poly(ethylene glycol) 800
PEF	Poly(ethylene furanoate)
PEMA	Poly(ethyl methacrylate)
PEN	Poly(ethylene naphthalate)
PET	Poly(ethylene terephthalate)
PFA	Perfluoroalkoxy alkane
PFAS	Polyfluoroalkyl substances
PFOA	Perfluorooctanoic acid
PFOS	Perfluorooctane sulfonate
PLA	Poly(lactic acid)
PMMA	Poly(methyl methacrylate)
PMS	Poly(α-methylstyrene)
PPhMA	Poly(phenyl methacrylate)
PiPMA	Poly(i-propyl methacrylate)
POLAG	Polymer-assisted grinding
PPM	Post-polymerization modification
PPS	Poly(phenylene sulfide)
PP	Polypropylene
PS	Polystyrene
PTFE	Poly(tetrafluoroethylene)
PU	Polyurethane
PVA	Poly(vinyl acetate)
PVC	Poly(vinyl chloride)
PVDF	Poly(vinylidene fluoride)
PVDF–HFP	Poly(vinylidene fluoride-*co*-hexafluoropropylene)
PVP	Poly(vinylpyrrolidone) polymer
PXRD	Powder X-ray diffraction
RAging	Reactive milling + aging
RH	Relative humidity
RT	Room temperature
SAM	Surface-activated mechanocatalysis
SEC	Size exclusion chromatography
SEM	Scanning electron microscopy
SS	Stainless steel
SZ	Sulfated zirconia
TBAF	Tetrabutylammonium fluoride
t-BuOH	*tert*-Butanol
TDI	Toluene-2,4-diisocyanate
TEM	Transmission electron microscopy
T_c	Ceiling temperature
T_g	Glass transition temperature
T_m	Melting point
TEMPO	(2,2,6,6-Tetramethylpiperidin-1-yl)oxyl
TFM-PS	Trifluoromethyl-grafted polystyrene
TGA	Thermogravimetric analysis
THF	Tetrahydrofuran
TMAF	Tetramethylammonium fluoride
TPA	Terephthalic acid
UV	Ultraviolet
WC	Tungsten carbide
WZ	Tungstated zirconia
X_c	Degree of crystallinity
XPS	X-ray photoelectron spectroscopy
ZrO_2	Zirconium dioxide

Data availability

No primary research results, software or code have been included and no new data were generated or analysed as part of this review.

Acknowledgements

The financial support was provided through the Ruđer Bošković Institute internal funding programme.

References

1 R. C. Thompson, S. H. Swan, C. J. Moore and F. S. vom Saal, Our plastic age, *Philos. Trans. R. Soc., B*, 2009, **364**, 1973–1976.
2 Plastics – the fast Facts 2024, Plastics Europe, source: https://www.plasticseurope.org/knowledge-hub.
3 W. Tan, D. Cui and B. Xi, Moving policy and regulation forward for single-use plastic alternatives, *Front. Environ. Sci. Eng.*, 2021, **15**, 1–4.
4 Y. Li, L. Tao, Q. Wang, F. Wang, G. Li and M. Song, Potential Health Impact of Microplastics: A Review of Environmental Distribution, Human Exposure, and Toxic Effects, *Environ. Health*, 2023, **1**, 249–257.
5 Z. O. G. Schyns and M. P. Shaver, Mechanical Recycling of Packaging Plastics: A Review, *Macromol. Rapid Commun.*, 2021, **42**, 2000415.
6 L. S. Kato and C. A. Conte-Junior, Safety of Plastic Food Packaging: The Challenges about Non-Intentionally Added Substances (NIAS) Discovery, Identification and Risk Assessment, *Polymers*, 2021, **13**(2077), 1–43.
7 S. Chen and Y. H. Hu, Advancements and future directions in waste plastics recycling: From mechanical

methods to innovative chemical processes, *Chem. Eng. J.*, 2024, **493**, 152727.
8 X. Chen, Y. Wang and L. Zhang, Recent Progresses in the Chemical Upcycling of Plastic Wastes, *ChemSusChem*, 2021, **14**, 4137–4151.
9 F. Cuccu, L. De Luca, F. Delogu, E. Colacino, N. Solin, R. Mocci and A. Porcheddu, Mechanochemistry: New Tools to Navigate the Uncharted Territory of "Impossible" Reactions, *ChemSusChem*, 2022, **15**, e202200362.
10 J. F. Reynes, F. Leon and F. Garcia, Mechanochemistry for Organic and Inorganic Synthesis, *ACS Org. Inorg. Au*, 2024, **4**, 432–470.
11 B. Szczęśniak, S. Borysiuk, J. Choma and M. Jaroniec, Mechanochemical synthesis of highly porous materials, *Mater. Horiz.*, 2020, **7**, 1457–1473.
12 P. Ying, J. Yu and W. Su, Liquid-Assisted Grinding Mechanochemistry in the Synthesis of Pharmaceuticals, *Adv. Synth. Catal.*, 2021, **363**, 1246–1271.
13 T. Friščić, D. G. Reid, I. Halasz, R. S. Stein, R. E. Dinnebier and M. J. Duer, Ion- and Liquid-Assisted Grinding: Improved Mechanochemical Synthesis of Metal–Organic Frameworks Reveals Salt Inclusion and Anion Templating, *Angew. Chem., Int. Ed.*, 2010, **49**, 712–715.
14 D. Hasa, E. Carlino and W. Jones, Polymer-Assisted Grinding, a Versatile Method for Polymorph Control of Cocrystallization, *Cryst. Growth Des.*, 2016, **16**, 1772–1779.
15 A. Mukherjee, R. D. Rogers and A. S. Myerson, Cocrystal formation by ionic liquid-assisted grinding: case study with cocrystals of caffeine, *CrystEngComm*, 2018, **20**, 3817–3821.
16 G. Félix, N. Fabregue, C. Leroy, T.-X. Métro, C.-H. Chen and D. Laurencin, Induction-heated ball-milling: a promising asset for mechanochemical reactions, *Phys. Chem. Chem. Phys.*, 2023, **25**, 23435–23447.
17 V. Štrukil and I. Sajko, Mechanochemically-assisted solid-state photocatalysis (MASSPC), *Chem. Commun.*, 2017, **53**, 9101–9104.
18 F. Effaty, L. Gonnet, S. G. Koenig, K. Nagapudi, X. Ottenwaelder and T. Friščić, Resonant acoustic mixing (RAM) for efficient mechanoredox catalysis without grinding or impact media, *Chem. Commun.*, 2023, **59**, 1010–1013.
19 K. Kubota, Y. Pang, A. Miura and H. Ito, Redox reactions of small organic molecules using ball milling and piezoelectric materials, *Science*, 2019, **366**, 1500–1504.
20 S. Lukin, L. S. Germann, T. Friščić and I. Halasz, Toward Mechanistic Understanding of Mechanochemical Reactions Using Real-Time In Situ Monitoring, *Acc. Chem. Res.*, 2022, **55**, 1262–1277.
21 S. Aydonat, A. H. Hergesell, C. L. Seitzinger, R. Lennarz, G. Chang, C. Sievers, J. Meisner, I. Vollmer and R. Göstl, Leveraging mechanochemistry for sustainable polymer degradation, *Polym. J.*, 2024, **56**, 249–268.
22 J. Li, C. Nagamani and J. S. Moore, Polymer Mechanochemistry: From Destructive to Productive, *Acc. Chem. Res.*, 2015, **48**, 2181–2190.
23 A. Rizzo and G. I. Peterson, Progress toward sustainable polymer technologies with ball-mill grinding, *Prog. Polym. Sci.*, 2024, **159**, 101900.
24 G. W. Coates and Y. D. Y. L. Getzler, Chemical recycling to monomer for an ideal, circular polymer economy, *Nat. Rev. Mater.*, 2020, **5**, 501–516.
25 M. Rabnawaz, I. Wyman, R. Auras and S. Cheng, A roadmap towards green packaging: the current status and future outlook for polyesters in the packaging industry, *Green Chem.*, 2017, **19**, 4737–4753.
26 H. Köpnick, M. Schmidt, W. Brügging, J. Rüter and W. Kaminsky, Polyesters, in *Ullmann's Encyclopedia of Industrial Chemistry*, 2000, vol. 28, pp. 623–649.
27 J. Scheirs, Additives for the Modification of Poly(Ethylene Terephthalate) to Produce Engineering-Grade Polymers, in *Modern Polyesters: Chemistry and Technology of Polyesters and Copolyesters*, 2004, pp. 495–540.
28 J. Payne and M. D. Jones, The Chemical Recycling of Polyesters for a Circular Plastics Economy: Challenges and Emerging Opportunities, *ChemSusChem*, 2021, **14**, 4041–4070.
29 V. Štrukil, Highly efficient Solid-State Hydrolysis of Waste Polyethylene Terephthalate by Mechanochemical Milling and Vapor-Assisted Aging, *ChemSusChem*, 2021, **14**, 330–338.
30 A. W. Tricker, A. A. Osibo, Y. Chang, J. X. Kang, A. Ganesan, E. Anglou, F. Boukouvala, S. Nair, C. W. Jones and C. Sievers, Stages and Kinetics of Mechanochemical Depolymerization of Poly(ethylene terephthalate) with Sodium Hydroxide, *ACS Sustainable Chem. Eng.*, 2022, **10**, 11338–11347.
31 B. P. Hutchings, D. E. Crawford, L. Gao, P. Hu and S. L. James, Feedback Kinetics in Mechanochemistry: The Importance of Cohesive States, *Angew. Chem., Int. Ed.*, 2017, **56**, 15252–15256.
32 C. Bai, R. J. Spontak, C. C. Koch, C. K. Saw and C. M. Balik, Structural changes in poly(ethylene terephthalate) induced by mechanical milling, *Polymer*, 2000, **41**, 7147–7157.
33 A. Zaker and K. Auclair, Impact of Ball Milling on the Microstructure of Polyethylene Terephthalate, *ChemSusChem*, 2025, **18**, e202401506.
34 E. Anglou, Y. Chang, W. Bradley, C. Sievers and F. Boukouvala, Modeling Mechanochemical Depolymerization of PET in Ball-Mill Reactors Using DEM Simulations, *ACS Sustainable Chem. Eng.*, 2024, **12**, 9003–9017.
35 C. Vasiliu Oprea, C. Neguleanu and C. Simionescu, On the mechano-chemical destruction of polyethylene terephthalate by vibratory milling, *Eur. Polym. J.*, 1970, **6**, 181–198.
36 P. A. May and J. S. Moore, Polymer mechanochemistry: techniques to generate molecular force via elongational flows, *Chem. Soc. Rev.*, 2013, **42**, 7497–7506.
37 S. Kaabel, J. P. D. Therien, C. E. Deschênes, D. Duncan, T. Friščić and K. Auclair, Enzymatic depolymerization of

highly crystalline polyethylene terephthalate enabled in moist-solid reaction mixtures, *Proc. Natl. Acad. Sci. U. S. A.*, 2021, **118**, e2026452118.

38 D. Jain, F. Cramer, P. Shamraienko, H.-J. Drexler, B. Voit and T. Beweries, Highly efficient mechanochemical depolymerisation of bio-based polyethylene furanoate and polybutylene furanoate, *RSC Sustainability*, 2025, **3**, 3513–3519, DOI: 10.1039/d5su00428d.

39 H. W. Lee, K. Yoo, L. Borchardt and J. G. Kim, Chemical recycling of polycarbonate and polyester without solvent and catalyst: mechanochemical methanolysis, *Green Chem.*, 2024, **26**, 2087–2093.

40 P. He, Z. Hu, Z. Dai, H. Bai, Z. Fan, R. Niu, J. Gong, Q. Zhao and T. Tang, Mechanochemistry Milling of Waste Poly(Ethylene Terephthalate) into Metal–Organic Frameworks, *ChemSusChem*, 2023, **16**, e202201935.

41 C.-A. Tao and J.-F. Wang, Synthesis of Metal Organic Frameworks by Ball-Milling, *Crystals*, 2021, **11**(15), 1–20.

42 S. Wu, S. Ma, Q. Zhang and C. Yang, A comprehensive review of polyurethane: Properties, applications and future perspectives, *Polymer*, 2025, **327**, 128361.

43 H. Sardon, D. Mecerreyes, A. Basterretxea, L. Avérous and C. Jehanno, From Lab to Market: Current Strategies for the Production of Biobased Polyols, *ACS Sustainable Chem. Eng.*, 2021, **9**, 10664–10677.

44 J. O. Akindoyo, M. D. H. Beg, S. Ghazali, M. R. Islam, N. Jeyaratnam and A. R. Yuvaraj, Polyurethane types, synthesis and applications – a review, *RSC Adv.*, 2016, **6**, 114453–114482.

45 G. Rossignolo, G. Malucelli and A. Lorenzetti, Recycling of polyurethanes: where we are and where we are going, *Green Chem.*, 2024, **26**, 1132–1152.

46 R. Donadini, C. Boaretti, L. Scopel, A. Lorenzetti and M. Modesti, Deamination of Polyols from the Glycolysis of Polyurethanez, *Chem. – Eur. J.*, 2024, **30**, e202301919.

47 R. Heiran, A. Ghaderian, A. Reghunadhan, F. Sedaghati, S. Thomas and A. H. Haghighi, Glycolysis: an efficient route for recycling of end of life polyurethane, *J. Polym. Res.*, 2021, **28**, 22.

48 J. Li, H. Zhu, D. Fang, X. Huang, C. Zhang and Y. Luo, Mechanochemistry recycling of polyurethane foam using urethane exchange reaction, *J. Environ. Chem. Eng.*, 2023, **11**, 110269.

49 S. Kim, K. Li, A. Alsbaiee, J. P. Brutman and W. R. Dichtel, Circular Reprocessing of Thermoset Polyurethane Foams, *Adv. Mater.*, 2023, **35**, 2305387.

50 B. Wang, J. Britschgi, N. K. Tran, I. Jevtovikj, P. Ingale, C. Mai, S. A. Schunk and F. Schüth, Recycling of Polyurethane via Mechanocatalytic Methanolysis/Hydrolysis, *ChemSusChem*, 2025, **18**, e202500253.

51 G. I. Peterson, W. Ko, Y.-J. Hwang and T.-L. Choi, Mechanochemical Degradation of Amorphous Polymers with Ball-Mill Grinding: Influence of the Glass Transition Temperature, *Macromolecules*, 2020, **53**, 7795–7802.

52 V. Lohmann, G. R. Jones, N. P. Truong and A. Anastasaki, The Thermodynamics and Kinetics of Depolymerization: What Makes Vinyl Monomer Regeneration Feasible?, *Chem. Sci.*, 2024, **15**, 832–853.

53 Y. Chang, V. S. Nguyen, A. H. Hergesell, C. L. Seitzinger, J. Meisner, I. Vollmer, F. J. Schorka and C. Sievers, Thermodynamic limits of the depolymerization of poly(olefin)s using mechanochemistry, *RSC Mechanochem.*, 2024, **1**, 504–513.

54 X. Wang, Y. Liang, Z. Pu, S. Yang, J. He and Y. Liang, Transforming waste to treasure: Superhydrophobic coatings from recycled polypropylene for high-value application, *Prog. Org. Coat.*, 2024, **188**, 108248.

55 Q. Sun, T. Liu, T. Wen and J. Yu, Coupling of carbonization method with high-energy ball milling: Towards submicron-sized graphite powders transforming from waste COVID-19 masks, *Mater. Chem. Phys.*, 2023, **307**, 128134.

56 I. Vollmer, M. J. F. Jenks, M. C. P. Roelands, R. J. White, T. van Harmelen, P. de Wild, G. P. van der Laan, F. Meirer, J. T. F. Keurentjes and B. M. Weckhuysen, Beyond Mechanical Recycling: Giving New Life to Plastic Waste, *Angew. Chem., Int. Ed.*, 2020, **59**, 15402–15423.

57 R. Mishra, A. Kumar, E. Singh and S. Kumar, Recent Research Advancements in Catalytic Pyrolysis of Plastic Waste, *ACS Sustainable Chem. Eng.*, 2023, **11**, 2033–2049.

58 D. K. Ratnasari, M. A. Nahil and P. T. Williams, Catalytic pyrolysis of waste plastics using staged catalysis for production of gasoline range hydrocarbon oils, *J. Anal. Appl. Pyrolysis*, 2017, **124**, 631–637.

59 M. Kusenberg, A. Eschenbacher, M. R. Djokic, A. Zayoud, K. Ragaert, S. De Meester and K. M. Van Geem, Opportunities and challenges for the application of post-consumer plastic waste pyrolysis oils as steam cracker feedstocks: To decontaminate or not to decontaminate?, *Waste Manage.*, 2022, **138**, 83–115.

60 A. Maisels, A. Hiller and F.-G. Simon, Chemical Recycling for Plastic Waste: Status and Perspectives, *ChemBioEng Rev.*, 2022, **9**, 541–555.

61 M. A. Bashir, T. Ji, J. Weidman, Y. Soong, M. Gray, F. Shi and P. Wang, Plastic waste gasification for low-carbon hydrogen production: a comprehensive review, *Energy Adv.*, 2025, **4**, 330–363.

62 M. J. Boel, H. Wang, A. Al Farra, L. Megido, J. M. Gonzalez-LaFuente and N. R. Shiju, Hydrothermal liquefaction of plastics: a survey of the effect of reaction conditions on the reaction efficiency, *React. Chem. Eng.*, 2024, **9**, 1014–1031.

63 Z. Chen, W. Wei, X. Chen, Y. Liu, Y. Shen and B.-J. Ni, Upcycling of plastic wastes for hydrogen production: Advances and perspectives, *Renewable Sustainable Energy Rev.*, 2024, **195**, 114333.

64 V. S. Nguyen, Y. Chang, E. V. Phillips, J. A. DeWitt and C. Sievers, Mechanocatalytic Oxidative Cracking of Poly(ethylene) Via a Heterogeneous Fenton Process, *ACS Sustainable Chem. Eng.*, 2023, **11**, 7617–7623.

65 L. Li, O. Vozniuk, Z. Cao, P. Losch, M. Felderhoff and F. Schüth, Hydrogenation of different carbon substrates

into light hydrocarbons by ball milling, *Nat. Commun.*, 2023, **14**(5257), 1–9.
66 L. Li, M. Leutzsch, P. Hesse, C. Wang, B. Wang and F. Schüth, Polyethylene Recycling via Water Activation by Ball Milling, *Angew. Chem., Int. Ed.*, 2025, **64**, e202413132.
67 G. Cagnetta, K. Zhang, Q. Zhang, J. Huang and G. Yu, Augmented hydrogen production by gasification of ball milled polyethylene with $Ca(OH)_2$ and $Ni(OH)_2$, *Front. Environ. Sci. Eng.*, 2019, **13**(11), 1–9.
68 R. Gu, T. Wang, Y. Ma, T.-X. Wang, R.-Q. Yao, Y. Zhao, Z. Wen, G.-F. Han, X.-Y. Lang and Q. Jiang, Upcycling Polyethylene to High-Purity Hydrogen under Ambient Conditions via Mechanocatalysis, *Angew. Chem., Int. Ed.*, 2025, **64**, e202417644.
69 K. Kubota, J. Jiang, Y. Kamakura, R. Hisazumi, T. Endo, D. Miura, S. Kubo, S. Maeda and H. Ito, Using Mechanochemistry to Activate Commodity Plastics as Initiators for Radical Chain Reactions of Small Organic Molecules, *J. Am. Chem. Soc.*, 2024, **146**, 1062–1070.
70 A. H. Hergesell, R. J. Baarslag, C. L. Seitzinger, R. Meena, P. Schara, Ž. Tomović, G. Li, B. M. Weckhuysen and I. Vollmer, Surface-Activated Mechano-Catalysis for Ambient Conversion of Plastic Waste, *J. Am. Chem. Soc.*, 2024, **146**, 26139–26147.
71 A. Porcheddu, E. Colacino, L. De Luca and F. Delogu, Metal-Mediated and Metal-Catalyzed Reactions Under Mechanochemical Conditions, *ACS Catal.*, 2020, **10**, 8344–8394.
72 H. Staudinger and W. Heuer, über hochpolymere Verbindungen, 93. Mitteil.: über das Zerreißen der Faden-Moleküle des Poly-styrols, *Ber. Dtsch. Chem. Ges.*, 1934, **67**, 1159–1164.
73 R. E. Eckert, T. R. Maykrantz and R. J. Salloum, The formation of free radicals in polystyrene by ball milling, *J. Polym. Sci., Part B: Polym. Phys.*, 1968, **6**, 213–218.
74 V. P. Balema, I. Z. Hlova, S. L. Carnahan, M. Seyedi, O. Dolotko, A. J. Rossini and I. Luzinov, Depolymerization of polystyrene under ambient conditions, *New J. Chem.*, 2021, **45**, 2935–2938.
75 E. Jung, D. Yim, H. Kim, G. I. Peterson and T. L. Choi, Depolymerization of poly(α-methyl styrene) with ball-mill grinding, *J. Polym. Sci.*, 2023, **61**, 553–560.
76 T. Yamamoto, S. Kato, D. Aoki and H. Otsuka, A Diarylacetonitrile as a Molecular Probe for the Detection of Polymeric Mechanoradicals in the Bulk State through a Radical Chain-Transfer Mechanism, *Angew. Chem., Int. Ed.*, 2021, **60**, 2680–2683.
77 Y. Chang, S. J. Blanton, R. Andraos, V. S. Nguyen, C. L. Liotta, F. J. Schork and C. Sievers, Kinetic Phenomena in Mechanochemical Depolymerization of Poly (styrene), *ACS Sustainable Chem. Eng.*, 2024, **12**, 178–191.
78 M. E. Skala, S. M. Zeitler and M. R. Golder, Liquid-assisted grinding enables a direct mechanochemical functionalization of polystyrene waste, *Chem. Sci.*, 2024, **15**, 10900–10907.
79 N. Ohn and J. G. Kim, Mechanochemical post-polymerization modification: solvent-free solid-state synthesis of functional polymers, *ACS Macro Lett.*, 2018, **7**, 561–565.
80 M. Ashlin and C. E. Hobbs, Post-polymerization thiol substitutions facilitated by mechanochemistry, *Macromol. Chem. Phys.*, 2019, **220**, 1900350.
81 G. Kim, B. Park, N. Kim, Y.-J. Hwang, A. Rizzo and G. I. Peterson, Waste polystyrene upcycling via the Birch reduction with ball-mill grinding, *Nat. Commun.*, 2025, **16**, 5924.
82 H. Wu, W. Zhao, H. Hu and G. Chen, One-step in situ ball milling synthesis of polymer-functionalized graphene nanocomposites, *J. Mater. Chem.*, 2011, **21**, 8626–8632.
83 J. Lin, D. Chen, J. Dong and G. Chen, Preparation of polyvinylpyrrolidone-decorated hydrophilic graphene via in situ ball milling, *J. Mater. Sci.*, 2015, **50**, 8057–8063.
84 K. Kubota, N. Toyoshima, D. Miura, J. Jiang, S. Maeda, M. Jin and H. Ito, Introduction of a Luminophore into Generic Polymers via Mechanoradical Coupling with a Prefluorescent Reagent, *Angew. Chem., Int. Ed.*, 2021, **60**, 16003–16008.
85 A. P. Smith, J. S. Shay, R. J. Spontak, C. M. Balik, H. Ade, S. D. Smith and C. C. Koch, High-energy mechanical milling of poly(methyl methacrylate), polyisoprene and poly(ethylene-*alt*-propylene), *Polymer*, 2000, **41**, 6271–6283.
86 S.-i. Kondo, Y. Sasai, S. Hosaka, T. Ishikawa and M. Kuzuya, Kinetic analysis of the mechanolysis of polymethylmethacrylate in the course of vibratory ball milling at various mechanical energy, *J. Polym. Sci., Part A: Polym. Chem.*, 2004, **42**, 4161–4167.
87 E. Jung, M. Cho, G. I. Peterson and T.-L. Choi, Depolymerization of Polymethacrylates with Ball-Mill Grinding, *Macromolecules*, 2024, **57**, 3131–3137.
88 F. Karasek and L. Dickson, Model studies of polychlorinated dibenzo-p-dioxin formation during municipal refuse incineration, *Science*, 1987, **237**, 754–756.
89 M. Baláž, Polymeric Waste, in *Environmental Mechanochemistry Recycling Waste into Materials Using High-Energy Ball Milling*, Springer, 2021, vol. 4, pp. 135–153.
90 G. Cagnetta, J. Robertson, J. Huang, K. Zhang and G. Yu, Mechanochemical destruction of halogenated organic pollutants: A critical review, *J. Hazard. Mater.*, 2016, **313**, 85–102.
91 F. Saito, W. Zhang and J. Kano, Mechanochemical dechlorination of waste PVC resin and feedstock recycling, *Powder Technol.*, 2024, **448**, 120330.
92 Q. Zhang, F. Saito, K. Shimme and S. Masuda, Dechlorination of PVC by a mechanochemical treatment under atmospheric condition, *J. Soc. Powder Technol., Jpn.*, 1999, **36**, 468–473.
93 S. Saeki, J. Kano, F. Saito, K. Shimme, S. Masuda and T. Inoue, Effect of additives on dechlorination of PVC by mechanochemical treatment, *J. Mater. Cycles Waste Manage.*, 2001, **3**, 20–23.

94 H. Mio, S. Saeki, J. Kano and F. Saito, Estimation of mechanochemical dechlorination of poly (vinyl chloride), *Environ. Sci. Technol.*, 2002, **36**, 1344–1348.
95 T. Inoue, M. Miyazaki, M. Kamitani, J. Kano and F. Saito, Mechanochemical dechlorination of polyvinyl chloride by co-grinding with various metal oxides, *Adv. Powder Technol.*, 2004, **15**, 215–225.
96 W. Tongamp, Q. Zhang and F. Saito, Mechanochemical decomposition of PVC by using La_2O_3 as additive, *J. Hazard. Mater.*, 2006, **137**, 1226–1230.
97 T. Inoue, J. Kano and F. Saito, Influence of polymer impurity on the mechanochemical dechlorination reaction of polyvinyl chloride, *Adv. Powder Technol.*, 2006, **17**, 425–432.
98 W. Tongamp, J. Kano, Q. Zhang and F. Saito, Mechanochemical dechlorination of polyvinyl chloride with calcium sulfates, *J. Mater. Cycles Waste Manage.*, 2008, **10**, 140–143.
99 W. Tongamp, J. Kano, Q. Zhang and F. Saito, Simultaneous treatment of PVC and oyster-shell wastes by mechanochemical means, *Waste Manage.*, 2008, **28**, 484–488.
100 C.-F. Chow, C.-S. Lam, K.-C. Lau and C.-B. Gong, Waste-to-Energy: Production of Fuel Gases from Plastic Wastes, *Polymers*, 2021, **13**(3672), 1–11.
101 N. Choudhury, A. Kim, M. Kim and B.-S. Kim, Mechanochemical Degradation of Poly(vinyl chloride) into Nontoxic Water-Soluble Products via Sequential Dechlorination, Heterolytic Oxirane Ring-Opening, and Hydrolysis, *Adv. Mater.*, 2023, **35**, 2304113.
102 W.-T. Yang, Y.-Y. Xie, S.-M. Xu, G. Wu and Y.-Z. Wang, Upcycling of polyvinyl chloride to porous carbon for high-performance electromagnetic wave absorption materials, *Chem. Eng. J.*, 2024, **496**, 154054.
103 E. S. A. Al-Sammarraie, W. A. K. Al-Ithawi, A. V. Baklykov, V. A. Platonov, A. M. K. Altobee, N. S. Glebov, A. F. Khasanov, I. S. Kovalev, I. L. Nikonov, D. S. Kopchuk, I. M. Sapozhnikova, T. M. Sabirova, Y. Jin, G. V. Zyryanov and V. L. Rusinov, (Mechano)chemical modification of polyvinyl chloride with azole-based drugs, *Chim. Techno Acta*, 2024, **11**, 202411211.
104 Z. Wang, A. M. BuserIan, T. Cousins, S. Demattio, W. Drost, O. Johansson, K. Ohno, G. Patlewicz, A. M. Richard, G. W. Walker, G. S. White and E. Leinala, A New OECD Definition for Per- and Polyfluoroalkyl Substances, *Environ. Sci. Technol.*, 2021, **55**, 15575–15578.
105 R. C. Buck, J. Franklin, U. Berger, J. M. Conder, I. T. Cousins, P. De Voogt, A. A. Jensen, K. Kannan, S. A. Mabury and S. P. J. van Leeuwen, Perfluoroalkyl and polyfluoroalkyl substances in the environment: Terminology, classification, and origins, *Integr. Environ. Assess. Manage.*, 2011, **7**, 513–541.
106 K. Zhang, J. Huang, G. Yu, Q. Zhang, S. Deng and B. Wang, Destruction of Perfluorooctane Sulfonate (PFOS) and Perfluorooctanoic Acid (PFOA) by Ball Milling, *Environ. Sci. Technol.*, 2013, **47**, 6471–6477.
107 L. P. Turner, B. H. Kueper, K. M. Jaansalu, D. J. Patch, N. Battye, O. El-Sharnouby, K. G. Mumford and K. P. Weber, Mechanochemical remediation of perfluorooctanesulfonic acid (PFOS) and perfluorooctanoic acid (PFOA) amended sand and aqueous film-forming foam (AFFF) impacted soil by planetary ball milling, *Sci. Total Environ.*, 2021, **765**, 142722.
108 L. P. Turner, B. H. Kueper, D. J. Patch and K. P. Weber, Elucidating the relationship between PFOA and PFOS destruction, particle size and electron generation in amended media commonly found in soils, *Sci. Total Environ.*, 2023, **888**, 164188.
109 N. J. Battye, D. J. Patch, D. M. D. Roberts, N. M. O'Connor, L. P. Turner, B. H. Kueper, M. E. Hulley and K. P. Weber, Use of a horizontal ball mill to remediate per- and polyfluoroalkyl substances in soil, *Sci. Total Environ.*, 2022, **835**, 155506.
110 K. Gobindlal, E. Shields, A. Whitehill, C. C. Weber and J. Sperry, Mechanochemical destruction of per- and polyfluoroalkyl substances in aqueous film-forming foams and contaminated soil, *Environ. Sci.: Adv.*, 2023, **2**, 982–989.
111 K. Gobindlal, Z. Zujovic, J. Jaine, C. C. Weber and J. Sperry, Solvent-Free, Ambient Temperature and Pressure Destruction of Per uorosulfonic Acids under Mechanochemical Conditions: Degradation Intermediates and Fluorine Fate, *Environ. Sci. Technol.*, 2023, **57**, 277–285.
112 N. Yang, S. Yang, Q. Ma, C. Beltran, Y. Guan, M. Morsey, E. Brown, S. Fernando, T. M. Holsen, W. Zhang and Y. Yang, Solvent-Free Nonthermal Destruction of PFAS Chemicals and PFAS in Sediment by Piezoelectric Ball Milling, *Environ. Sci. Technol. Lett.*, 2023, **10**, 198–203.
113 L. Yang, Z. Chen, C. A. Goult, T. Schlatzer, R. S. Paton and V. Gouverneur, Phosphate-enabled mechanochemical PFAS destruction for fluoride reuse, *Nature*, 2025, **640**, 100–106.
114 M. Pérez-Venegas and E. Juaristi, Mechanoenzymology: State of the Art and Challenges towards Highly Sustainable Biocatalysis, *ChemSusChem*, 2021, **14**, 2682–2688.
115 C. Bolm and J. G. Hernández, From Synthesis of Amino Acids and Peptides to Enzymatic Catalysis: A Bottom-Up Approach in Mechanochemistry, *ChemSusChem*, 2018, **11**, 1410–1420.
116 R. Hollenbach and K. Ochsenreither, Mechanoenzymatic Reactions – Challenges and Perspectives, *ChemCatChem*, 2023, **15**, e202300656.
117 S. Kaabel, T. Friščić and K. Auclair, Mechanoenzymatic Transformations in the Absence of Bulk Water: A More Natural Way of Using Enzymes, *ChemBioChem*, 2020, **21**, 742–758.
118 F. Hammerer, L. Loots, J.-L. Do, J. P. D. Therien, C. W. Nickels, T. Friščić and K. Auclair, Solvent-Free Enzyme Activity: Quick, High-Yielding Mechanoenzymatic

Hydrolysis of Cellulose into Glucose, *Angew. Chem., Int. Ed.*, 2018, **57**, 2621–2624.

119 S. Kaabel, J. Arciszewski, T. H. Borchers, J. P. D. Therien, T. Friščić and K. Auclair, Solid-State Enzymatic Hydrolysis of Mixed PET/Cotton Textiles, *ChemSusChem*, 2023, **16**, e202201613.

120 E. Ambrose-Dempster, L. Leipold, D. Dobrijevic, M. Bawn, E. M. Carter, G. Stojanovski, T. D. Sheppard, J. W. E. Jeffries, J. M. Ward and H. C. Hailes, Mechanoenzymatic reactions for the hydrolysis of PET, *RSC Adv.*, 2023, **13**, 9954–9962.

121 D. Shingwekar, H. Laster, H. Kemp and J. L. Mellies, Two-Step Chemo-Microbial Degradation of Post-Consumer Polyethylene Terephthalate (PET) Plastic Enabled by a Biomass-Waste Catalyst, *Bioengineering*, 2023, **10**(1253), 1–17.

122 D. Shingwekar, N. Lutz, D. S. Botes, E. J. Cabrera-Vega, G. Campillo-Alvarado, J. L. Mellies and J. D. Loya, Polymorphism control of polyethylene terephthalate (PET) degradation product via mechanochemistry leads to accelerated microbial degradation, *RSC Mechanochem.*, 2024, **1**, 514–519.

123 M. Pérez-Venegas, T. Friščić and K. Auclair, Efficient Mechano-Enzymatic Hydrolysis of Polylactic Acid under Moist-Solid Conditions, *ACS Sustainable Chem. Eng.*, 2023, **11**, 9924–9931.

124 Y. Xia and K. Auclair, Mechanoenzymatic Depolymerization of Highly Crystalline Polyethylene Naphthalate under Moist-Solid Conditions, *ACS Sustainable Chem. Eng.*, 2024, **12**, 14832–14840.

125 V. Tournier, C. M. Topham, A. Gilles, B. David, C. Folgoas, E. Moya-Leclair, E. Kamionka, M.-L. Desrousseaux, H. Texier, S. Gavalda, M. Cot, E. Guémard, M. Dalibey, J. Nomme, G. Cioci, S. Barbe, M. Chateau, I. André, S. Duquesne and A. Marty, An engineered PET depolymerase to break down and recycle plastic bottles, *Nature*, 2020, **580**, 216–219.

126 J. F. Reynes, V. Isoni and F. Garcia, Tinkering with Mechanochemical Tools for Scale Up, *Angew. Chem., Int. Ed.*, 2023, **62**, e202300819.

127 L. Biermann, D. Quast, E. Brepohl, C. Eichert and S. Scholl, Alkali Depolymerization of Poly(ethylene terephthalate) in a Quasi-solid-solid Kneading Reaction, *Chem. Eng. Technol.*, 2021, **44**, 2300–2308.

128 T. Yalçinyuva, M. R. Kamal, R. A. Lai-Fook and S. Özgümüs, Hydrolytic Depolymerization of Polyethylene Terephthalate by Reactive Extrusion, *Int. Polym. Process.*, 2000, **XV**, 137–146.

129 L. Biermann, E. Brepohl, C. Eichert, M. Paschetag, M. Watts and S. Scholl, Development of a continuous PET depolymerization process as a basis for a back to-monomer recycling method, *Green Process. Synth.*, 2021, **10**, 361–373.

130 J. Lu, S. Borjigin, S. Kumagai, T. Kameda, Y. Saito and T. Yoshioka, Practical dechlorination of polyvinyl chloride wastes in NaOH/ethylene glycol using an up-scale ball mill reactor and validation by discrete element method simulations, *Waste Manage.*, 2019, **99**, 31–41.

131 J. Lu, S. Kumagai, Y. Fukushima, H. Ohno, S. Borjigin, T. Kameda, Y. Saito and T. Yoshioka, Sustainable Advance of Cl Recovery from Polyvinyl Chloride Waste Based on Experiment, Simulation, and Ex Ante Life-Cycle Assessment, *ACS Sustainable Chem. Eng.*, 2021, **9**, 14112–14123.

132 M. Baláž, Z. Bujňáková, M. Achimovičová, M. Tešinský and P. Baláž, Simultaneous valorization of polyvinyl chloride and eggshell wastes by a semi-industrial mechanochemical approach, *Environ. Res.*, 2019, **170**, 332–336.

133 F. Gomollón-Bel, Ten Chemical Innovations That Will Change Our World: IUPAC identifies emerging technologies in Chemistry with potential to make our planet more sustainable, *Chem. Int.*, 2019, **41**, 12–17.

134 T. Yamamoto, K. Kubota, Y. Harabuchi and H. Ito, Scaling theory for the kinetics of mechanochemical reactions with convective flow, *RSC Mechanochem.*, 2025, **2**, 230–239.

135 M. Alonso, T. Bettens, J. Eeckhoudt, P. Geerlings and F. De Proft, Wandering through quantum-mechanochemistry: from concepts to reactivity and switches, *Phys. Chem. Chem. Phys.*, 2024, **26**, 21–35.